10/78

NASA CR-135278
R77AEG439

QUIET CLEAN SHORT-HAUL EXPERIMENTAL ENGINE (QCSEE) COMPOSITE FAN FRAME DESIGN REPORT

September, 1978

by

Stephen C. Mitchell

GENERAL ELECTRIC COMPANY

Prepared for

National Aeronautics and Space Administration

FOREWORD

The Quiet Clean Short-Haul Experimental Engine (QCSEE) Program is currently being conducted by the General Electric Company, Aircraft Engine Group, under NASA Contract NAS3-18021. The QCSEE Program is under the direction of Mr. C.C. Ciepluch, NASA Project Manager.

This report presents the results of the Composite Fan Frame Design. The NASA program director and technical advisor for this effort was Mr. M.P. Hanson. The program was performed under the direction of Mr. C.L. Stotler, Jr., Technical Manager-General Electric Company, with Mr. S.C. Mitchell responsible for the frame design and analysis.

TABLE OF CONTENTS

LIST OF ILLUSTRATIONS

LIST OF ILLUSTRATIONS (Continued)

LIST OF ILLUSTRATIONS (Concluded)

LIST OF TABLES

1.0 SUMMARY

One of the advanced technology items of the Quiet Clean Short-Haul Experimental Engine (QCSEE) Program is the design, fabrication, and test of an advanced composite frame which is flight-weight and integrates the functions of several structures. The program produced two nearly identical frames, one for the over-the-wing (OTW) engine and the other for the under-the-wing (UTW) engine. Both the OTW and UTW frames are flight-weight, integrated designs that are constructed of advanced composite materials and are identical except for several minor differences not connected with structural integrity. Design integration is achieved by combining the functions of the fan stator vanes, fan outer casing, and fan frame into the one unitized structure shown in Figure 1. This approach saves considerable duplication of structure resulting in a significantly lighter-weight design. The unitized approach is particularly suited to the use of composite materials, since these materials are more efficient when employed in large bonded structures rather than small structures which are bolted together. The composite design concepts used for the frame are essentially those which were developed for, and demonstrated by, the F101 simulated composite front frame shown in Figure 2 and funded under Air Force Contract AFML-TR-73-158.

The composite material system selected as the basic material for the frame is Type AS graphite fiber in a Hercules 3501 epoxy resin matrix. This material was selected because of the rather extensive data base for the material, its good mechanical properties, its cost, and its ready availability.

The frame was analyzed using a finite-element digital computer program. A three-dimensional view of the computer model utilized in the analysis of the QCSEE composite frame is shown in Figure 3. This program was used in an iterative fashion to arrive at practical thicknesses and ply orientations to achieve a final design that met all strength and stiffness requirements for critical conditions. Using this information, the detail design of each of the individual parts of the frame was completed and released. On the basis of these designs, the required tooling was designed to fabricate the various component parts of the frame.

To verify the structural integrity of the critical joint areas, a full-scale test was conducted on the frame before engine testing. The testing of the frame established critical spring constants and subjected the frame to three critical load cases. The successful static load test was followed by 153 and 58 hours respectively of successful running on the UTW and OTW engines. Figure 4 shows the UTW engine on Pad IVD at the GE Outdoor Peebles test facility shown in Figure 5.

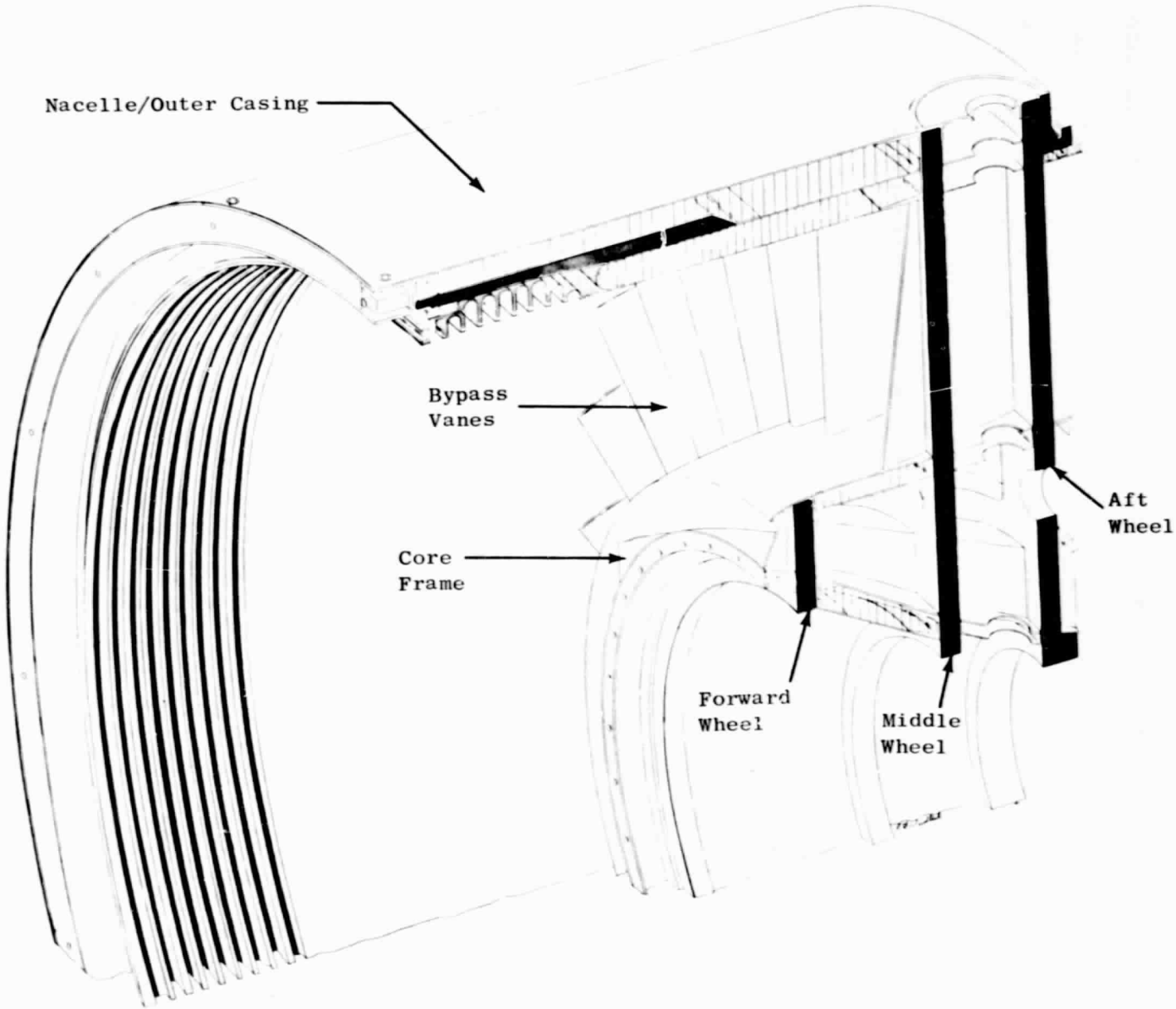

Figure 1. OCSEE Frame Trimetric.

Figure 2. F101 Composite Frame.

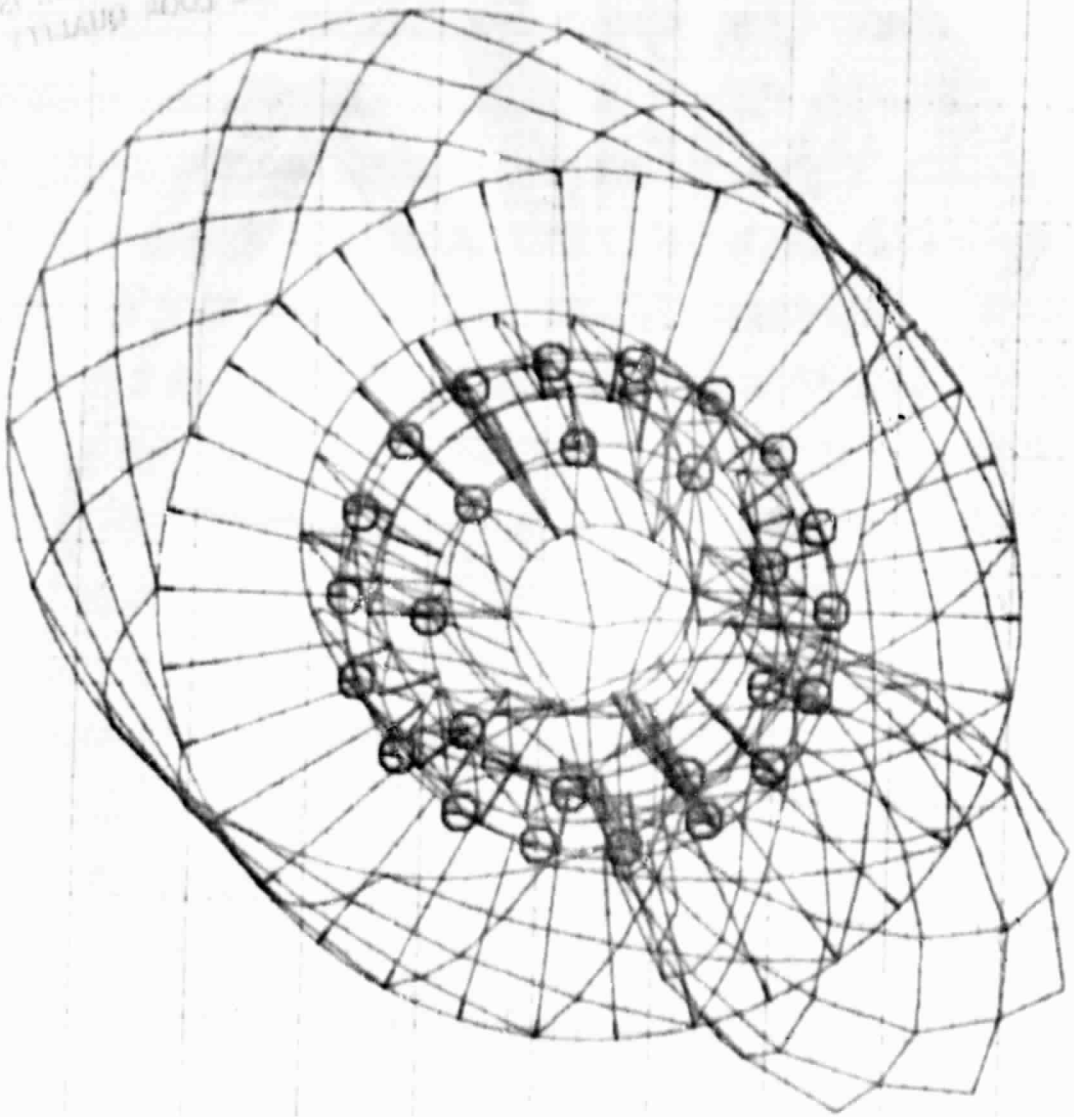

Figure 3. Analytical Model Trimetric.

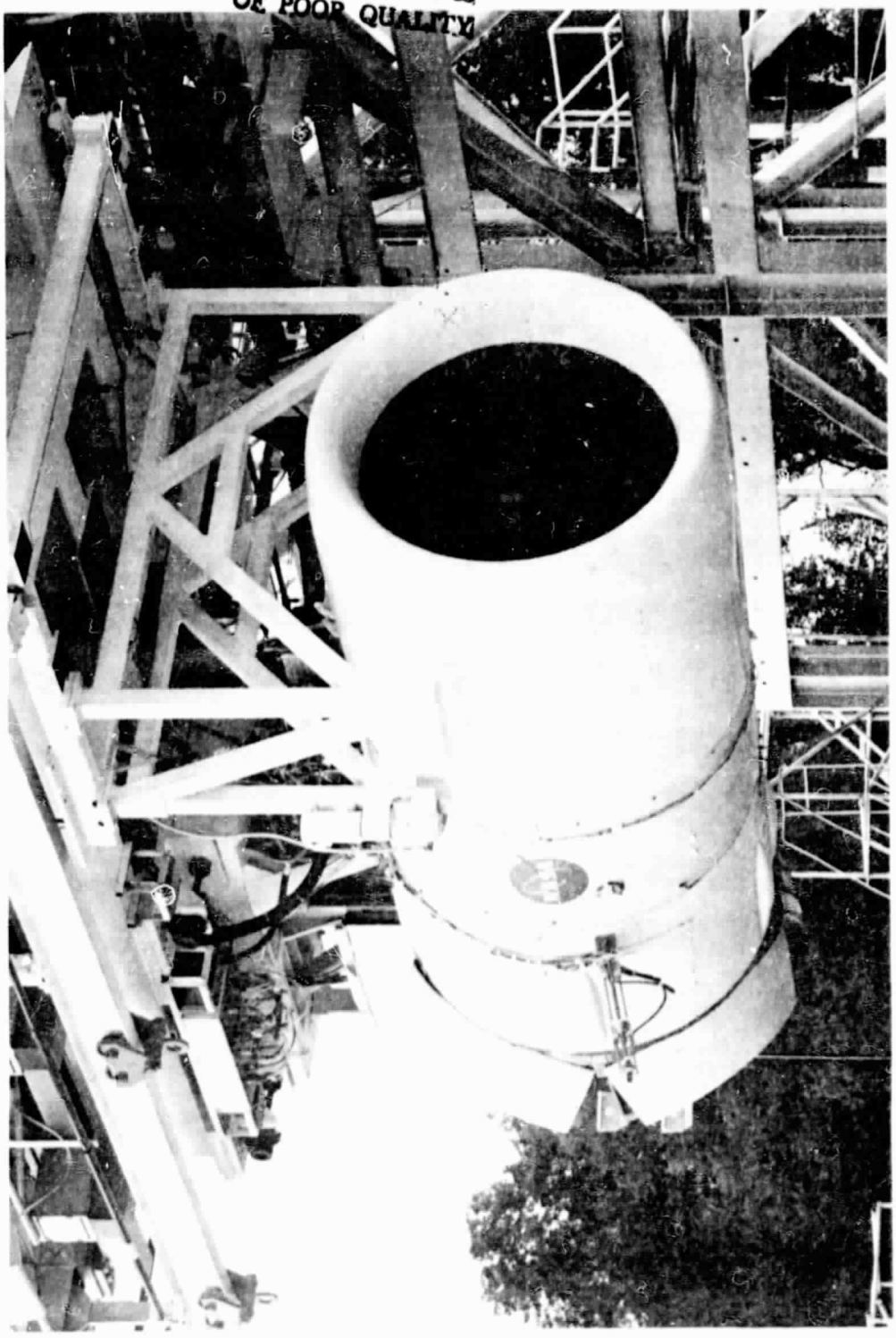

Figure 4. QCSEE UTW Engine on Test.

Figure 5. Site IV at Peebles Test Facility.

2.0 INTRODUCTION

The QCSEE fan frame is a flight-weight integrated design constructed of advanced composite materials. Design integration is achieved by combining the functions of the fan stator vanes, fan outer casing, and fan frame into one unitized structure as shown in Figure 1. This approach saves considerable duplication of structure resulting in a significantly lighter-weight design. The unitized approach is particularly suited to the use of composite materials since these materials are more efficient when employed in large bonded structures rather than smaller structures that must be bolted together.

The composite material system selected as the basic material for the frame is Type AS graphite fiber in Hercules 3501 epoxy resin matrix. This material was selected because of the rather extensive data base for the material, its good mechanical properties, its cost, and its ready availability.

The frame was analyzed using a finite-element computer program. This program was used in an iterative fashion to arrive at practical thicknesses and ply orientations to achieve a final design that met all strength and stiffness requirements for all of the critical conditions. Using this information, the detail design of each of the individual parts of the frame was completed and released. On the basis of these designs, the tooling required to fabricate the various component parts of the frame was designed and released to manufacturing.

The composite design concepts used for the frame are essentially those which were developed for, and demonstrated by, the F101 simulated composite front frame shown in Figure 2 and funded under Air Force Contract AFML-TR-73-158. The basic concept consists of "wheels" in which the inner, mid, and outer rings and the spokes are fabricated as a one-piece integral structure. Two or more of the wheels are then joined together by flowpath panels to form the basic frame. This concept, as applied to the QCSEE fan frame, is shown in Figures 1 and 6. Its primary advantage is that the major radial load-carrying structure (the spokes of the wheels) and the major circumferential load-carrying structure (the ring or hubs of the wheels) are integrally bonded structures rather than separate structures which must transfer load by means of bolted joints.

The structural integrity of the frame was verified by a full-scale frame test in which the frame was loaded to critical flight loads and ultimate loads. The highest loading - the ultimate load condition - subjected the frame to loads encountered from a blade-out condition at maximum thrust and maximum torque. After the successful static load test the frame was incorporated into the engine buildup. To date, both frames have performed successfully after 153 hours of UTW running and 48 hours of OTW running.

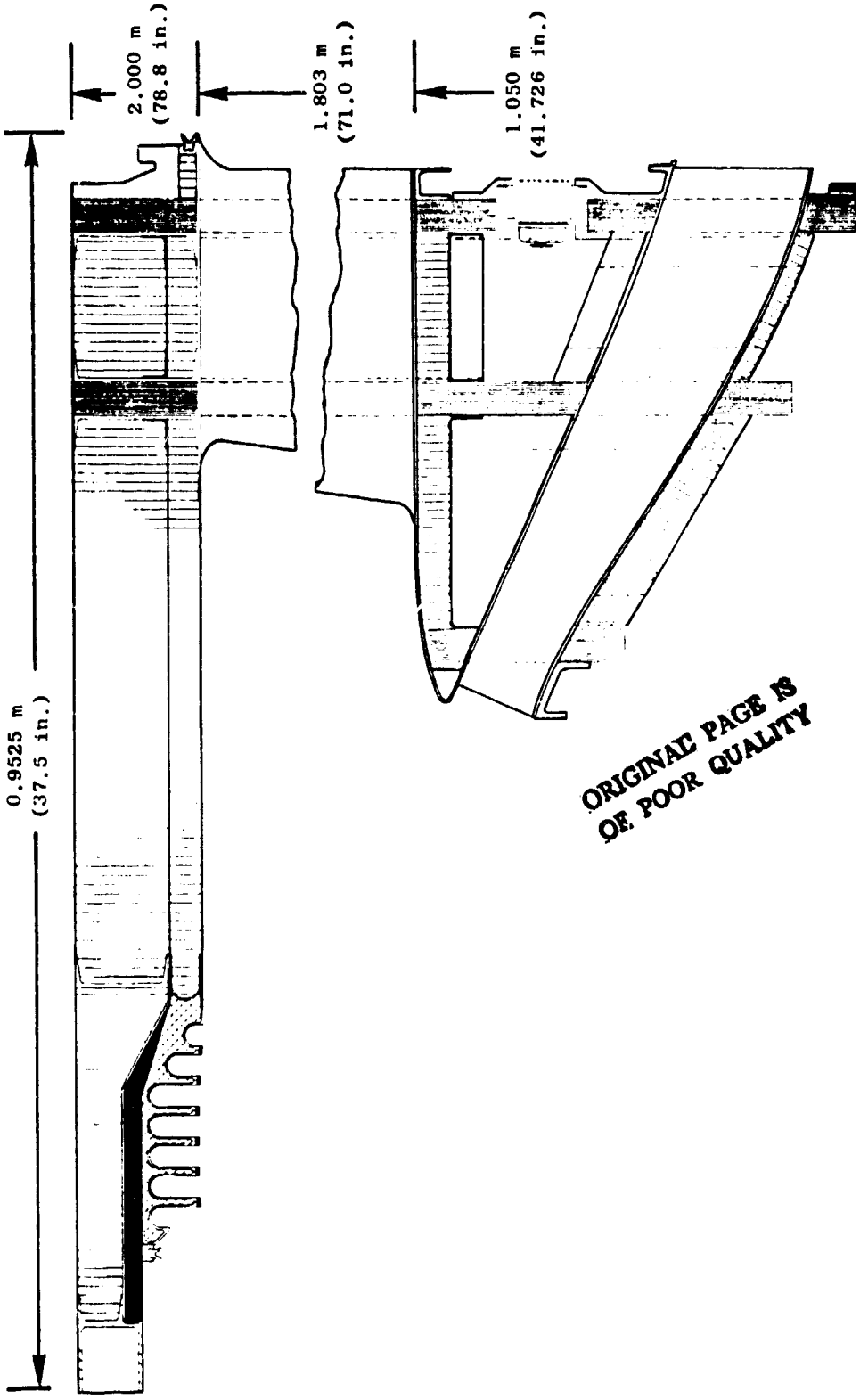

Figure 6. QCSEE Frame Cross Section.

3.0 DEVELOPMENT

The development of the QCSEE frame can be divided into three distinct phases: Mechanical Design, Analysis, and Fabrication. The Mechanical Design section describes the basic structural concept embodied by the frame geometry. Other topics covered in this section are the mechanical, aerodynamic, acoustic, and engine system functions and loads that affect both the UTW and OTW frames. The Analysis section describes primarily the iterative design analysis cycle and the different computer programs used in optimizing the frame design. Also discussed in this section are design criteria and the highest loads on the frame. The Fabrication section explains the sequence of primary events within the fabrication cycle. Although it does not describe in detail the fabrication of each component, it does describe the fabrication of the forward, mid, and aft "wheels".

3.1 MECHANICAL DESIGN

3.1.1 Basic Structural Concept

The QCSEE composite frame design concept not only satisfies the requirement of high structural integrity but also yields significant payoff in weight compared to similar mechanical metallic constructions. In essence, the overall structural concept consists of two basic elements; i.e., structural wheels and shear panels, with each element designed to perform a specific load-carrying function. For the QCSEE frame application the frame consisted of three structural wheels and eight styles of airfoil-shaped shear panels. Figure 2 depicts a simplified version of this design concept for a single-annulus frame, and as seen by the figure the structural wheels are tied together by the bonded, airfoil-shaped, shear panels.

The structural wheel satisfies several load-transfer requirements. The three basic requirements are: (1) that it transfer tensile and compressive radial load through the struts from one casing to another; (2) that it transfer both circumferential normal and bending ring loads within any ring of the wheel; and (3) that it transfer any existent forward overturning bending moments from one casing to another.

The shear panels are bonded to the four sides of each wheel flow cavity and serve not only as the basic load-carrying members between wheels but, also, as airflow surfaces within the frame cavities. The panels perform the following structural functions. First, they transfer shear forces between wheels imposed on the frame through the ring flanges. Second, they transfer radial forces between casings imposed on the struts by a tangential bending moment. Third, they transfer axial tensile and compressive forces between wheels.

The design of the composite frame in the QCSEE engine is based on the above mentioned wheel/shear panel concept but, in addition to the wheels and

shear panels, the frame also has a large outer cylinder. This cylinder attaches to the outer forward portion of the wheel/shear panel frame to form the nacelle/outer casing structure of the frame. The skeletal structure of the frame is comprised of three wheels referred to as a forward wheel, a midwheel, and an aft wheel.

The forward wheel is shown in Figure 7 and is comprised of an inner ring (hub), an outer ring (splitter), and six spokes. The wheel is a solid one-piece structure comprised of graphite/epoxy laminates. The mid and aft wheels are shown in Figures 8 and 9, respectively. Although these two wheels have different dimensions, they are constructed identically. Both wheels are comprised of an inner ring (hub), 6 core spokes, a midring (splitter), 33 bypass spokes, and an outer ring. The 6 core spokes of the midwheel are located at the center of the core strut; the 33 bypass spokes are located in the leading edge of the bypass vanes. The 6 core spokes of the aft wheel are located in the trailing edge of the core struts; 32 of the 33 bypass spokes are located in the trailing edge of the bypass vanes. The aft spoke in the pylon vane is not the trailing edge since it forms the interface between the forward nose of the pylon and the main pylon structure. The core frame is constructed by bonding core airflow panels (Figure 10) to the core spokes, the inner (hub) rings, and the splitter rings. Reinforcement of the bonded wheel/shear panel interface is accomplished by composite "L" flanges bonded to both the wheel ring, or spoke, and the panel. The sump is formed by bonding the one-piece graphite/epoxy truncated cone shown in Figure 11 to the inner (hub) rings of the forward and midwheels. The top of the splitter flowpath is constructed by bonding the airflow panels shown in Figure 12 to the top of the forward, mid, and aft wheel splitter rings. The bypass vanes are formed by bonding the airfoil panels shown in Figure 13 to the bypass spokes of the mid and aft wheels. The outer nacelle/casing is a multilayered honeycomb structure formed from graphite/epoxy panels and aluminum honeycomb. This casing structure is bonded to the outer rings of the mid and aft wheels. Figure 14 depicts the outer casing panels and Figure 15 shows the outer casing cylinder before attachment to the frame. As shown in Figure 16, the nacelle/fan casing structure is integral with the frame from the bypass vanes forward to the inlet. The high strength and stiffness in the frame provide the nacelle support and also support the radial drive gearbox, the digital control, and other equipment. In addition to equipment support, the entire wall thickness of the nacelle/fan case is utilized to provide fan shroud stiffness and to support the blade-containment structure. The full-depth honeycomb was lighter and less expensive to fabricate compared to the conventional double-walled structure.

The region of the casing over the fan blades was designed to improve the aerodynamics and the acoustics of the QCSEE fan. These improvements were brought about by providing continuous slots in the flowpath over the fan region. As shown in Figure 17, the edges of the webs between the slots contained frangible honeycomb to minimize abrasion from a fan blade rub. The interior of the fan casing in the region of the tip treatment contained the blade-containment structure. As seen in Figure 17, the blade containment was provided by 30 continuous plies of unimpregnated Style 328 Kevlar woven

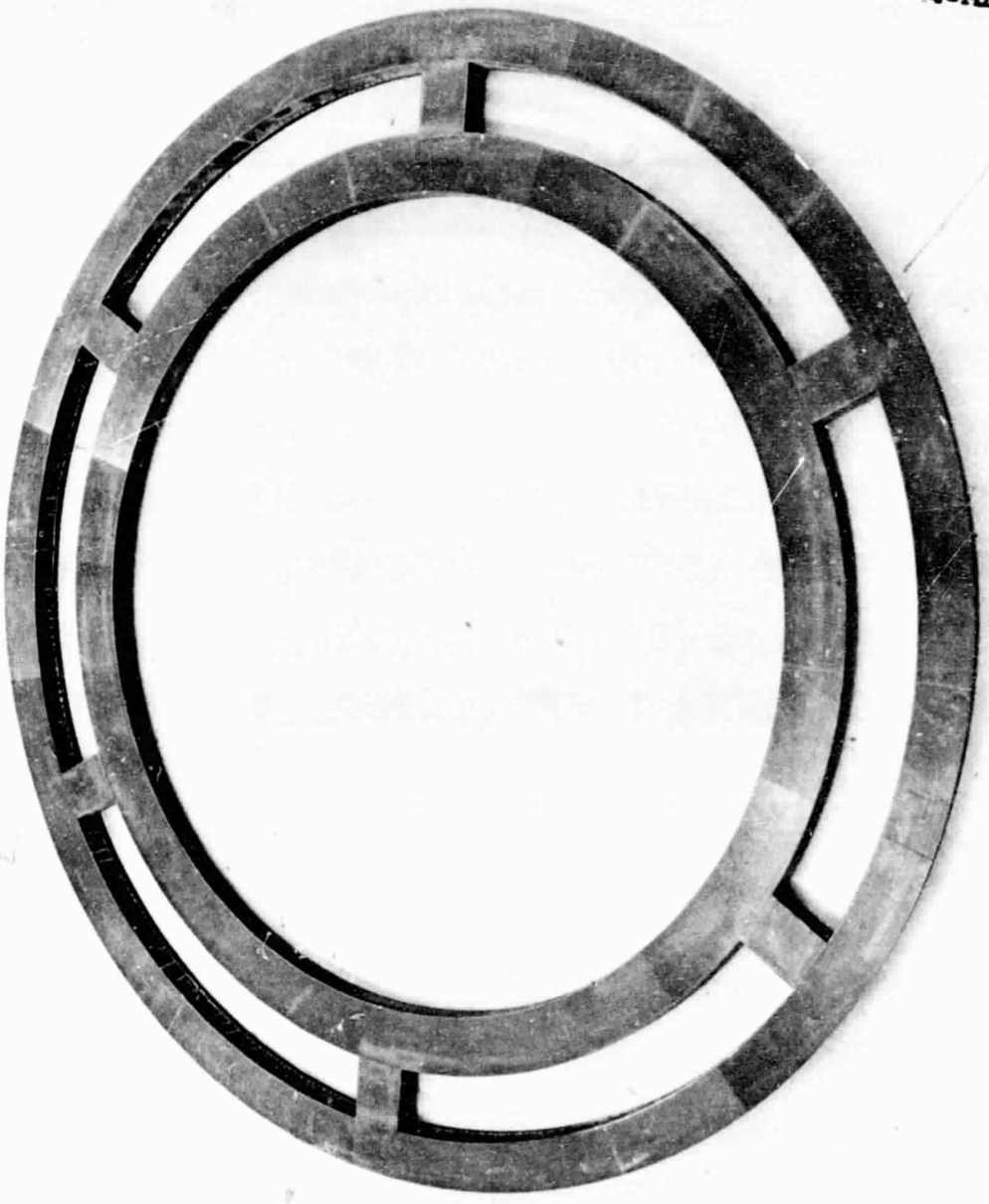

Figure 7. Forward Frame Wheel.

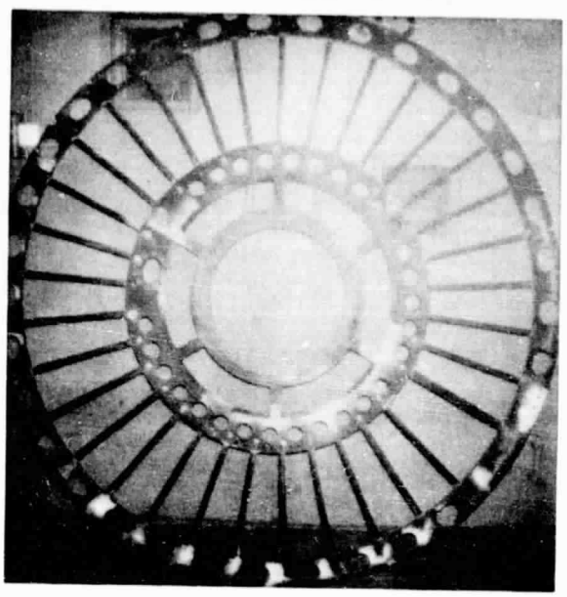

Figure 8. Middle Frame Wheel.

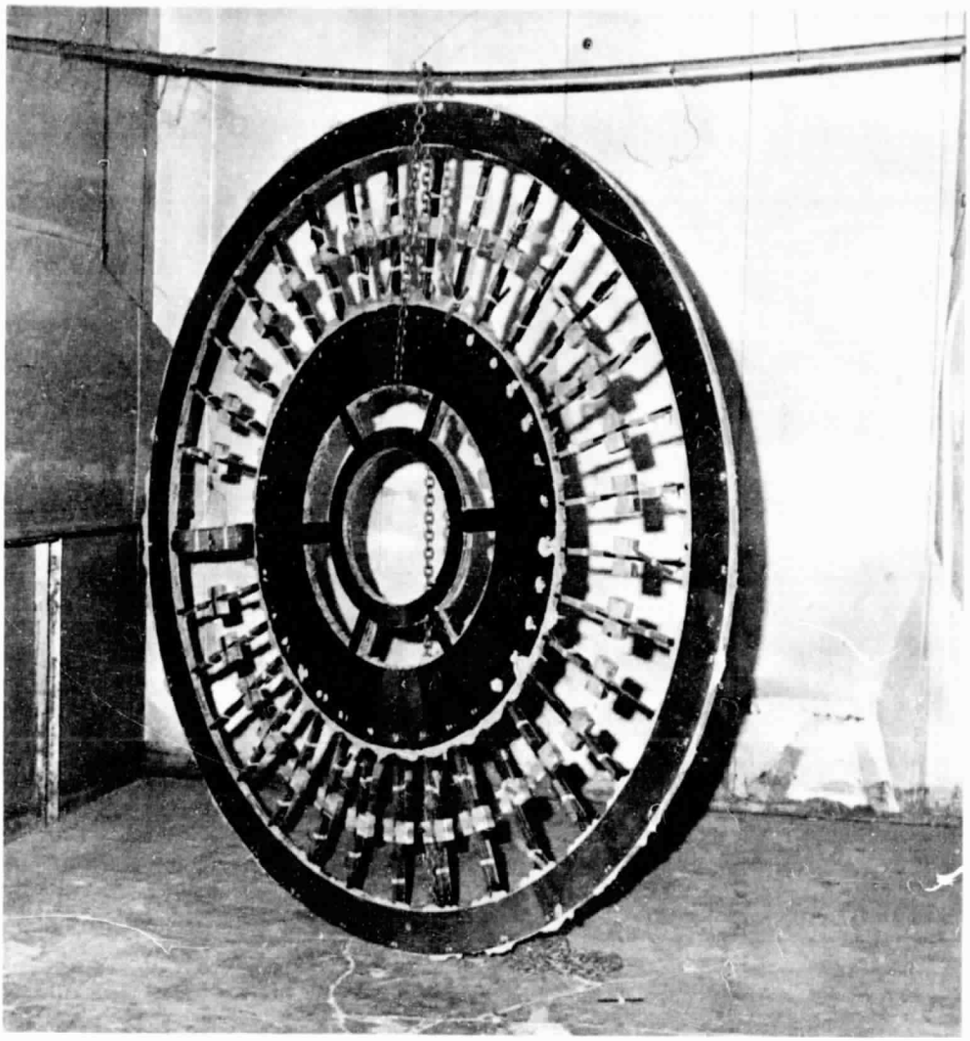

Figure 9. Aft Frame Wheel.

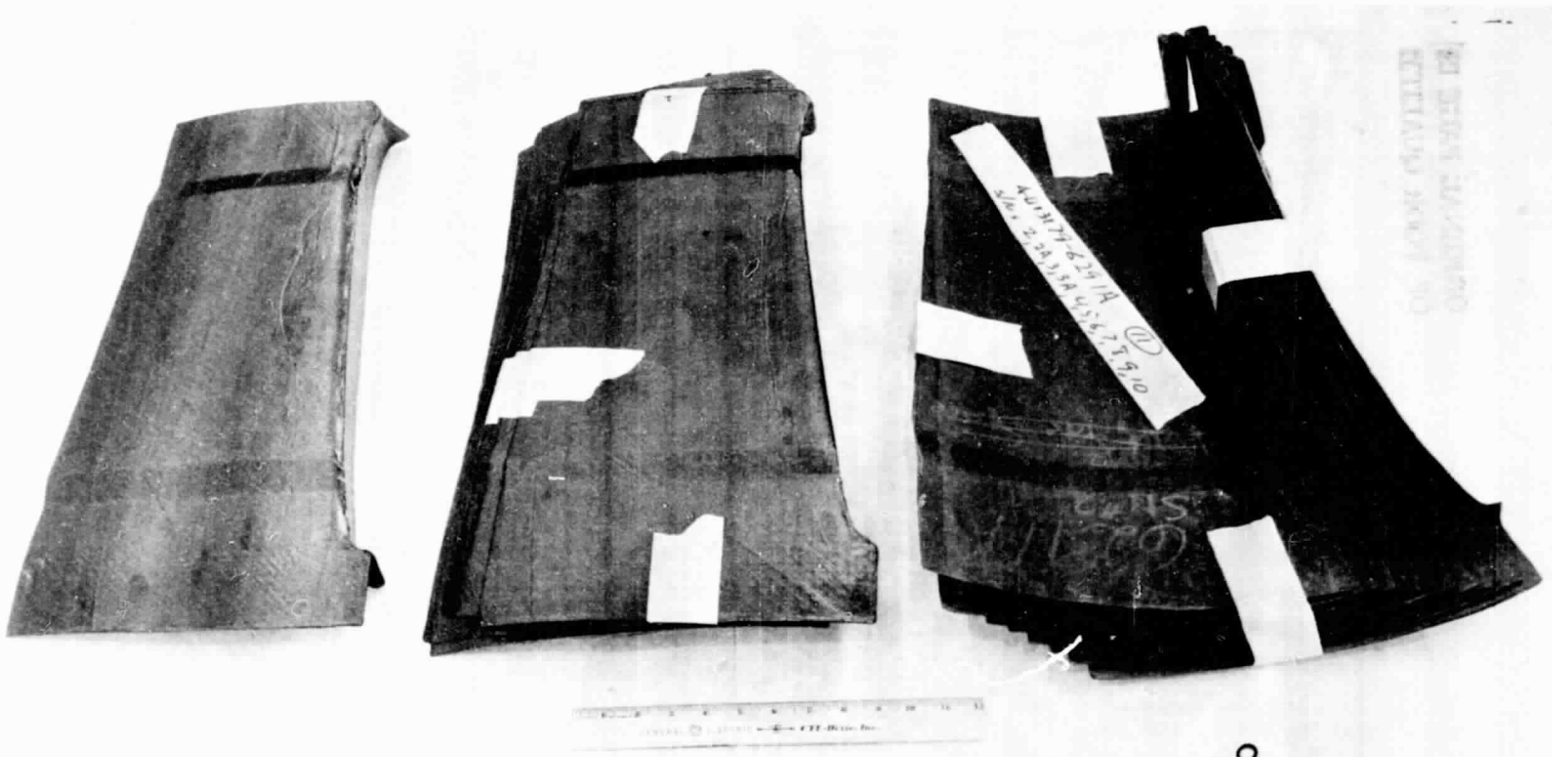

Figure 10. Core Flowpath Panels.

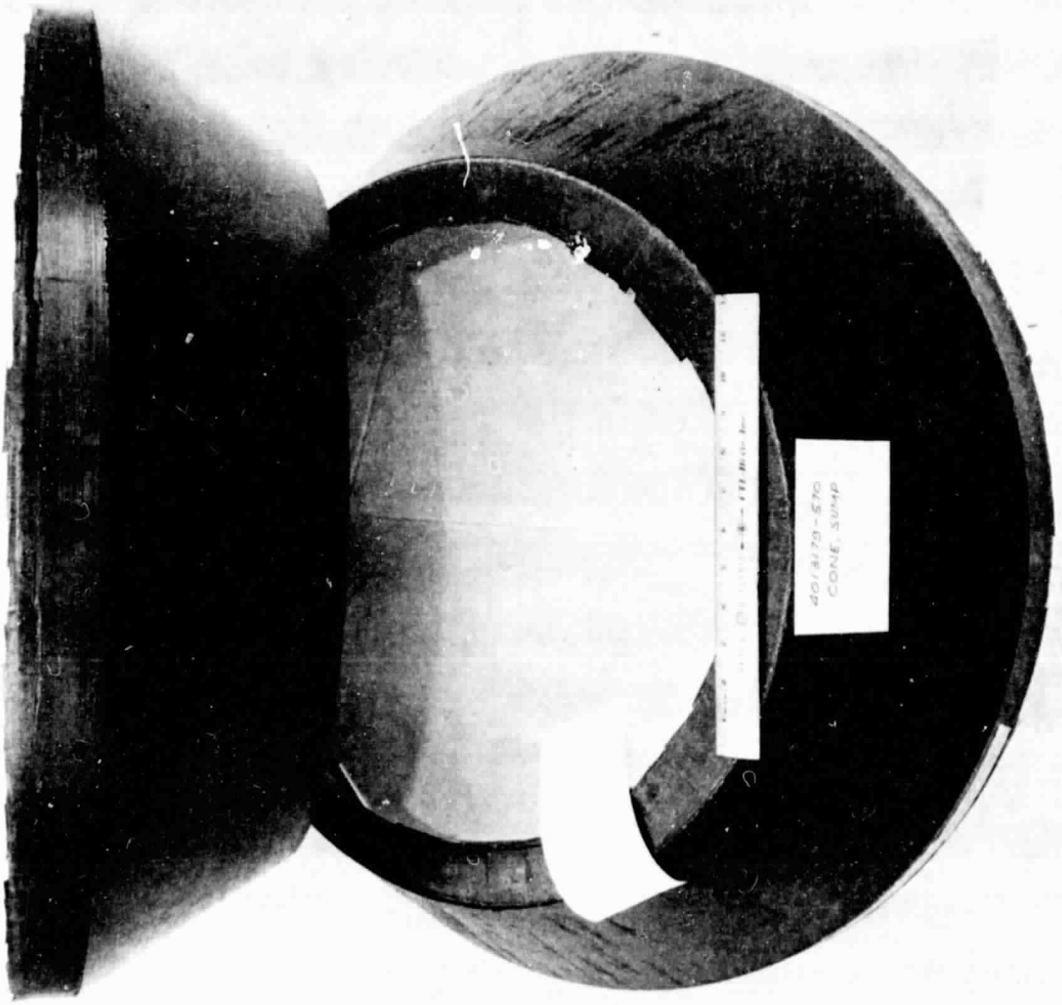

Figure 11. Forward Sump Cone.

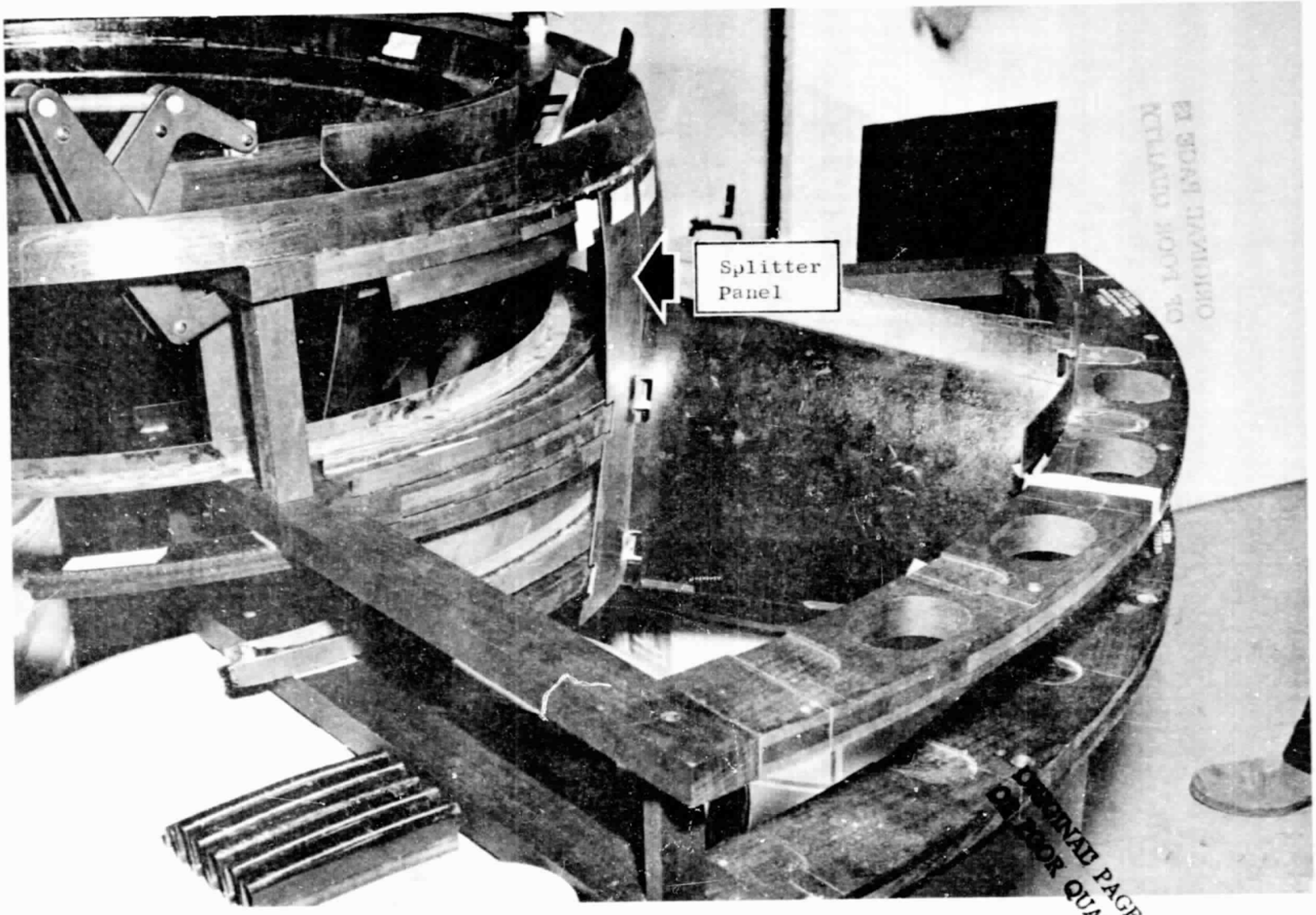

Figure 12. Splitter Flowpath Panel on Fitup Model.

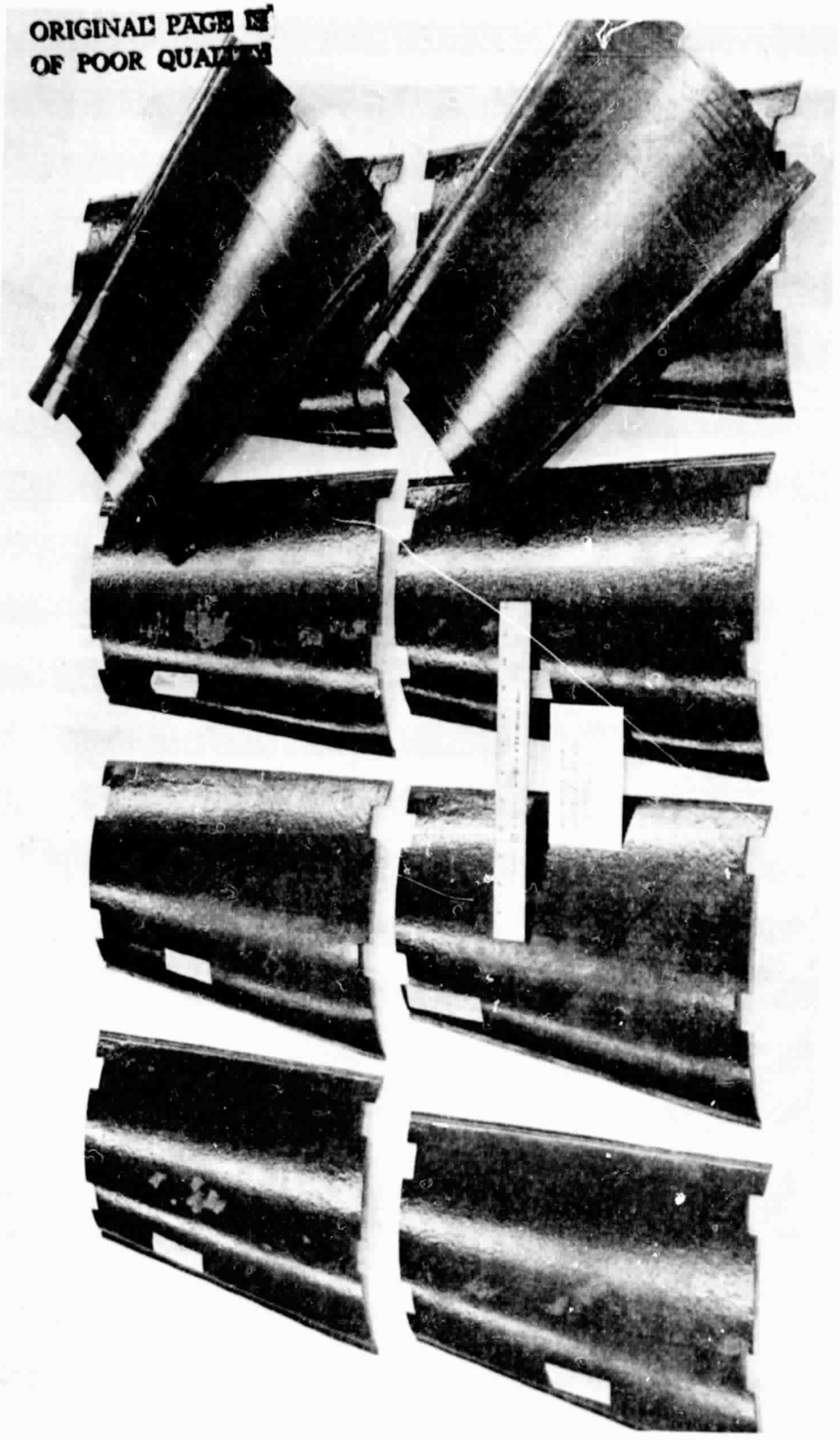

Figure 13. Bypass Vane Panels.

Figure 14. Outer Casing Panels.

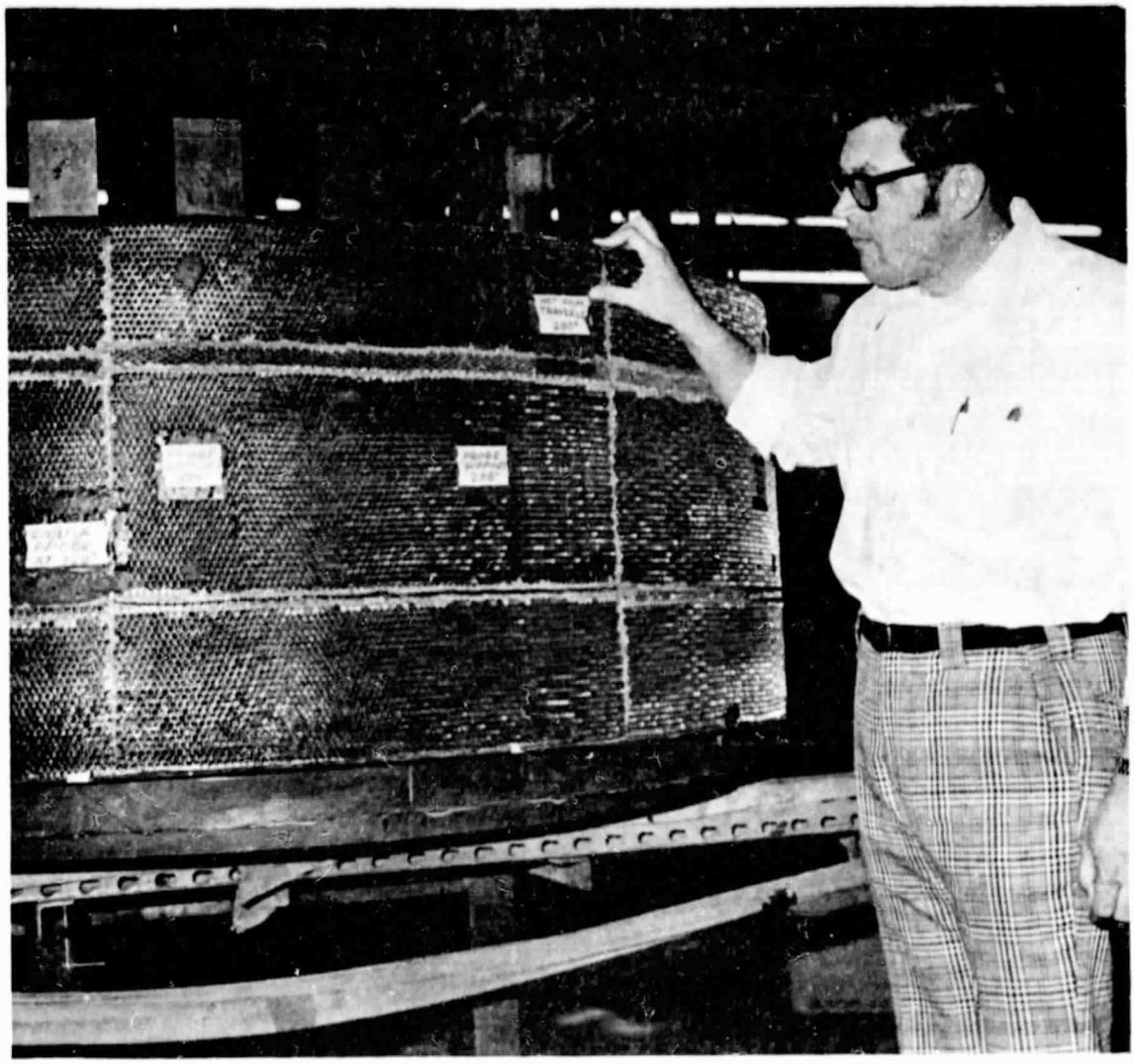

Figure 15. Outer Casing Without Outer Panel.

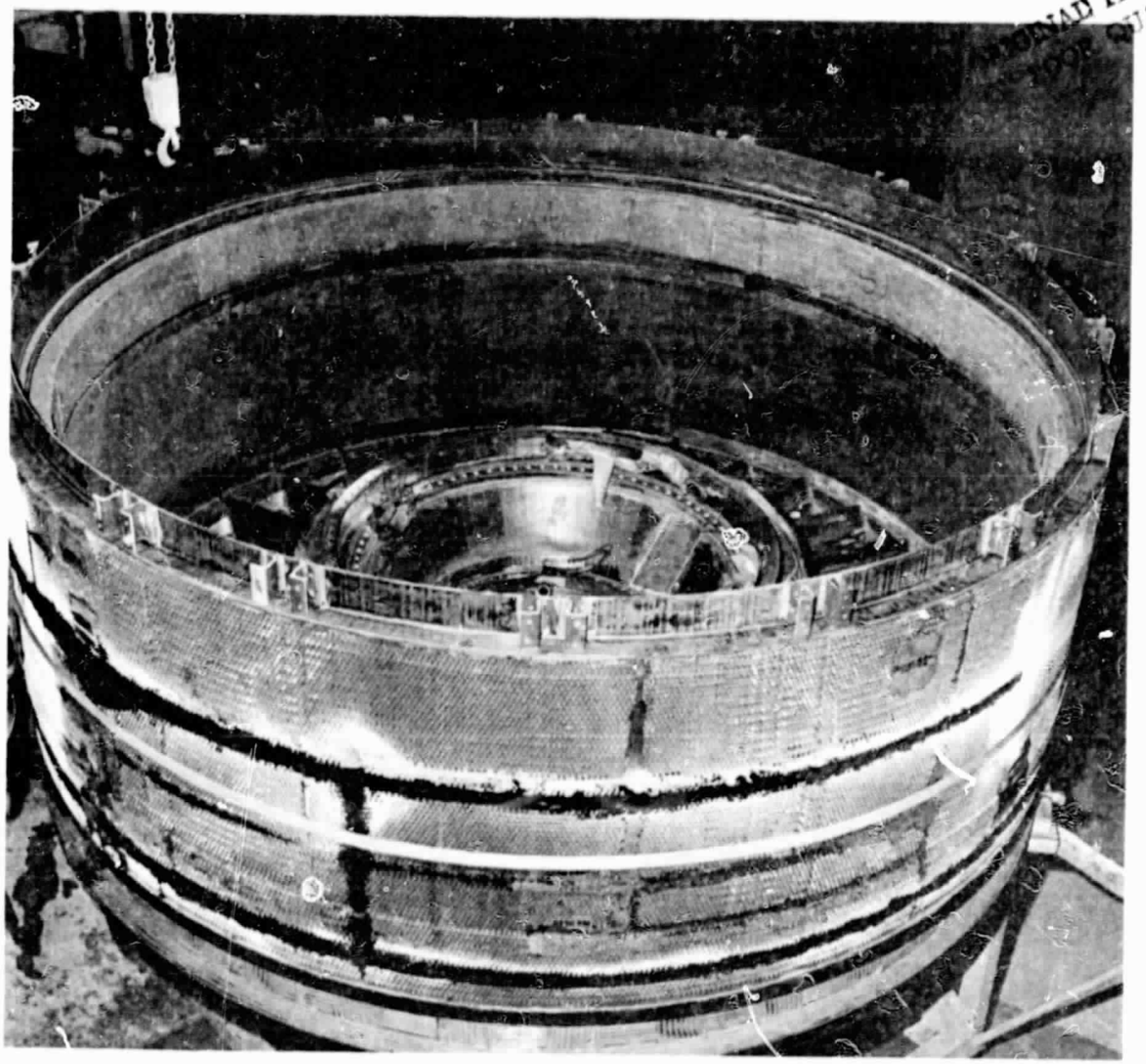

Figure 16. Outer Casing After First Bond Cycle to Frame.

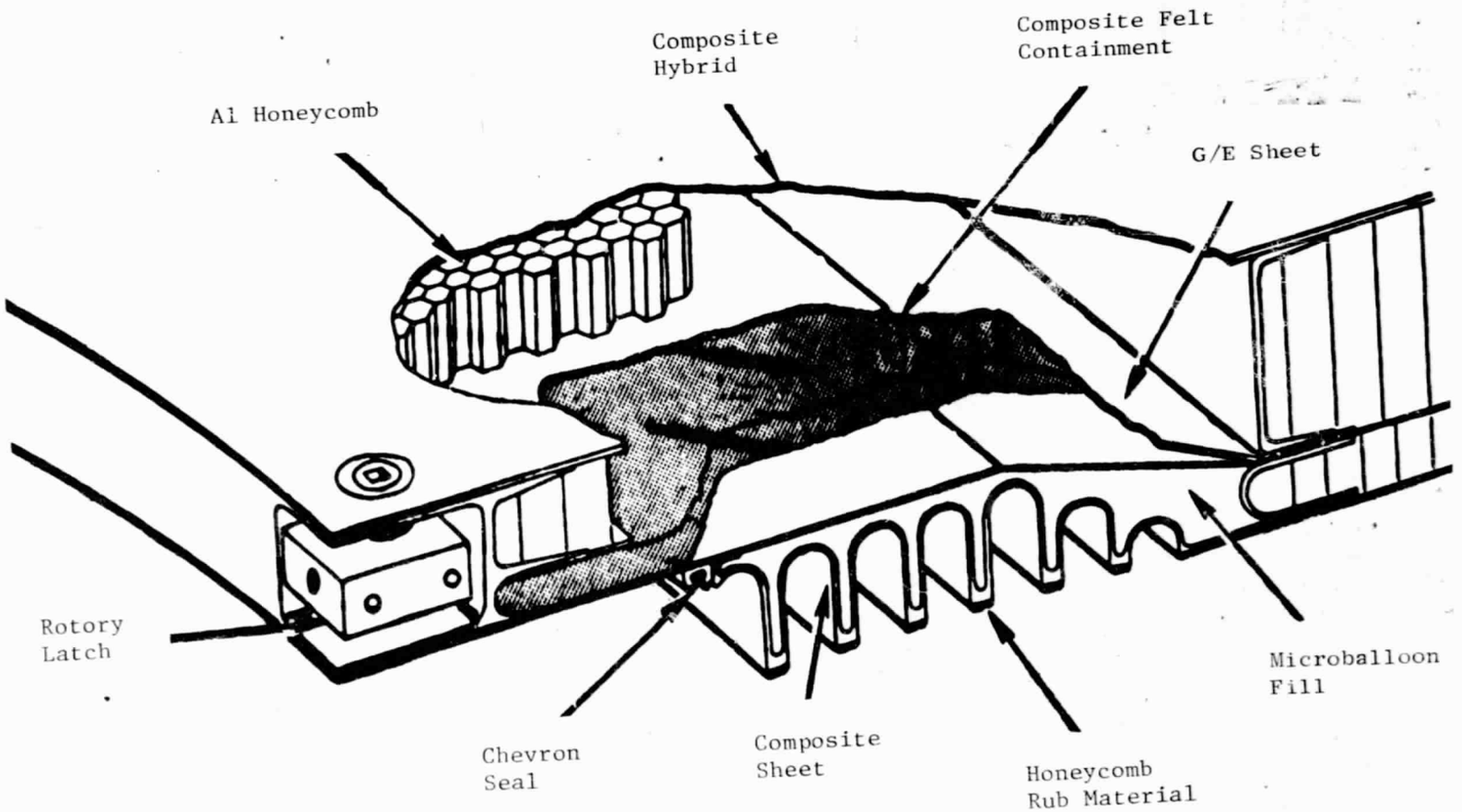

Figure 17. Containment/Tip Treatment.

cloth. These cloth belts are kept in place by closure of the cavity after the cloth is installed.

The frame section of the engine mounting system consists of three engine mount attachment points located on the aft wheel splitter ring. The first attachment point is located at the 0° (12 o'clock) position and consists of a metal uniball which supports both vertical and side loads. At 45° down from either side of the metal uniball are metal brackets that support all thrust loads of the engine. Figure 18 shows the top vertical mount and the right-hand thrust bracket. All of the above-mentioned metal mount hardware are attached to the aft wheel by mechanical fastening.

3.1.2 Structural Description

The forward frame of the QCSEE engine is an all-composite structure that integrates the functions of three conventional structures. As shown in Figures 1, 19, and 20, the frame is a combination of a fan frame, a bypass vane assembly, and a nacelle cowling. Integration of these three structures into one unit offers a high weight payoff by avoiding the duplication of numerous interface joints typical of current designs. Utilization of the integrated frame concept offers an especially large weight payoff in the QCSEE engine because the frame is a large structure which can readily take advantage of the low-density and high-strength weight ratio of composites.

The composite material system utilized as the basic material for the frame is the Type AS graphite fiber in a Hercules 3501 epoxy resin matrix. The selection of this material was due to the rather extensive data base for the material, its good mechanical properties, its ready availability, and its low cost.

For the QCSEE program two composite frames were constructed. The first frame was built for the UTW QCSEE (Figure 21); the second frame was for the OTW QCSEE (Figure 22). The differences between the two frames were small, the main differences occurring in the flowpath contour. Other differences occur in the geometry of the tip treatment, the depth of the outer casing treatment, and the fan Outlet Guide Vane (OGV) attachment. These changes are seen in Figures 23, 24, and 25. Aside from these three changes, all other interfaces and contours are the same for both the UTW and OTW frames; therefore, aside from the outer casing acoustic treatment, a small amount of rework can make both frames interchangeable.

The QCSEE composite frame has a maximum outer diameter of 2.00 m (78.8 in.) and an overall length of 0.95 m (37.5 in.). As seen in Figure 20, the core flowpath is divided by 6 equally spaced symmetrical airfoil struts. Although symmetrical, the top and bottom core struts are thicker than the other four in order to provide shafting accessibility. The bypass of the frame is spanned by 33 vanes which are shaped into 6 different contours arranged in groups of 1, 6, 6, 8, 6, and 6 (see Figure 20). At top vertical is the pylon; next to it (clockwise, aft looking forward) is the vane group with highest camber, Closed 2. Then come (still clockwise) Closed 1, Nominal,

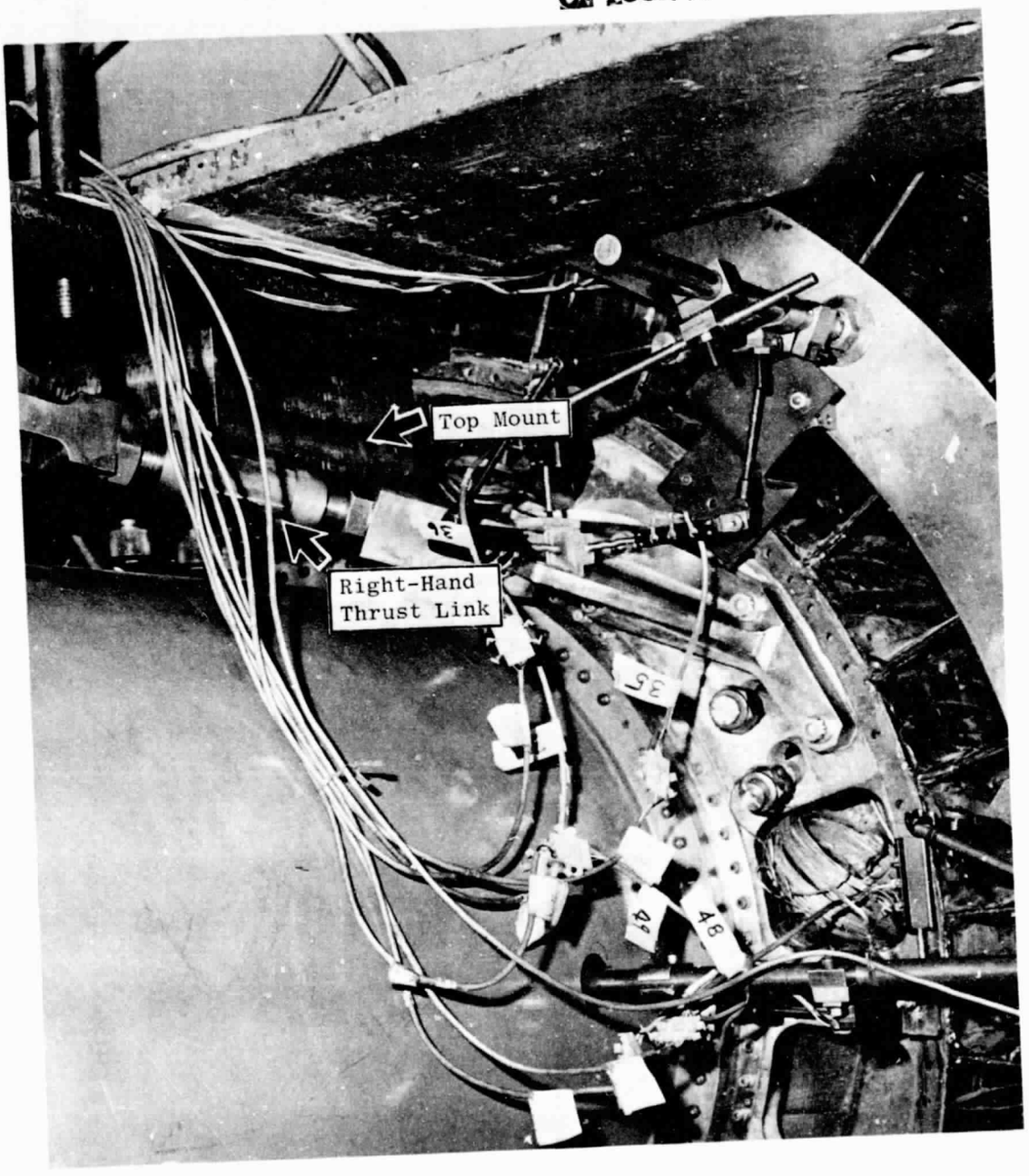

Figure 18. Frame Mounting Configuration.

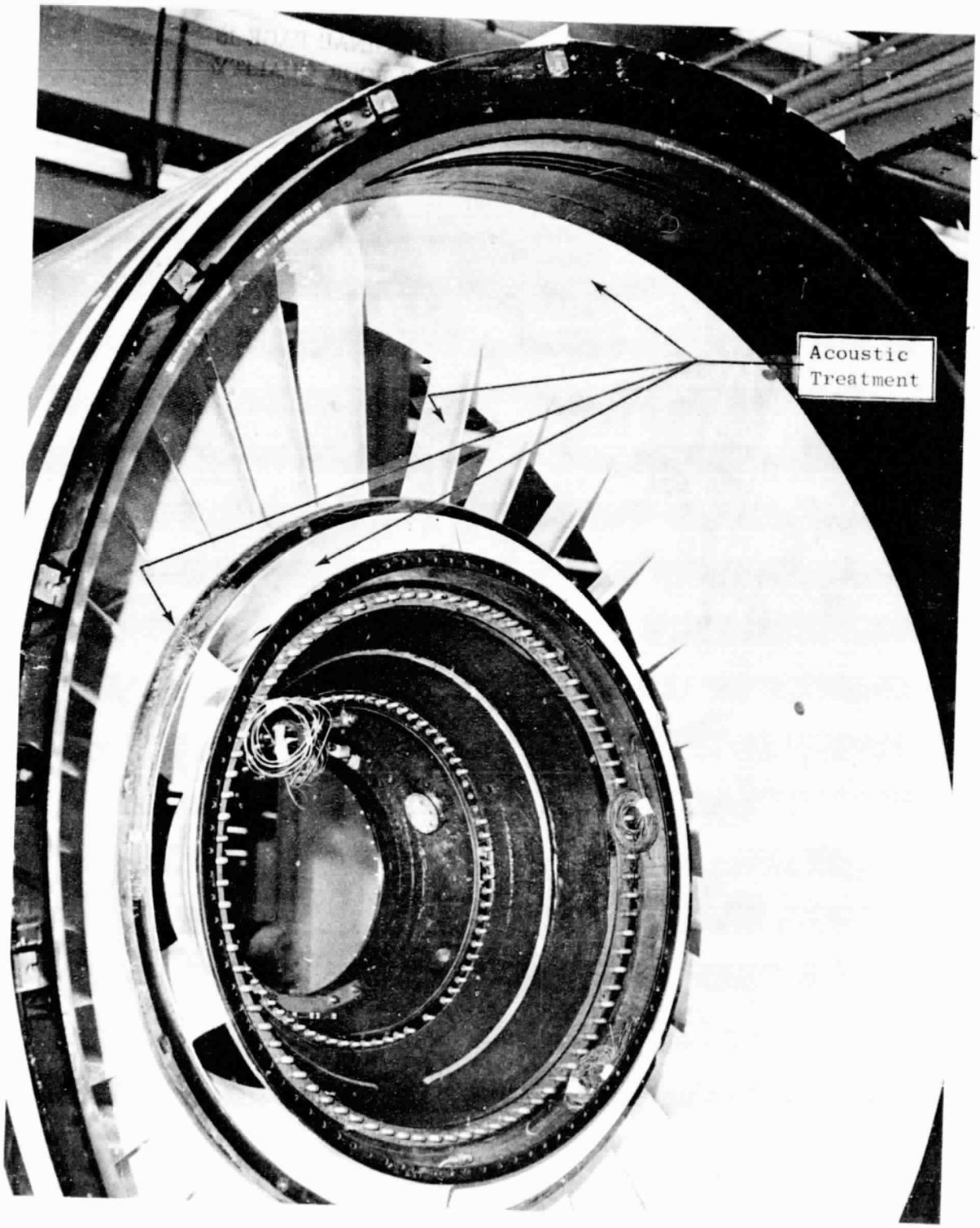

Figure 19. QCSEE OTW Frame, Forward View.

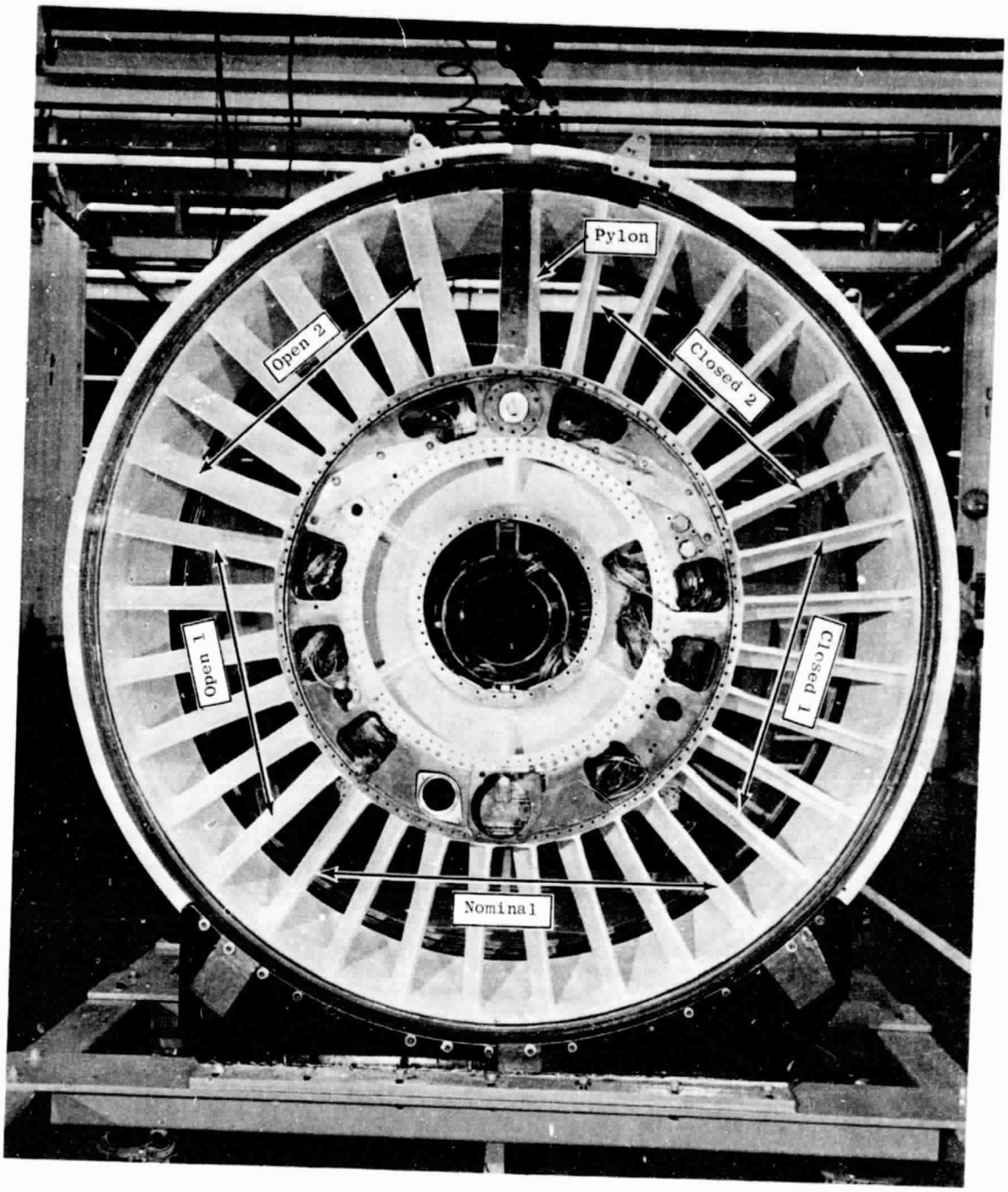

Figure 20. QCSEE UTW Frame, Aft View.

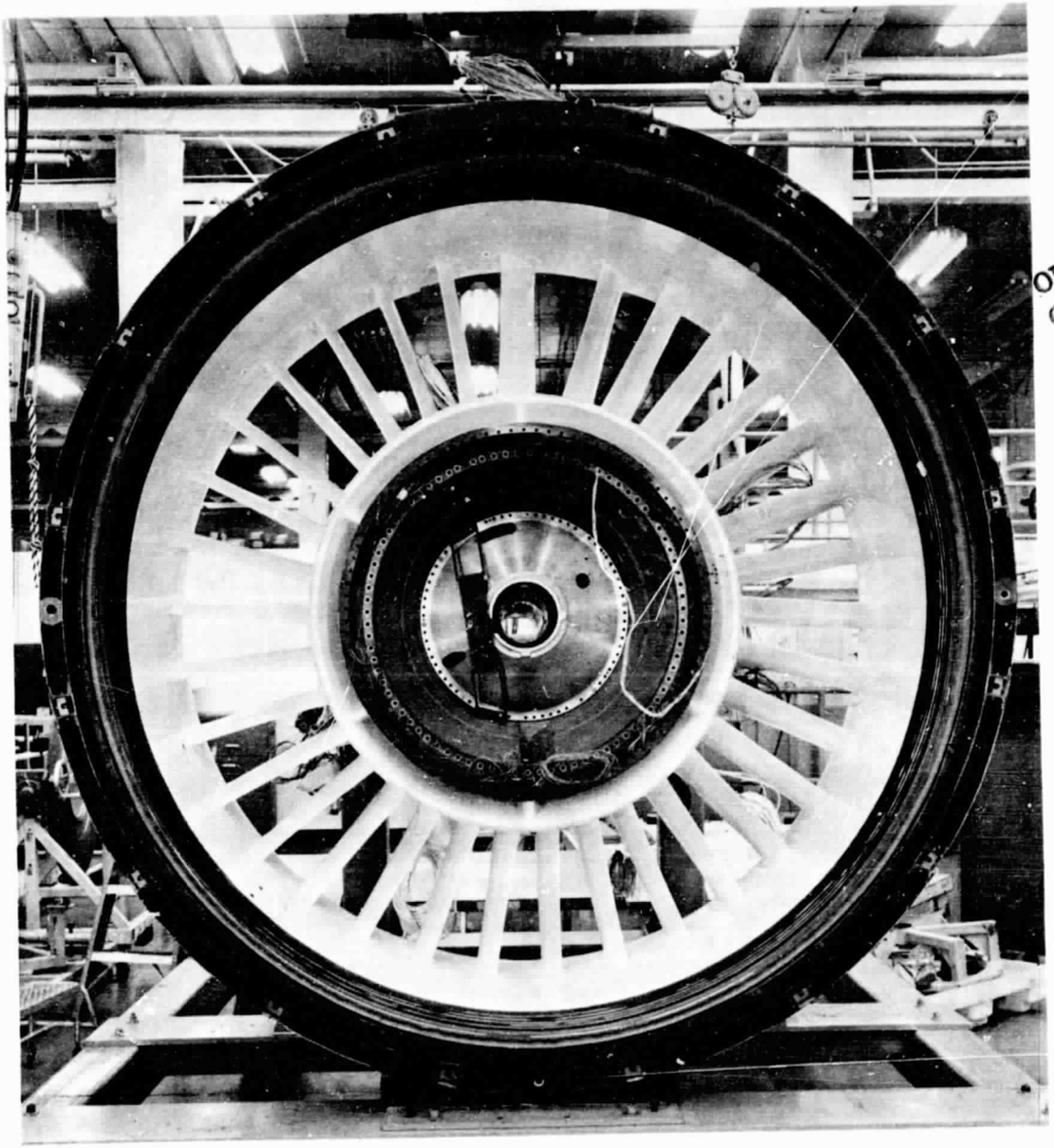

Figure 21. QCSEE UTW Frame, Forward View.

Figure 22. QCSEE OTW Frame, Aft View.

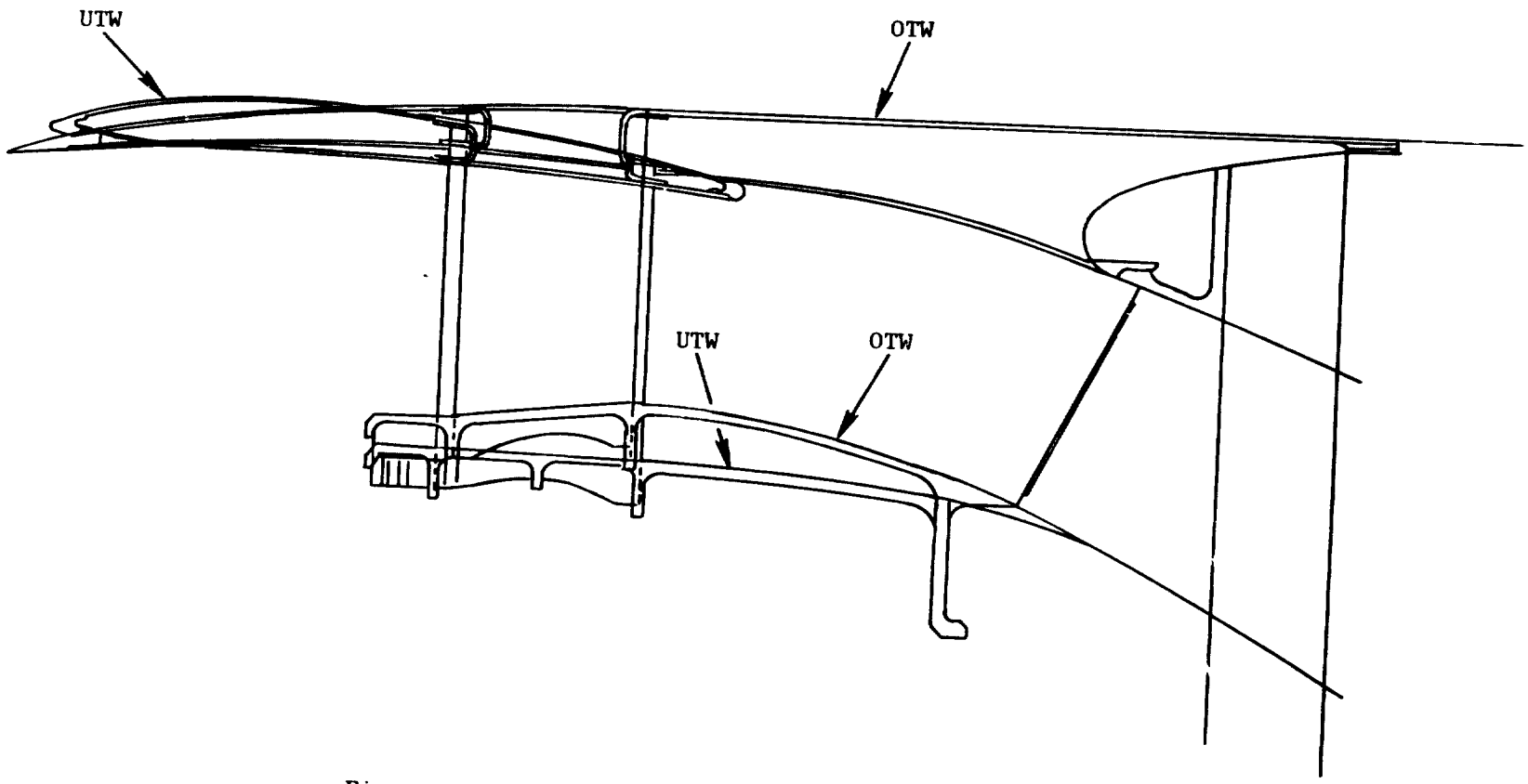

Figure 23. UTW and OTW OGV Comparison.

FOLDOUT FRAME

ORIGINAL PAGE IS
OF POOR QUALITY

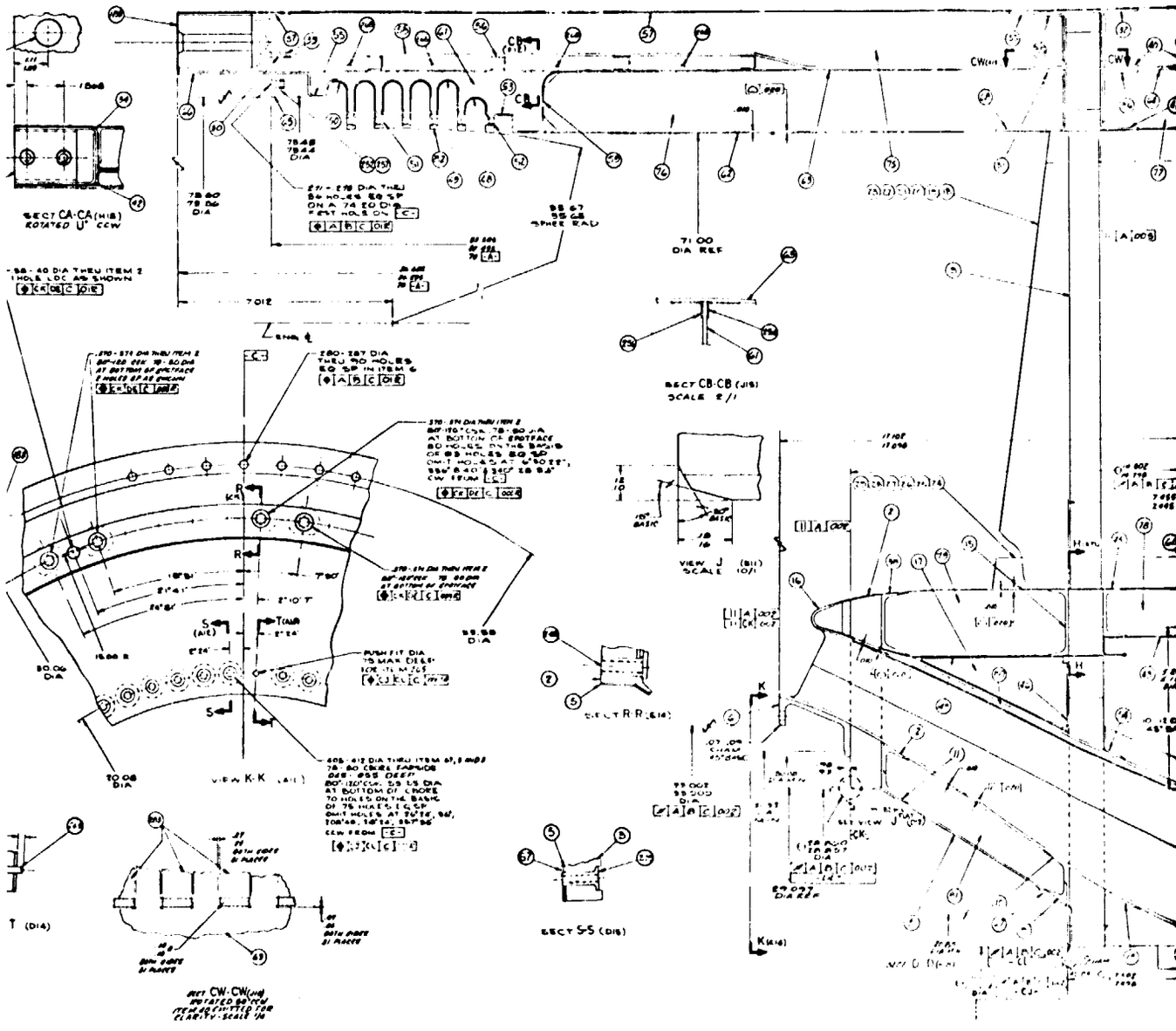

Figure 24. UTW Outer Ca

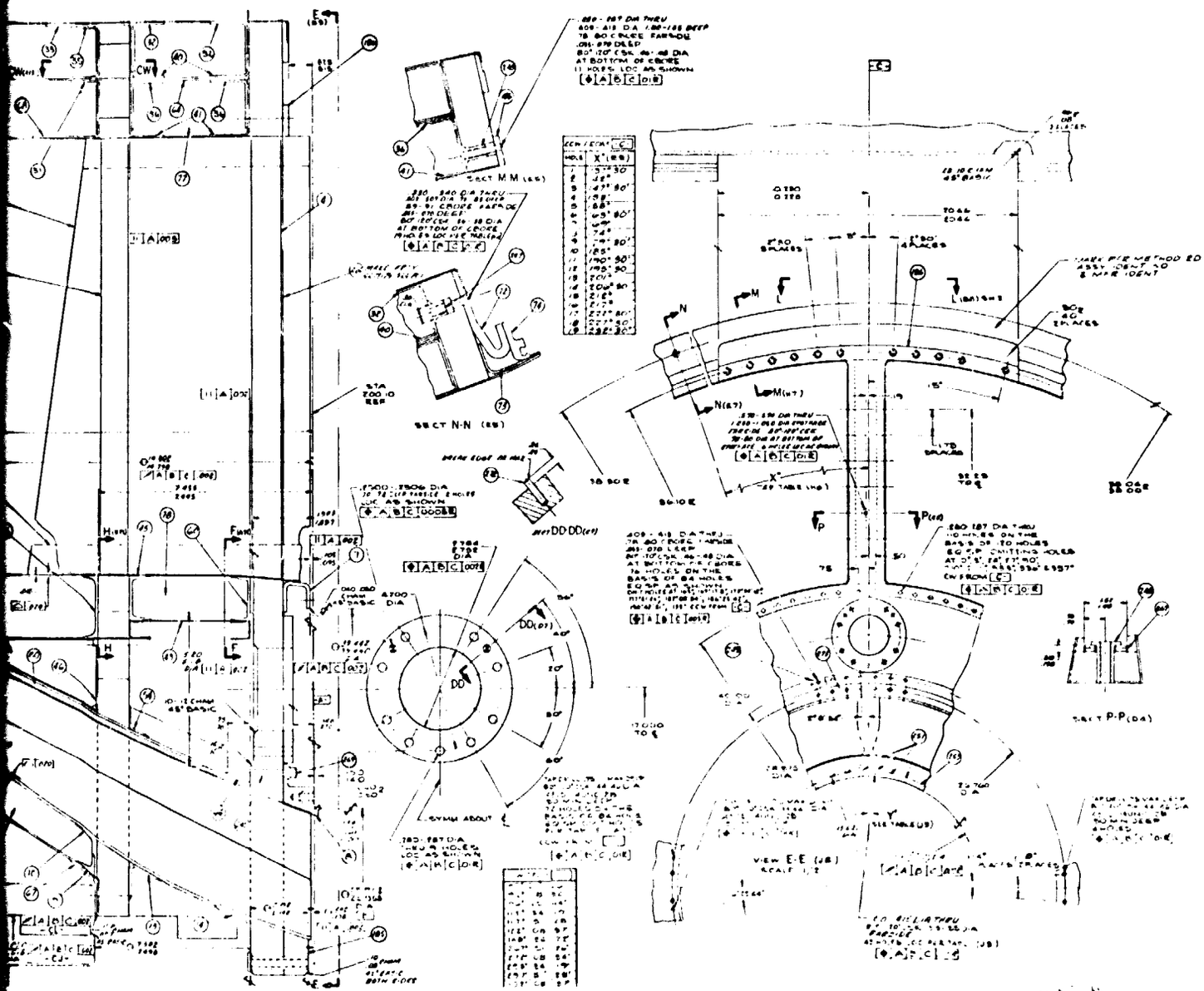

. UTW Outer Casing Configuration.

2. FOLDOUT FRAME

ORIGINAL PAGE IS
OE POOR QUALITY

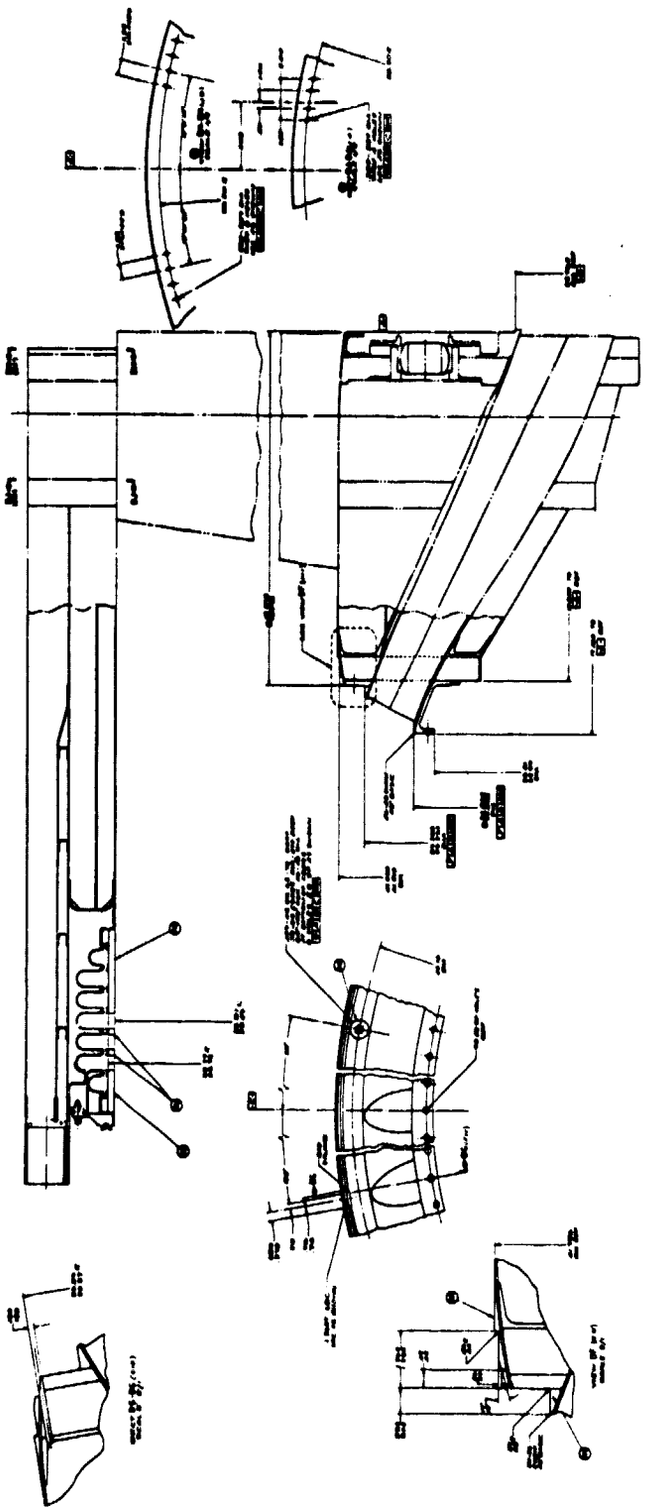

ORIGINAL PAGE IS
OF POOR QUALITY

Figure 25. OTW Outer Casing Configuration.

Open 1, and finally - the vane grouping with the lowest camber - Open 2. The main purpose of the various vane shapes is to equally distribute the bypass airflow around the large pylon at top vertical. Another unique feature on the frame is the extensive acoustic treatment; as seen in Figure 19, the treatment exists not only in the outer casing, but also on the splitter flowpath, the outer core flowpath, and on all bypass vanes (except pylon).

From a mechanical function standpoint, large frame structures are complex. In the QCSEE engine this is especially true since the frame is responsible for even more functions and interfaces due to the integrated concept. Listed below are the primary QCSEE frame mechanical functions.

- Inlet attachment
- Blade containment
- Seal drain eductor attachment
- Digital control attachment
- Hydromechanical control attachments
- Gearbox mounts
- Aft fan duct attachment
- Midspan bearing mount
- Core cowl attachment
- Pylon extension and pylon tubing attachment
- Fan OGV attachment
- Sump bearing cone attachments (4)
- Core engine attachment
- Vertical and side load mount
- Thrust mount
- Oil screen attachment

Figures 20 and 21 show the location of the majority of the above-mentioned attachments. In addition to the above mechanical functions, the frame also provides the following aerodynamic, acoustic, and engine system functions.

- Internal sump system
- Aerodynamic split between the core and bypass
- Extensive instrumentation sensors
- Sump vent passages
- Several oil drain passages
- Fan blade tip treatment
- Perforated panels for acoustic treatment

All of the above mentioned attachments to the frame are accomplished through one or another of the following four methods.

- Bolt and nut
- Stud and nut
- Latch
- Tongue and groove

The inner core doors, pylon extension, mounts, OGV's, UTW bearing cones, and remaining hardware are attached with bolts and nuts. The OTW bearing cones are attached with studs and nuts. The inlet is attached with rotary latches and the aft outer casing is connected to the frame through a tongue-and-groove joint.

3.1.3 Loads

In addition to the normal range and combination of steady-state pressure, thermal, thrust, and torque loads, the engine (including all nacelle and aircraft-furnished components attached to or mounted on the engine and supported through the engine mounts) has been designed to withstand, within the limits specified, the loads defined in Conditions I through VI, which are listed in Table I. Table II summarizes the bearing loads on the frame for the following set of conditions: 1 g down, 1 radian/sec, and one composite fan blade-out. The OTW frame is designed for five composite blade-outs even though the OTW experimental engine has metal blades. This was done to maintain structural commonality with the UTW frame. The loads caused by five composite blade-outs are slightly greater than a two OTW metal blade-out condition. Air loading on the bypass vane, for both the UTW and OTW, is shown in Figure 26.

Table 1. QCSEE Engine Load Conditions.

Limit Loads

For any one of the following load conditions, all stresses shall remain within the material elastic limits.

Condition I: (Flight and Landing) - See load diagram, Table III.

Condition II: (Gust Load) - An equivalent load from a 51.44-m/sec (100-kn) crosswind acting at any angle within a plane 1.5708 radians (90 degrees) to the axis of the engine, zero-to-maximum thrust.

Condition III: (Side Load) - A 4-g side load combined with 1/3 the equivalent load as defined in Condition II, zero-to-maximum thrust.

Ultimate Loads

The engine shall not separate from the aircraft when subjected to Conditions IV, V, and VI and for static loads equivalent to 1.5 times the loads specified as limit loads in metal parts, and 3.0 times the loads specified as limit loads in composite parts.

Condition IV: (Flight-Engine Seizure) - The seizure loads are due to the fan and engine basic gas generator decelerating from maximum-to-zero engine speed in one second.

Condition V: (Crash Load) - The crash load is defined as 10-g forward, 2.25-g side, and 4.5-g down at maximum thrust or up to zero thrust.

Condition VI: (5-blades-out) - The engine shall be capable of withstanding unbalance loads caused by the loss of 5 adjacent fan blades at maximum rpm (composite blades only).

Table II. Frame Radial Bearing Loads.

1 g Down Bearing No.	UTW Radial Load N	UTW Radial Load lb	OTW Radial Load N	OTW Radial Load lb
1	3,425	(770)	4,822	(1,084)
2	1,099	(247)	1,882	(423)
3	364	(82)	364	(82)
4	823	(185)	823	(185)
1 radian/sec Bearing No.				
1	27,397	(6,159)	69,232	(15,564)
2	27,397	(6,149)	69,232	(15,564)
3	1,699	(382)	1,739	(391)
4	9,559	(2,149)	9,906	(2,227)
1 Fan Blade-Out Bearing No.				
1	235,627	(52,971)	226,458	(50,910)
2	82,852	(18,626)	58,454	(13,141)
3	7,491	(1,684)	7,451	(1,675)
4	28,989	(6,517)	19,359	(4,352)

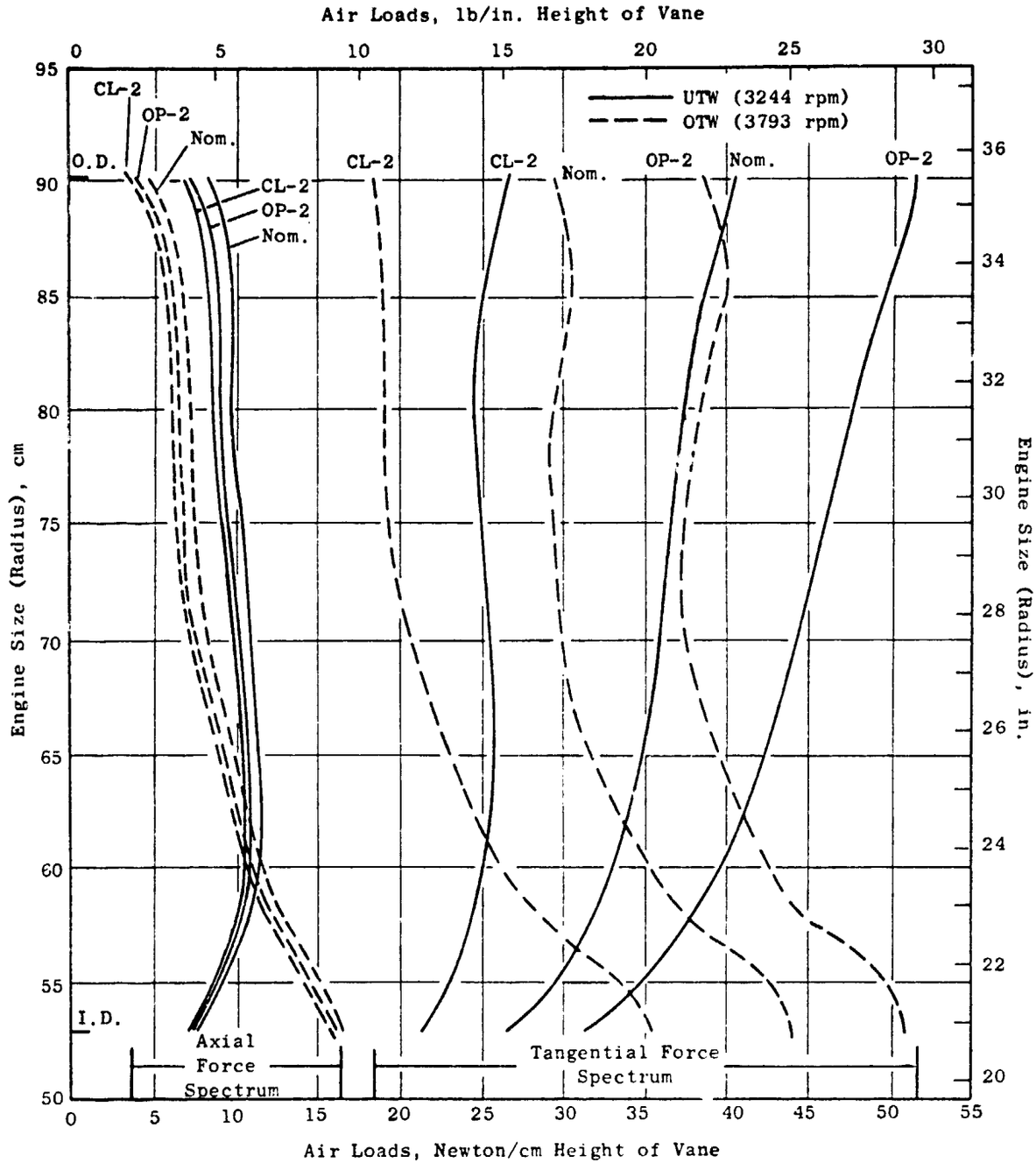

Figure 26. Bypass Vane Air Loading.

3.2 ANALYSIS

The first step of the analysis procedure was to establish an iterative design analysis cycle for the composite frame. Figure 27 illustrates the design analysis cycle. As seen in the figure, this cycle reflects the design optimization parameters embodied in a typical composite static structure. Refinement of each structural component is accomplished by cycling each component through the above-mentioned process until its ply orientation, geometry, and cost have been optimized for the particular loading environment.

The optimization procedure was initiated by assuming practical orientations and thicknesses for all of the component parts of the basic design. Next, a finite-element model of the QCSEE composite frame was constructed and is shown in Figures 3, 28, and 29. Due to the simple design philosophy of the frame, wheels (curved beams and straight beams), and skins (plates), the computer model quite accurately represents the actual frame structure. This similarity is shown in Figure 28.

In order to accurately model the load-extraction structures that are attached to the frame, both the engine mounting system and the core engine were also modeled. Figure 29 depicts the similarity of the computer model and the actual frame/core engine structure.

The iterative optimization procedure shown in Figure 27 is based on the philosophy that if (at some region) the margin of safety at ultimate load is high, weight savings can be realized by diminishing the amount of load-carrying material in that region. Conversely, if the margin of safety is low, material can be added locally to maintain structural integrity. The designer utilizing reinforced composite materials has the additional option of tailoring the fiber orientations to suit his strength and stiffness requirements.

This particular iterative procedure was specifically established for designs using composite materials. For isotropic materials, the method degenerates into a finite-element analysis since elastic and strength properties of the materials are available from handbooks. These properties can be directly coordinated with the finite-element program.

The basic frame analysis was performed using General Electric's computer program system (entitled "MASS") for the analysis of 3-D redundant structures. The MASS system provides the means of analyzing almost any structure. The variety of available elements gives the program a great deal of versatility; with care, most structures can be modeled accurately or closely approximated. The basic elements available for modeling are the two-ended curved or straight beam; the four-sided curved or flat trapezoidal plate; the six-sided tetrahedron; rigid connectors, springs, and tubes. A modification of the plate subprogram permits the analysis of sandwich panel structures with orthotropic faces.

The types of analyses available in MASS are: mechanical loading, thermal gradients, maneuver loads, forced response, and determination of critical

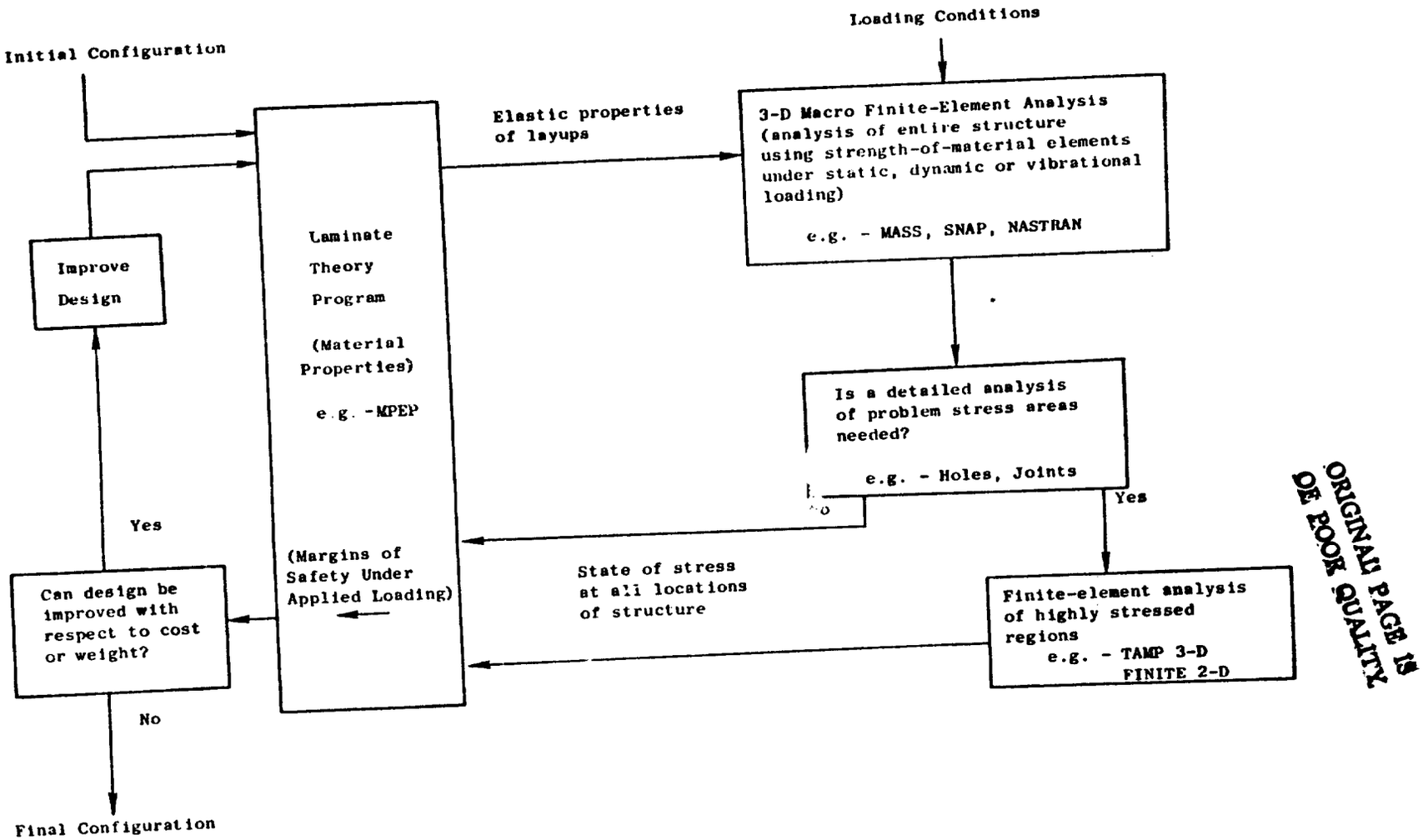

Figure 27. Design Optimization Cycle.

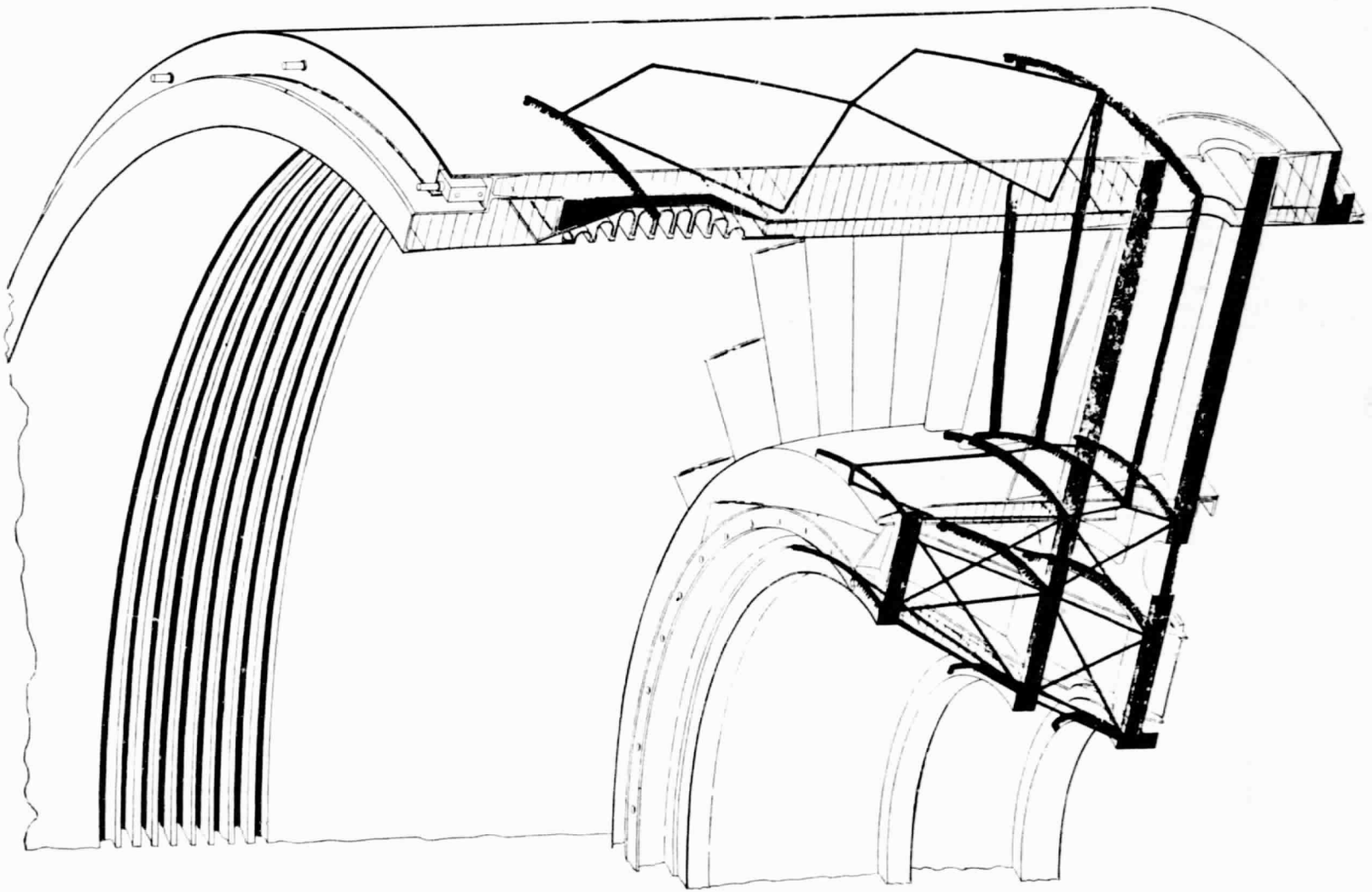

Figure 28. Analytical Model Representation.

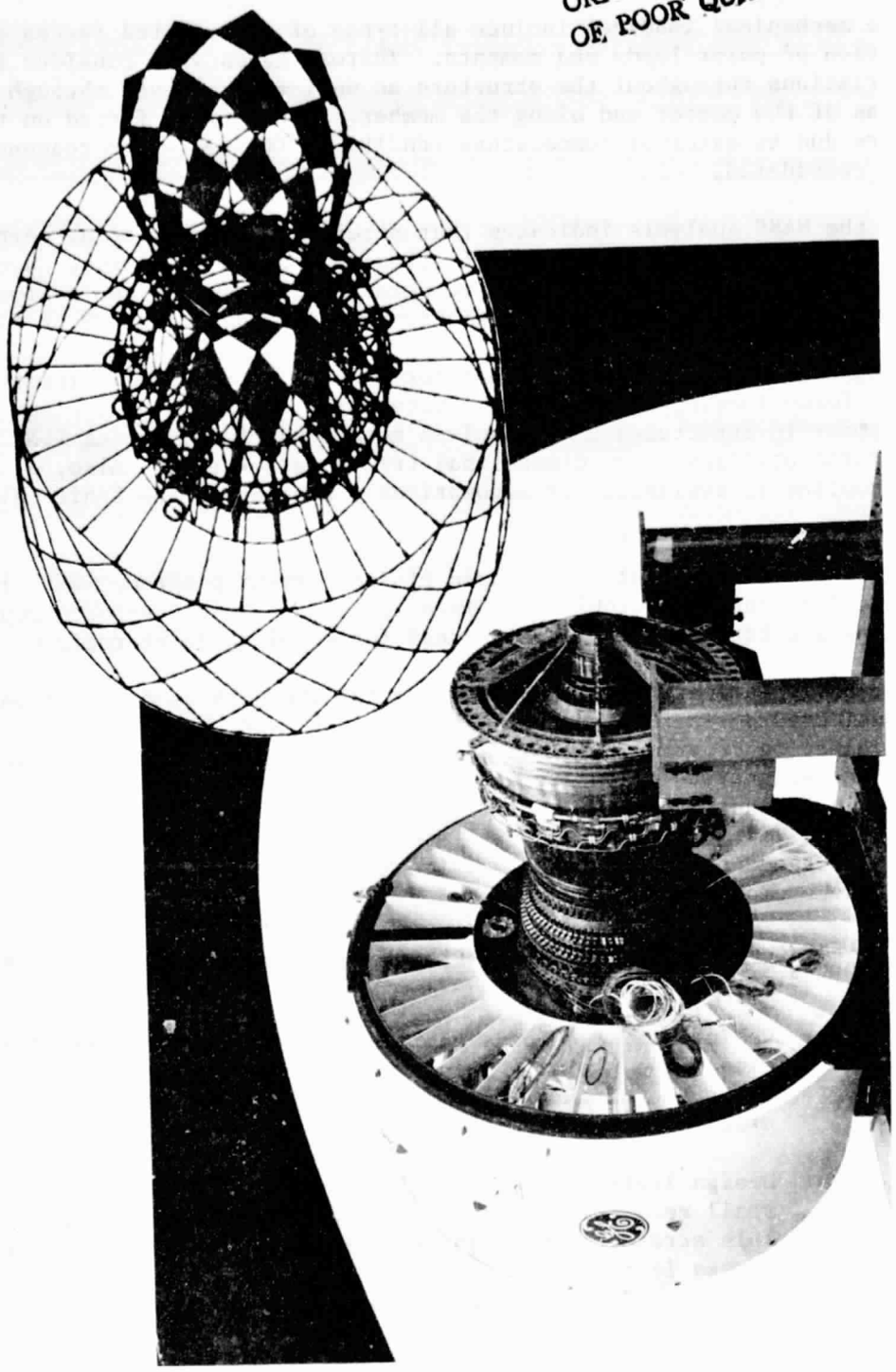

Figure 29. Analytical Model Comparison.

frequencies. An instability check is optional. Resulting output is in the form of loads, stresses and deflections.

The mechanical loadings include all types of distributed forces and application of point loads and moments. Thermal cases will consider temperature variations throughout the structure as well as gradients through the thickness of the member and along the member. Deflections forced on the structure due to external temperature conditions (or for other reasons) can also be considered.

If the MASS analysis indicates that stress problems exist at certain locations within the structure (or if stress concentrations exist that were not accounted for in modeling), a more detailed analysis of the region in question can be performed with the finite-element programs, TAMP or FINITE.

Both FINITE and TAMP can account for thermal, mechanical, vibrational, and body force loading or orthotropic materials. Plane stress, plane strain, or axisymmetric structures can be solved more economically using FINITE since this program utilizes a two-dimensional triangular element. Also, a computerized routine is available for automatically generating the finite-element grid work.

The three-dimensional orthotropic finite-element program, TAMP, is available for nonplanar problems. Since spring and friction-force boundary conditions are permissible, TAMP is ideal for modeling joint regions.

The basic laminate elastic properties for the various orientations that were considered during the program were obtained using MPEP (Material Property Evaluation Program). If the properties of a single ply are known, MPEP allows the designer to calculate the elastic properties of any chosen layup using basic laminate theory.

With respect to the use of composite materials, the following design criteria were employed for the proposed program.

1. For composite laminate structures subjected to significant biaxial loading, the material allowableness criteria shall be as follows:

   (a) Design ultimate loads shall result in a stress that does not exceed the ultimate allowable stress for the laminate used, where the ultimate allowable stress is the maximum laminate stress attainable without rupture of any lamina.

   (b) Design limit loads, as defined by the vehicle specifications, shall result in a stress that does not exceed the limit allowable stress for the laminate used, where limit allowable stress is that stress below which no lamina suffers intolerable degradation of stiffness, permanent deformation, or matrix failure in any lamina.

2. For laminate structures which are only subjected to primarly uniaxial loads (σ_L > 10 times σ_T), the criteria shall be as follows:

   (a) Design ultimate loads shall result in a stress that does not exceed the ultimate allowable stress for the laminate used, where ultimate allowable stress is the maximum laminate stress attainable. Matrix failure in off-axis lamina is permitted.

   (b) Same as (b) in Item 1 above.

3. All adhesive-bonded joints shall be designed using long-term temperature data.

4. No purely adhesive-bonded joint shall be subjected to large peel stresses.

5. Mechanically fastened joints shall, insofar as practical, be designed to fail in bearing rather than shear-out or net tension, so that catastrophic failure is prevented.

6. All composite material properties used for design shall be "B" basis properties as defined in MIL-HDBK-5B.

7. All composite areas that might be subjected to an adverse environment (e.g., hot oil, sand, etc.) shall be either isolated from that environment or protected by external coatings.

The next step of the analysis procedure was to establish the worst loading environments for the frame. The frame structure, in conjunction with the engine mounts, must withstand the maneuver loads as imposed by the conditions depicted in Table III. The frame must withstand these loads and maintain structural integrity without permanent deformation. In addition to the normal range of maneuver loads and combinations of steady-state pressure, thrust, and torque loads, the engine must withstand the loads defined in Conditions I through VI listed in Table I. Table II summarizes the bearing loads on the frame for 1 g down, 1 radian/sec, and one composite fan blade-out conditions collectively for UTW/OTW engines. Air Loading on the UTW/OTW frame bypass vanes is shown in Figure 26.

This structure must also be capable of transmitting mount loads equivalent to three times the worst possible combination of maneuver loads without experiencing collapsing - even though the members may acquire permanent deformation. All ultimate load conditions occur at a room-temperature environment. Investigation of the total mission requirements yielded the following two critical loading cases.

The first case is Condition II (gust loading). Design conditions require the frame to withstand three times the loads of a 51.44-m/sec (100-kn) crosswind acting at any angle within a plane perpendicular to the axis of the engine at zero-to-maximum thrust. This condition sizes the outer nacelle shell and bypass vanes.

Table III. Maneuver Load Map.

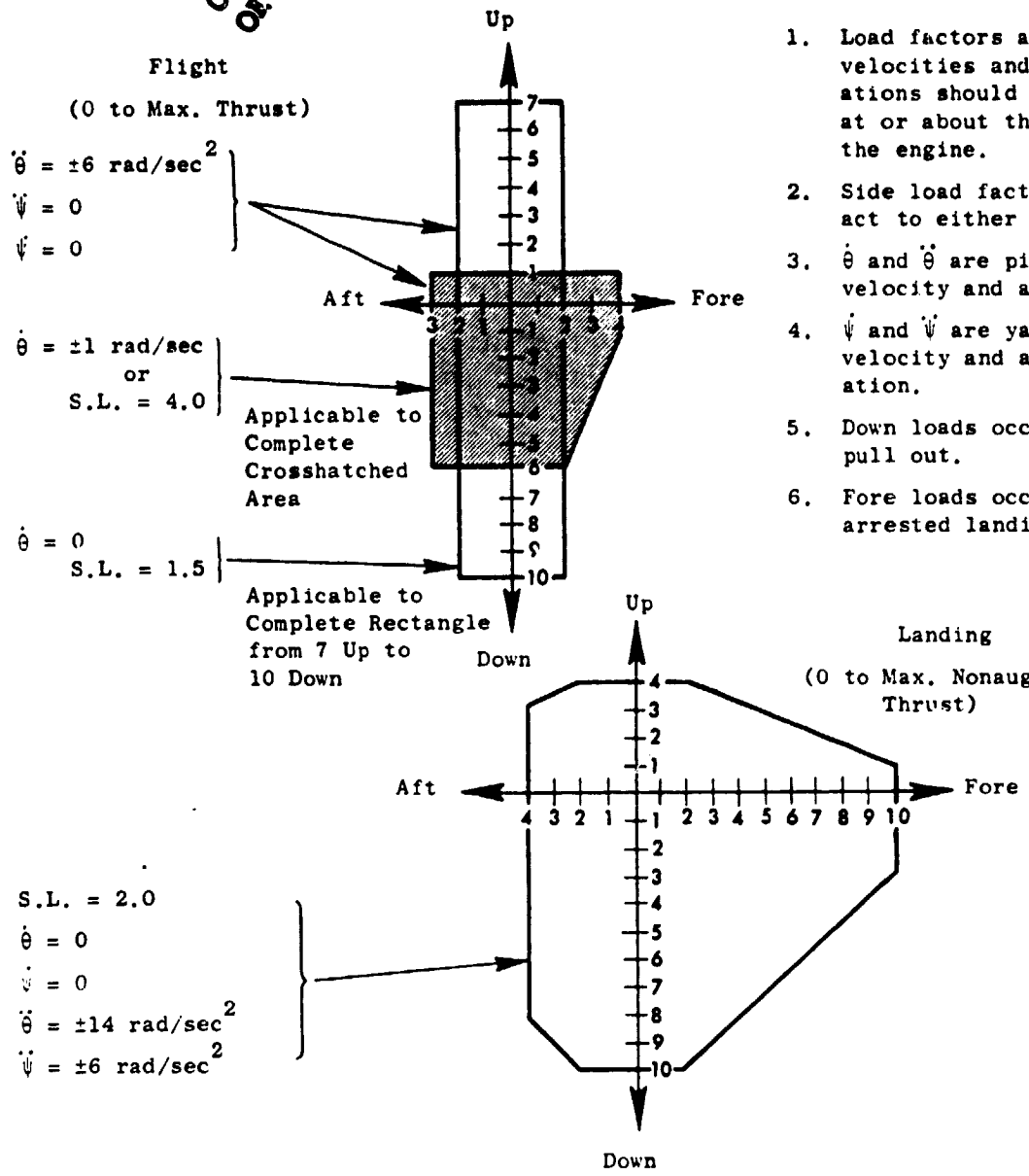

1. Load factors and angular velocities and accelerations should be taken at or about the C.G. of the engine.
2. Side load factors (S.L.) act to either side.
3. $\dot{\theta}$ and $\ddot{\theta}$ are pitching velocity and acceleration.
4. $\dot{\psi}$ and $\ddot{\psi}$ are yawing velocity and acceleration.
5. Down loads occur during pull out.
6. Fore loads occur during arrested landing.

The second case is Condition VI (blade-out). The five-blade-out condition requires the frame to withstand the unbalanced load resulting from a five-composite-blade-out condition on the fan rotor, a condition that would cause a dynamic 1/rev radial load on the No. 1 bearing support. This condition sizes the core struts, hub, and splitter.

Internal loads, stresses, and deflections in the frame incurred by the above-mentioned load conditions were analyzed using the MASS computer program and the finite-element model of the frame illustrated in Figure 28. Maximum frame component stresses and bond shear stresses for Conditions II and VI are shown in Tables IV and V. Geometry and material properties of the various critical composite frame components selected for the QCSEE frame design are shown in Table VI.

3.3 FABRICATION

The fabrication of the QCSEE composite frame was basically a cyclic manufacturing process of bonding together (in many steps) numerous premolded graphite/epoxy parts and machining certain interfaces in preparation for the next bonding cycle. The following discussion will deal mostly with the bonding events of major components and subassemblies and will not discuss the fabrication of the many separate components.

The first step of the fabrication process was to divide the frame into two major structures in order to efficiently complete the fabrication cycle. The frame was divided at a station on the outer casing just forward of the leading edge of the bypass vanes. This division separated the frame into an outer casing and a frame and, therefore, allowed both structures to be fabricated to near completion before bonding together for final fabrication and machining.

The outer casing was fabricated by positioning the perforated, graphite/epoxy, inner flowpath cylinder shown in Figure 30 onto the bonding fixture shown in Figure 31. The next step consisted of bonding the tip-treatment channels together and to the inner flowpath cylinder. The inner layer of honeycomb and the associated forward and aft flanges were the next to be bonded; this stage is shown in Figure 32. The next step was to bond the midskin to the flanges and honeycomb (Figure 33). After the midskin bonding, four separate belts of unimpregnated Kevlar cloth were wrapped around the cylinder to form a section of the containment structure. This wrapping is shown in Figure 34. The next three major steps consisted of (1) bonding the shell over the Kevlar belts, (2) bonding the fore and aft flanges to the midskin, and (3) bonding the second layer of honeycomb to the structure. After this cycle the structure was ready for bonding to the frame structure; Figure 35 depicts this stage of completion.

The other structure to be fabricated was the frame structure, but before this could be fabricated three basic components were needed: the forward, mid, and aft "wheels". The forward wheel was a one-piece, graphite/epoxy laminate part that was molded in a matched metal die and then machined to

Table IV. Critical Frame Component Stresses.

Load Case No.(1)	Location	Stress		Allowable Stress		Temperature	
		N/m^2	(psi)	N/m^2	(psi)	K	° F
2	Bypass Vane	402.90×10^6	(58,430)	565.4×10^6	(82,000)	338.7	(150)
6	Fwd Core Ring	687.06×10^6	(99,650)	841.2×10^5	(122,000)	450.0	(350)
6	Fwd Core Spoke	690.40×10^6	(100,136)	930.8×10^6	(135,000)	450.0	(350)

(1) Case 2 - 154.33-m/sec (300-kn) crosswind gust load + maximum maneuver
Case 6 - 5 composite blade-out

Table V. Critical Bond Shear Stresses.

Load Case No.(1)	Location	Design Stress(2)		Allowable Stress	
		N/m^2	(psi)	N/m^2	(psi)
2	Vane/Splitter	6.05×10^6	(878)	10.34×10^6	(1500)
6	Panel/Outer Radius Fwd "Wheel"	7.48×10^6	(1085)	10.34×10^6	(1500)
6	Panel/Spoke Fwd "Wheel"	8.06×10^6	(1169)	10.34×10^6	(1500)
6	Panel/Inner Radius Fwd "Wheel"	4.81×10^6	(698)	10.34×10^6	(1500)

(1) Case 2 - 154.33-m/sec (300-kn) crosswind gust load + maximum maneuver
Case 6 - 5 composite blade-out + maximum maneuver

(2) Design Stress - 3 times actual for flight and actual for emergency conditions

Table VI. Geometry and Material Properties of Composite Frame Components.

Item	Forward "Wheel"	Middle "Wheel"	Aft "Wheel"	Nacelle Panel	Bypass Vane Panel	Bypass Vane Spoke	Core Outer Panel	Core Inner Panel
% Plies	(50,20,30)	(30,20,50)	(30,20,50)	(29,57,14)	(40,40,20)	(80,20,0)	(25,50,25)	(40,40,20)
Thickness cm (in.)	2.54(1.00)	2.87(1.13)	2.87(1.13)	0.089(0.035)	0.127(0.05)	2.54(1.00)	0.203(0.080)	0.254(0.10)
0° Datum	Radial	Radial	Radial	Axial	Radial	Radial	Axial	Axial
Properties Temperature K (° F)	405 (270)	405 (270)	405 (270)	294 (70)	294 (70)	294 (70)	405 (270)	405 (270)
E_L^t (10^6) N/cm^2 (psi)	6.7 (9.7)	4.5 (6.5)	4.5 (6.5)	5.0 (7.2)	6.0 (8.7)	9.7 (14.0)	4.5 (6.5)	5.7 (8.2)
E_T^t (10^6) N/cm^2 (psi)	4.5 (6.5)	6.7 (9.7)	6.7 (9.7)	3.5 (5.1)	4.1 (6.0)	1.6 (2.3)	4.5 (6.5)	3.9 (5.7)
G_{LT} (10^6) N/cm^2 (psi)	0.8 (1.2)	0.8 (1.2)	0.8 (1.2)	1.9 (2.8)	1.5 (2.2)	1.0 (1.4)	1.7 (2.4)	1.4 (2.0)
F_L^{tu} (10^3) N/cm^2 (psi)	59 (86)	42 (61)	42 (61)	48 (70)	57 (83)	93 (135)	41 (59)	54 (78)
F_T^{tu} (10^3) N/cm^2 (psi)	42 (61)	59 (86)	59 (86)	36 (52)	39 (56)	10 (15)	41 (59)	36 (52)
F_L^{cu} (10^3) N/cm^2 (psi)	48 (70)	33 (48)	33 (48)	49 (71)	57 (84)	92 (134)	34 (50)	44 (64)
F_T^{cu} (10^3) N/cm^2 (psi)	33 (48)	48 (70)	48 (70)	36 (52)	41 (59)	19 (27)	34 (50)	30 (43)
F_{LT}^{su} (10^3) N/cm^2 (psi)	10 (14)	10 (14)	10 (14)	22 (32)	17 (25)	11 (16)	17 (25)	15 (22)
α_L (10^{-6}) cm/cm/K (in./in./°F)	2.3 (1.3)	4.3 (2.4)	4.3 (2.4)	2.2 (1.2)	2.2 (1.2)	0.2 (0.1)	3.2 (1.8)	2.2 (1.2)
α_T (10^{-6}) cm/cm/K (in./in./°F)	4.3 (2.4)	2.3 (1.3)	2.3 (1.3)	4.5 (2.5)	4.6 (2.6)	16.4 (9.3)	3.2 (1.8)	4.6 (2.6)

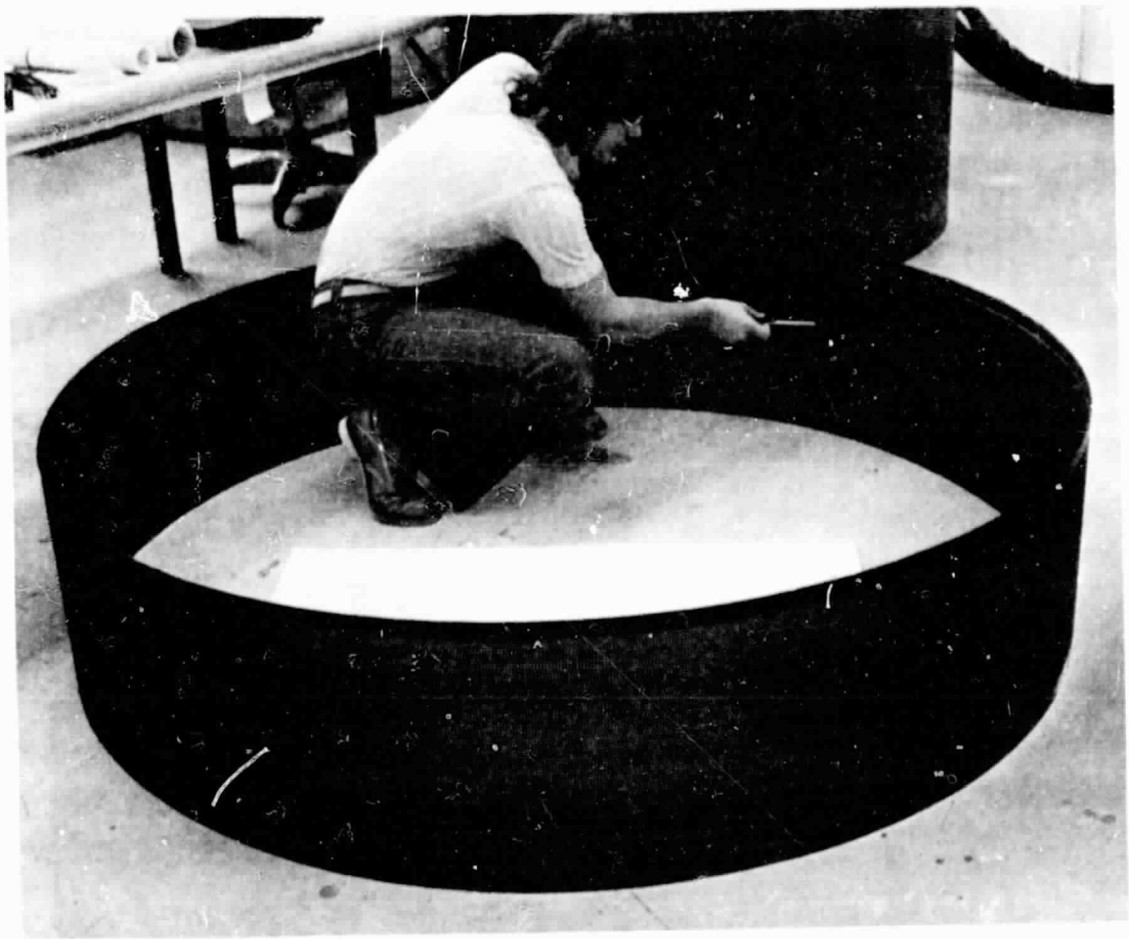

Figure 30. Outer Casing Acoustic Panel.

Figure 31. Outer Casing Assembly Fixture.

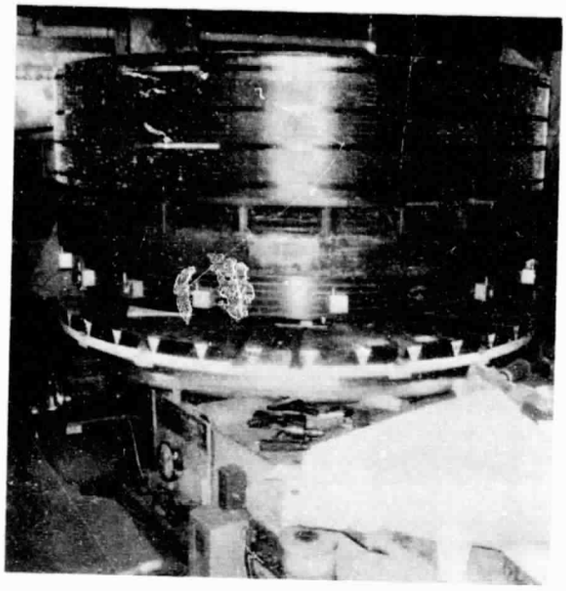

Figure 32. Tip Treatment and Inner Honeycomb Bonding.

Figure 33. Outer Casing Midpanel Bonding.

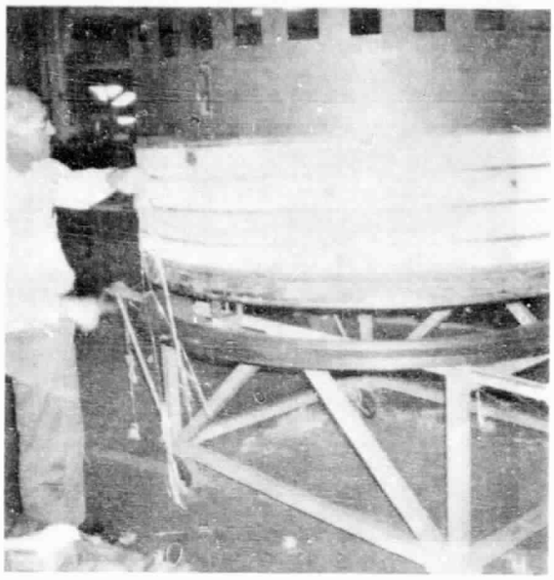

Figure 34. Kevlar Belts in Outer Casing Containment.

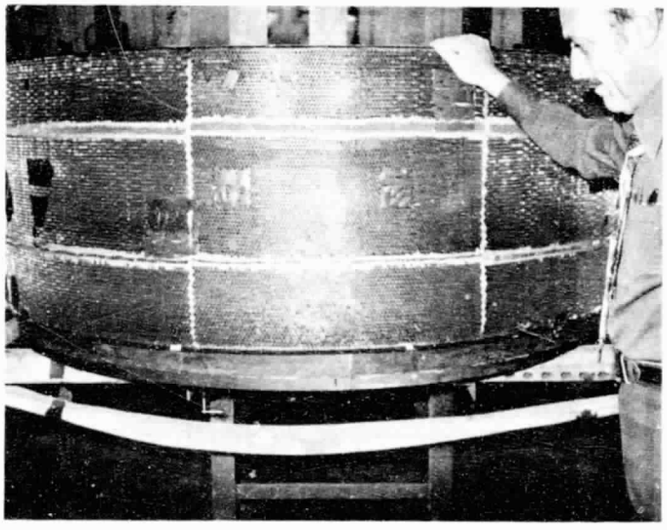

Figure 35. Outer Bypass Duct.

final dimensions. Figures 36 and 37 depict this wheel before and during machining. The mid and aft wheels were fabricated by bonding together many premolded, graphite/epoxy pieces to form the final wheel structure. The mid and aft wheels are identical in construction because they are comprised of 6 inner core wheels, 165 bypass spokes, and 6 outer casing rings. The layup sequence of the wheel is shown in Figure 38; as shown in the figure, the first layer of the wheel consists of 1 inner core wheel, 33 bypass spokes, and 1 outer ring. After the first layer was positioned on the fixture, a layer of film adhesive was placed over all of the components. This process was then repeated four more times to complete one wheel structure. Figure 39 depicts a completed wheel structure before bonding. Figures 40 and 41 illustrate the assembly of the core rings, bypass spokes, and casing rings. After being bonded the wheel was final-machined at all flowpath interfaces and rough-machined at all other interfaces. Figure 42 depicts an aft wheel after bonding. After all three wheels were complete the frame assembly was initiated by first bonding the midwheel to the aft wheel using modules of composite "U" flanges around honeycomb. Figure 43 shows the midwheel bonded to the aft wheel. Figure 44 depicts the next operation, the bonding of the forward wheel to the mid/aft wheel assembly through the use of six "U" flange/honeycomb modules. The next step consisted of bonding the core skins to the forward, mid, and aft wheels (Figure 45), and then bonding the splitter flowpath panels and concave bypass panels to the mid and aft wheels. Figure 46 illustrates the bypass panels being bonded to the spokes of the wheels. After this bond cycle the sump of the frame was fabricated by bonding the sump cone (Figure 11) and honeycomb to the hub of the frame between the forward and midwheels. "L" flanges were also bonded into the hub where the mid and aft hub rings meet the inner core flowpath panel. This bond cycle marked the end of the fabrication of two separate structures.

The next step in the fabrication was to bond the semifinished prebonded outer cylinder to the frame to form one structure. This bond sequence is shown in Figures 47, 48, and 49. After bonding the two structures together the outermost layer of honeycomb was bonded to the outer casing. Next, the honeycomb of the outer casing was ground concentric to the center of the core frame, and in areas of undersized honeycomb a layer of fiberglass/epoxy was added to establish the proper radial dimension. After honeycomb grinding, the outer skins shown in Figure 14 were bonded to the frame in the manner shown in Figure 50. The next step was to bond all convex bypass skins to the bypass spokes, and after these were bonded the bypass collars were fitted and then bonded to the vanes. The bonding of the collars to the vanes marked the end of bonding major structural graphite/epoxy components to the frame.

The next phase of the fabrication process was the drilling of all insert holes. After bonding the inserts, the frame was machined to all final dimensions. The last phase of the frame fabrication consisted of providing closeouts and sealing around all tubes that penetrate the sump of the frame. In many cases the tubes were sealed by conventional O-rings captured in a graphite/epoxy block, but in some cases the tubes were "soft-sealed" by placing a few wraps of fiberglass/epoxy around the tube/frame junction. A detailed view of this sealing approach is shown in Figure 51.

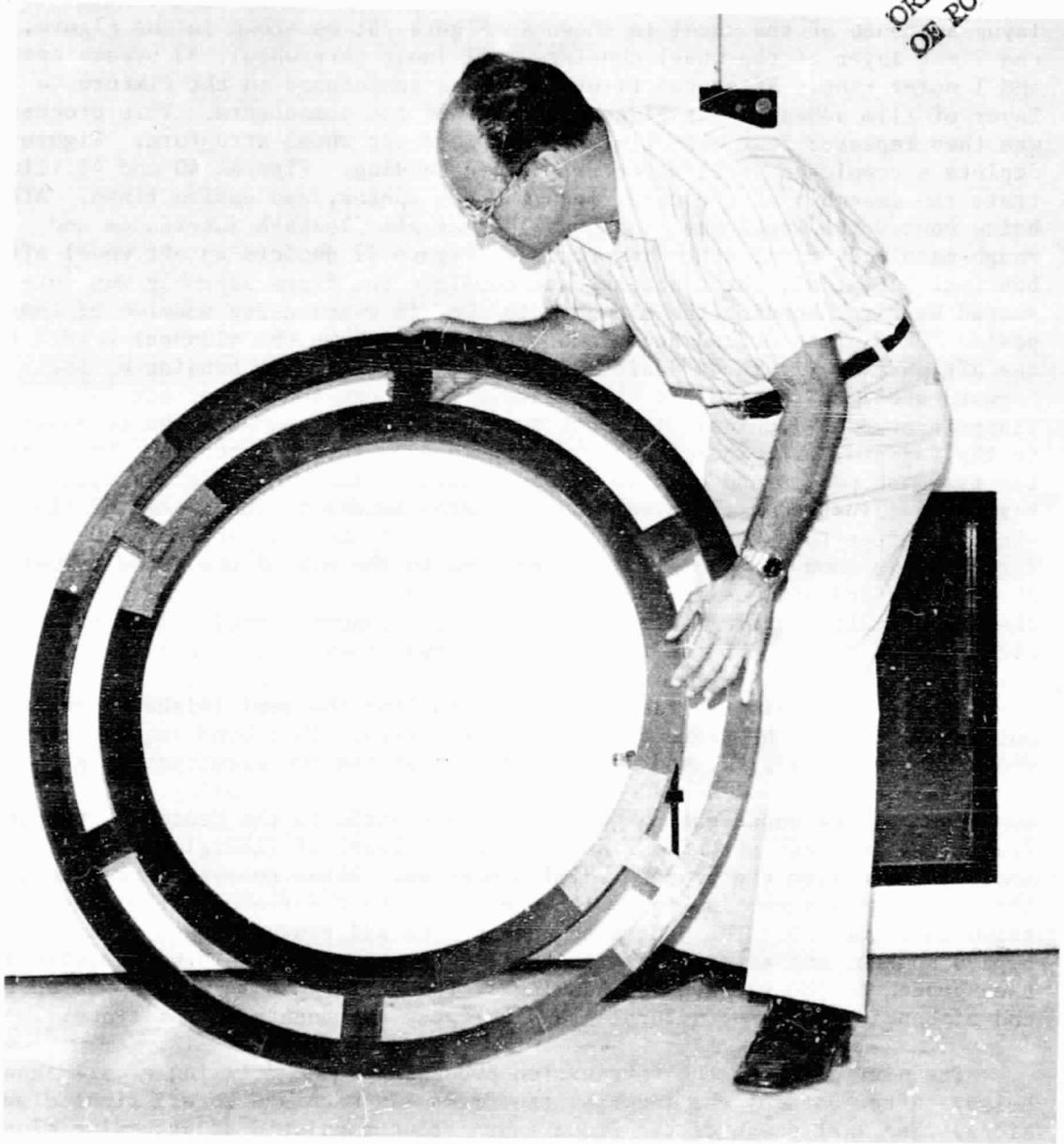

Figure 36. Forward Wheel Before Machining.

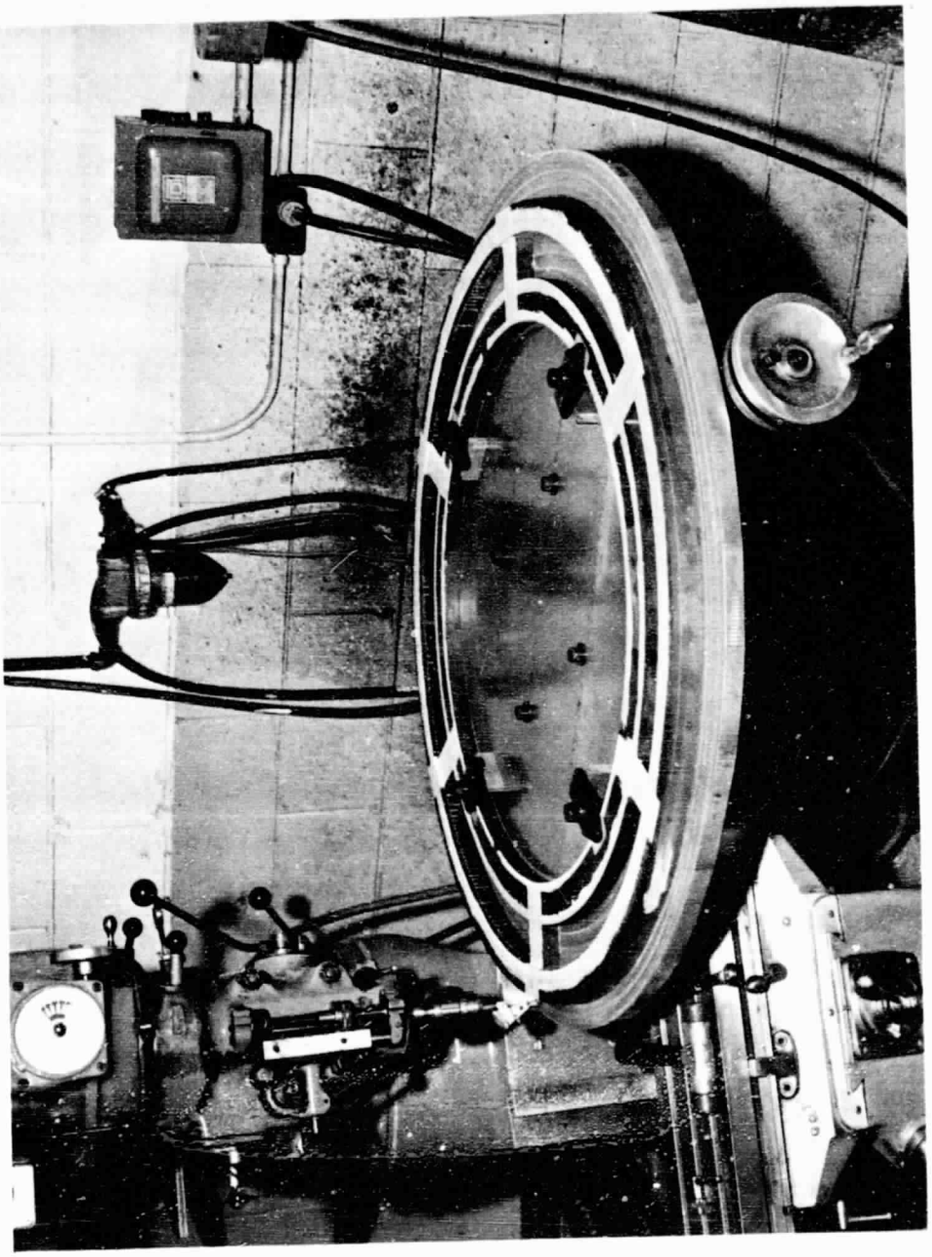

Figure 37. Forward Wheel During Machining.

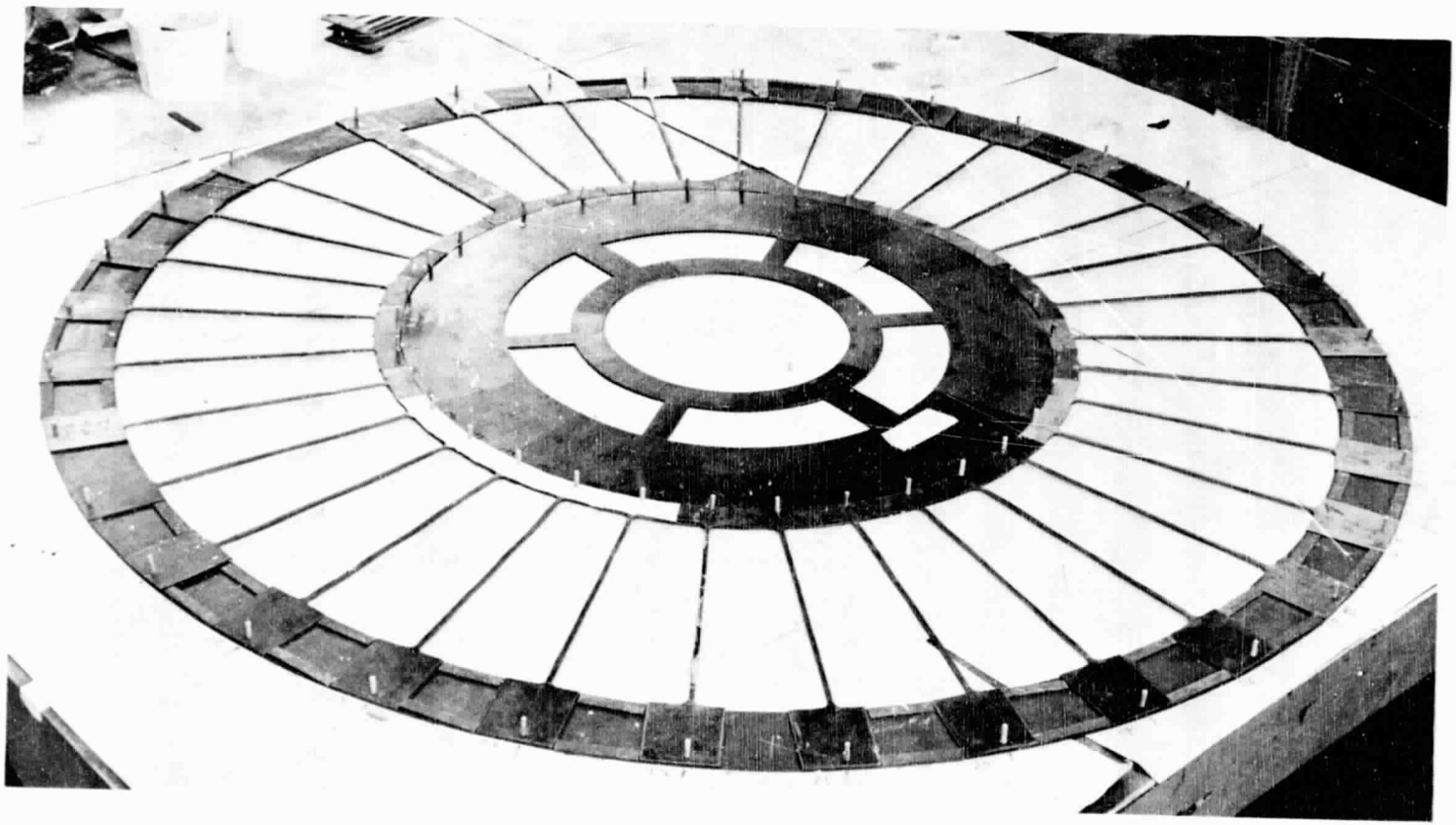

Figure 38. Aft Wheel Construction, First Layer.

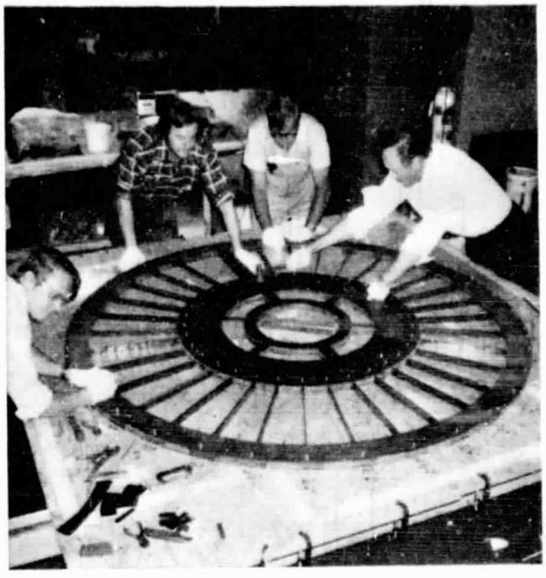

Figure 39. Aft Wheel Before Bonding.

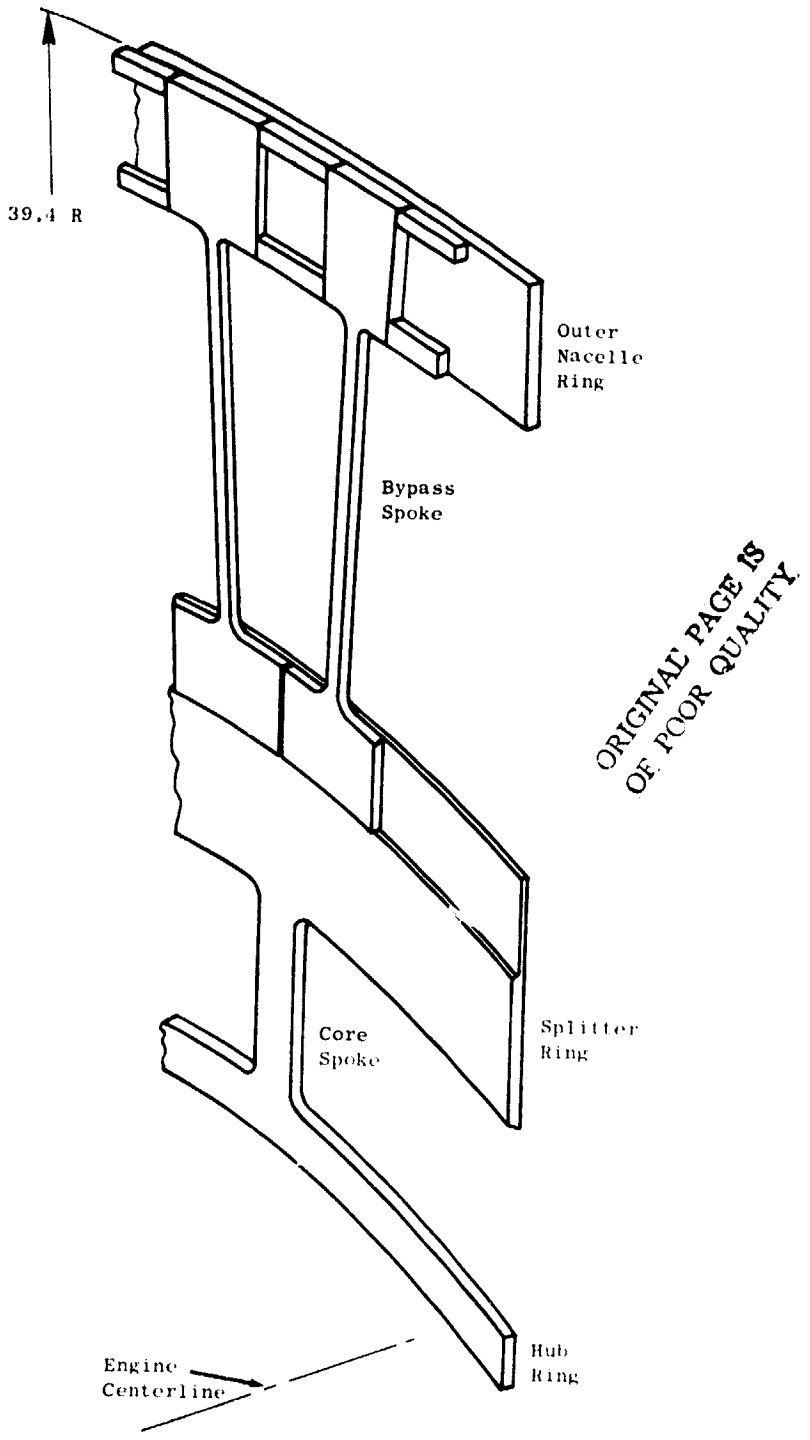

Figure 40. Frame Wheel Construction, Single Layer.

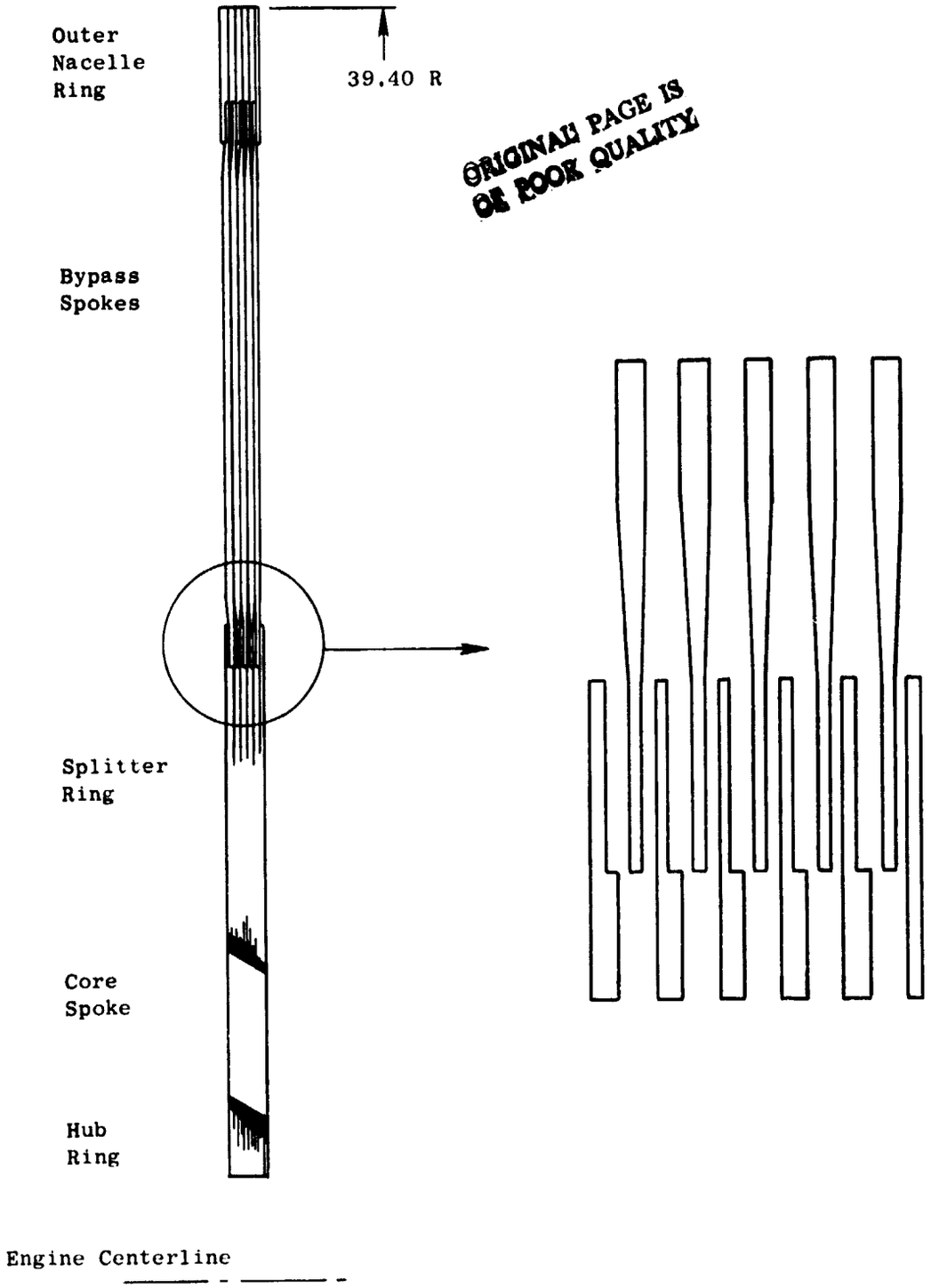

Figure 41. Frame Wheel Construction, Complete.

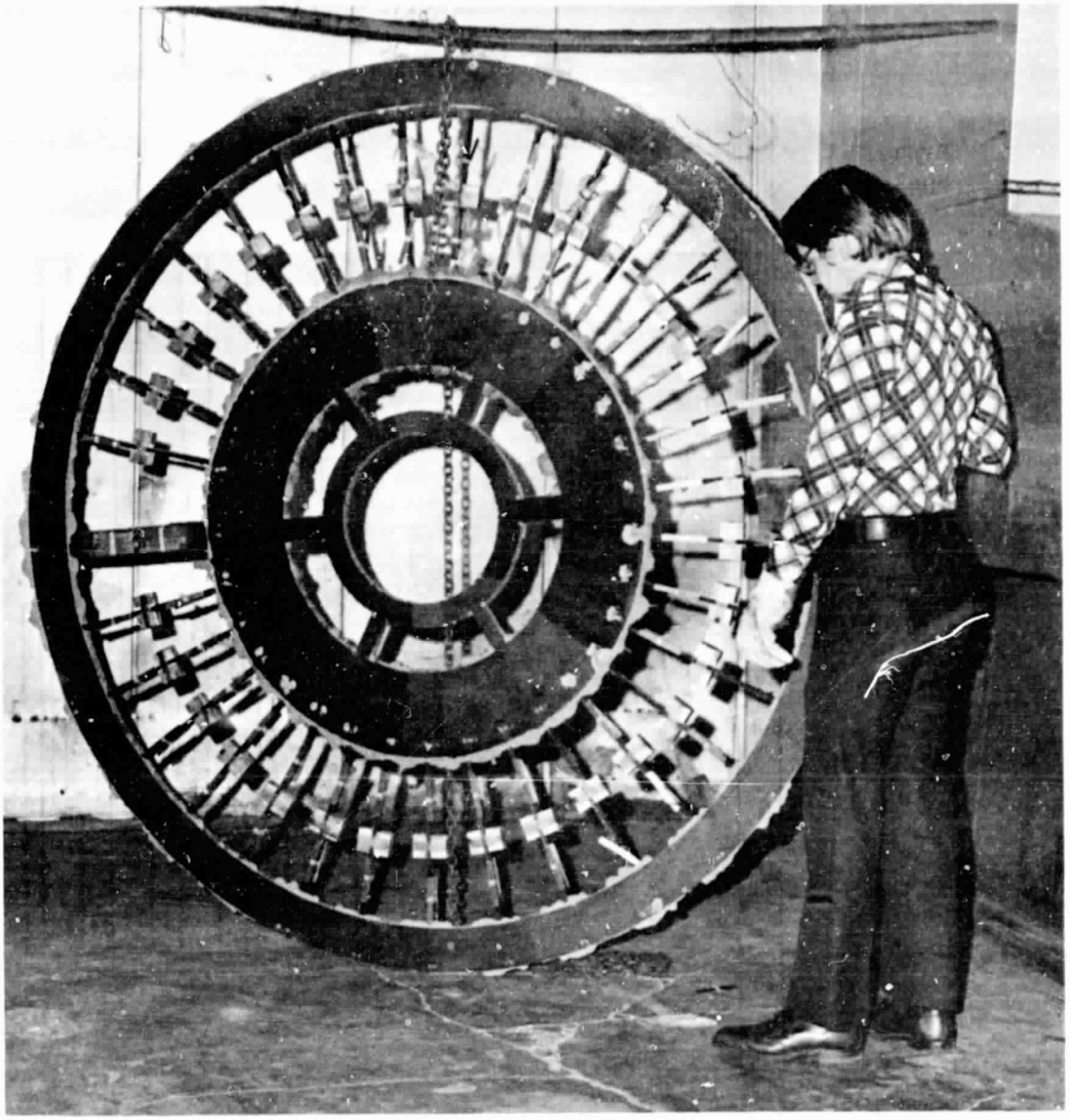

Figure 42. Molded Aft Wheel.

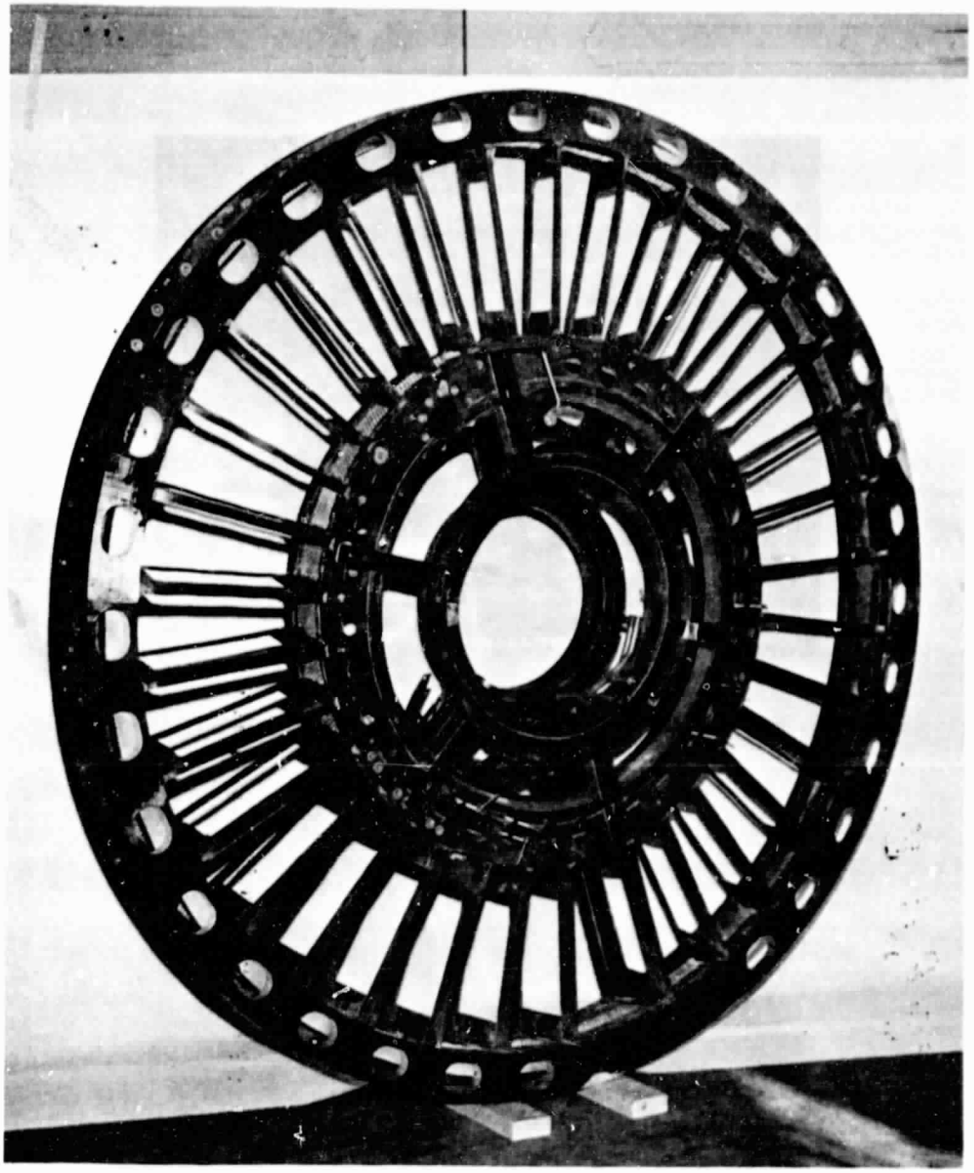

Figure 43. Mid/Aft Wheel Structure.

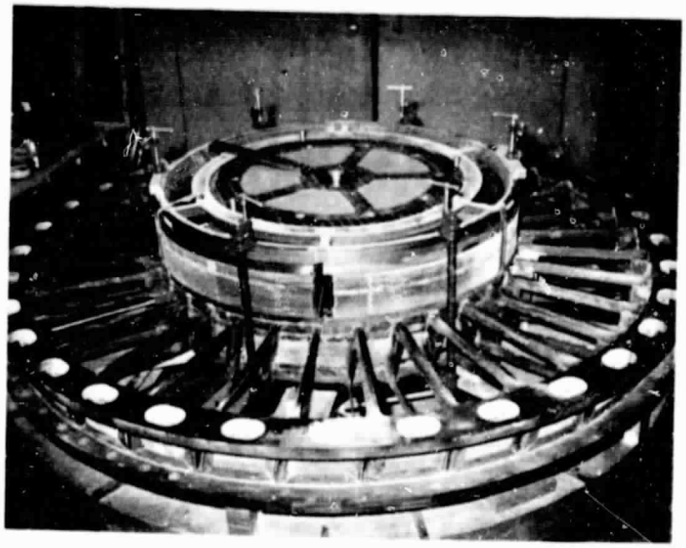

Figure 44. Three-Wheel Bonded Structure.

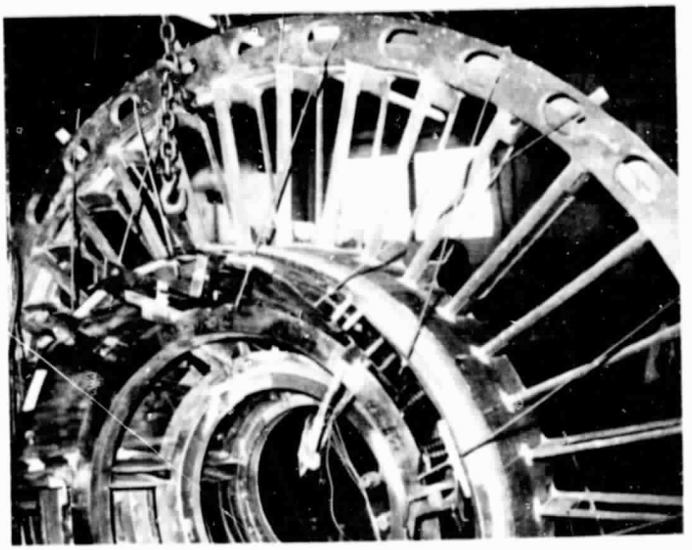

Figure 45. Core Flowpath Panel Bonding.

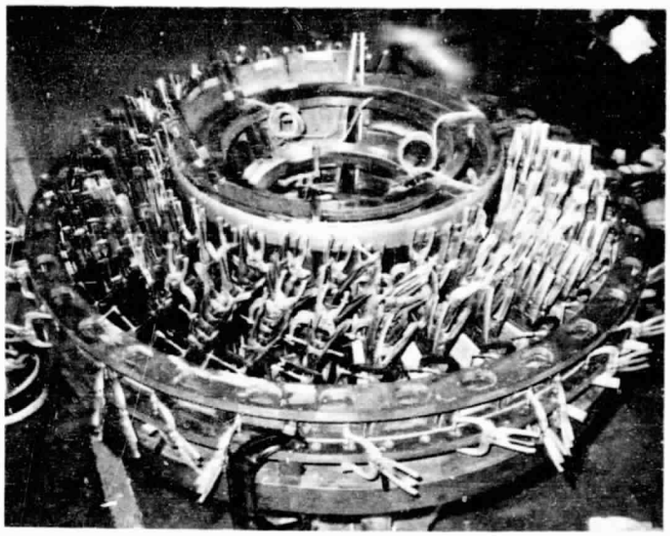

Figure 46. Bypass Vane Panel Bonding.

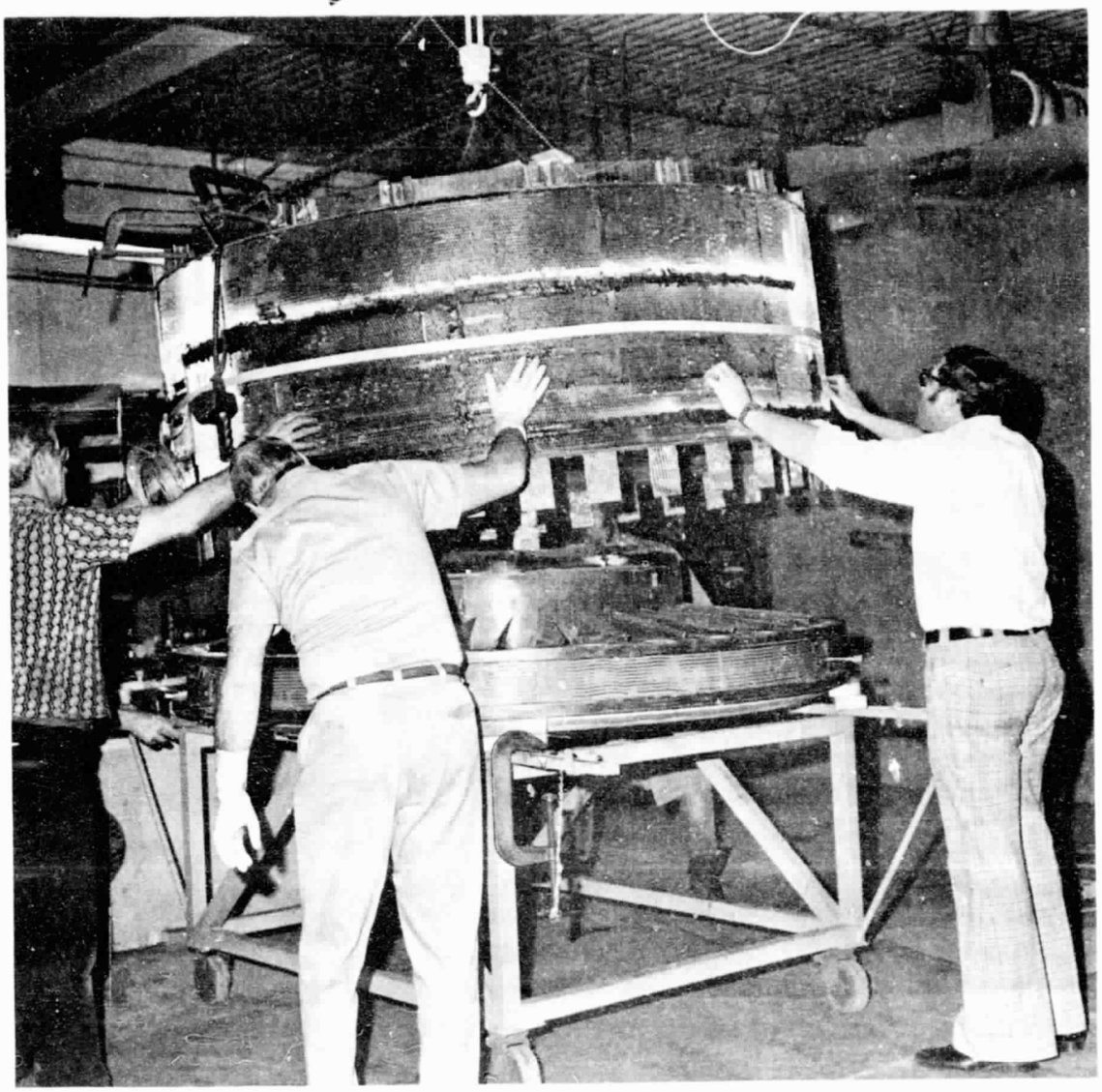

Figure 47. Lifting Outer Casing.

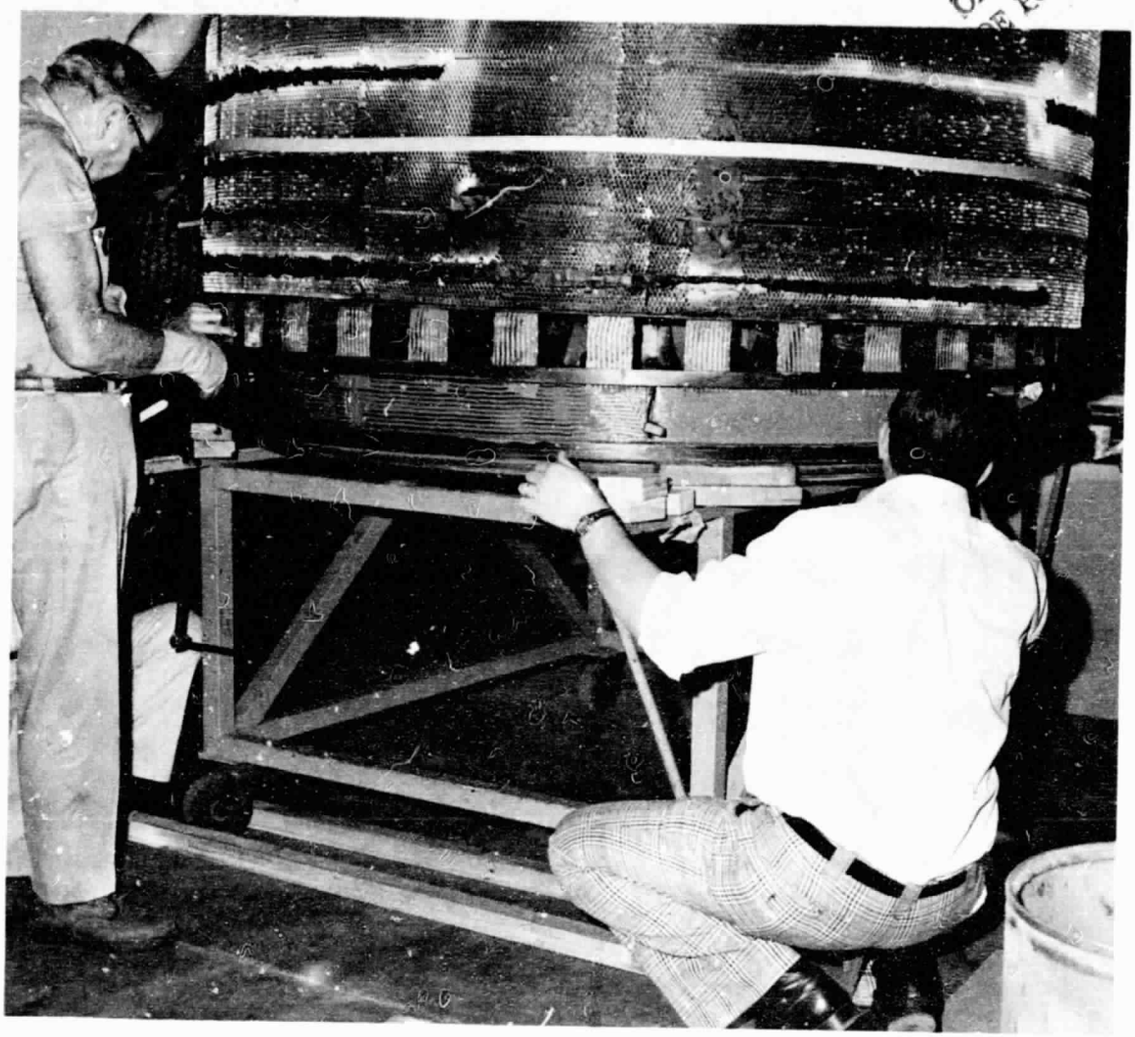

Figure 48. Positioning Outer Casing.

Figure 49. Full Engagement of Outer Casing.

Figure 50. Bonding Outer Casing Panels to Casing.

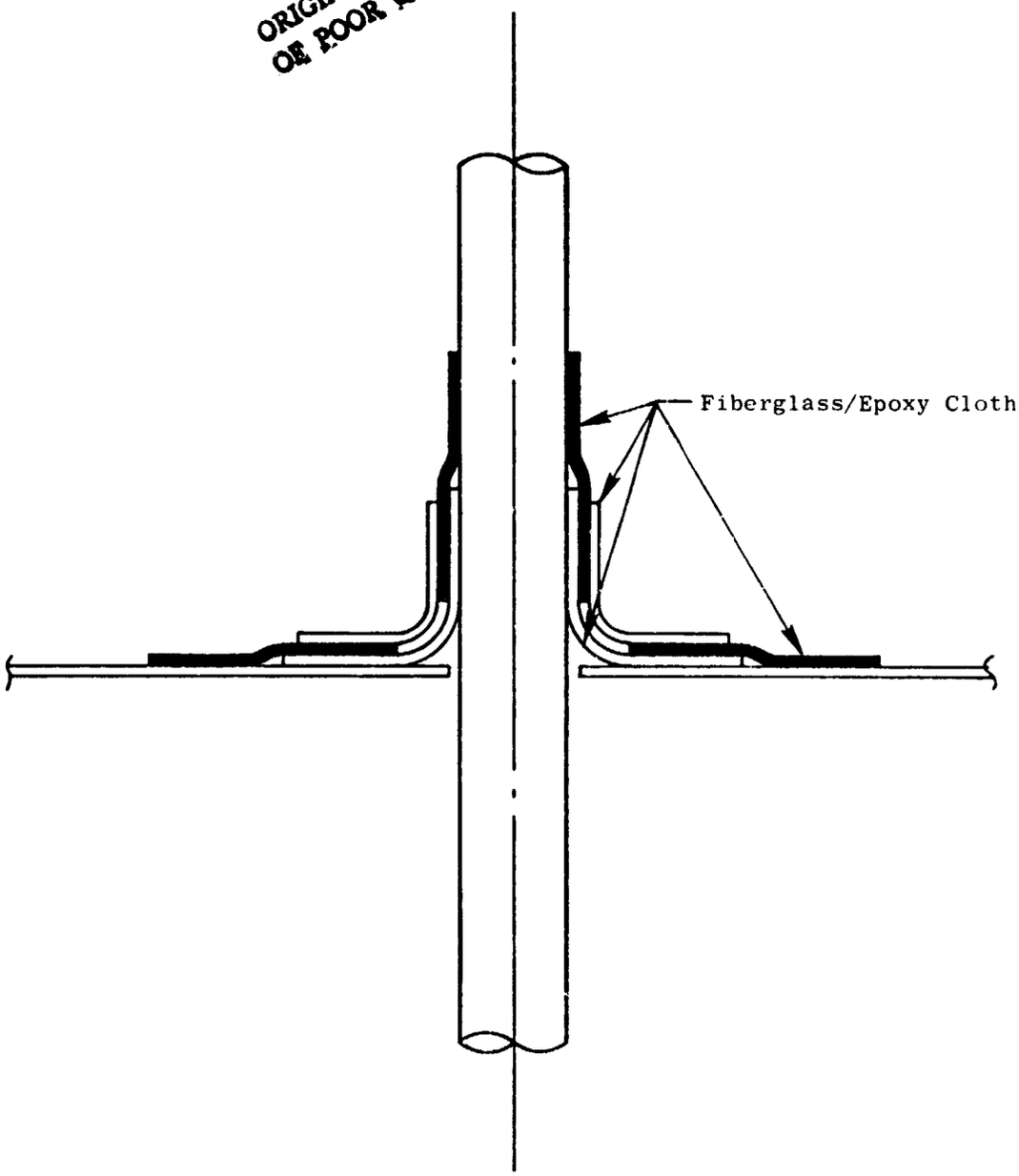

Figure 51. Tube Penetration Sealing Technique.

The last step of the fabrication process was to coat the sump of the frame with an oil-impervious substance. The UTW was coated with a fluorosilicone, whereas the OTW was coated with VITON. After sump coating, the frame was final inspected and then sent to assembly for incorporation into the engine buildup schedule.

3.4 FRAME WEIGHT

The production flight-weight bogey of the QCSEE frame is 192 kg (423 lb). Based on the actual weight of the QCSEE experimental frames, the projected weight of the production flight-weight QCSEE frame would be 204 kg (450 lb). The following discussion provides a reconcilation of the QCSEE test frame weight with the weight of a production flight-weight frame of the same design.

The average weight of the QCSEE UTW and OTW frames was 318 kg (702 lb). The following table is a breakdown of the weight by material.

Material	Weight kg (lb)	Reference
Graphite/Epoxy	152 (337)	Table VII
Honeycomb	29 (63)	
Glass/Epoxy	15 (33)	
Adhesive	34 (75)	Table VIII
Potting Compound	56 (124)	Table IX
Metal	32 (70)	Table X
Total	318 (702)	

The weight of the above-mentioned materials can be reduced for the following reasons.

Graphite/Epoxy - Redesign of the aft outer cowl door attachment and wheel structures, and reduction of the 5-blade-out condition to a 2-1/2-blade-out condition would result in an 18-kg (40-lb) weight savings. (See Table VII for details.)

Honeycomb - The structural analysis indicated a core requirement of 30.4-kg/m^3 (1.9-lb/ft^3) density; however, an acoustic analysis indicated that a 49.6-kg/m^3 (3.1-lb/ft^3) core would be needed. Based on present testing, a return to the 30.4-kg/m^3 (1.9-lb/ft^3) density is possible and, if enacted, would provide an 11.4-kg (25-pound) weight savings.

Table VII. Graphite/Epoxy Components.

	Item	Weight kg	Weight (lb)
(A)	Forward Wheel	11.34	(25.00)
(a)	Midwheel	29.48	(65.00)
(a)	Aft Wheel	38.56	(85.00)
(b)	Vane Skins	11.28	(24.88)
(b)	Vane Boots	4.09	(9.02)
(b)	Outer Core Panels	9.60	(21.16)
(b)	Outer Perforated Core Panels	1.09	(5.29)
(b)	Inner Core Panels	5.22	(11.50)
(a)	Sump Core	0.85	(1.88)
(a)	Outer Nacelle Panel	7.95	(17.53)
(a)	Separator Panel	3.94	(8.69)
(a)	Inner Nacelle Panel	3.42	(7.56)
(a)	Containment and Structure	1.97	(4.35)
(a)	Tip Treatment	5.12	(11.28)
(a)	Inlet Latch Channels	1.31	(2.89)
(a)	Hook Ring	12.79	(28.20)
(a)	Aft Splitter Ring	0.73	(1.60)
(a)	Miscellaneous	2.65	(5.84)
(a)	Calculated Total	151.39	(336.67)
(b)	Weighed		

Glass/Epoxy - a 0.18-cm (0.070-in.) thick glass/epoxy shell was required because the honeycomb received from the vendor was too thin. This part is not required when the proper depth honeycomb is procured. Its absence would result in a 15-kg (33-pound) reduction.

Adhesive - The insertion of the glass/epoxy shell required 2.72 kg (6 pounds) of adhesive which will not be required in the flight design. Improper fitting of parts required much use of paste adhesive with an average bond thickness of 0.06 cm (0.025 in.). Better fit up of parts will produce a 0.04-cm (0.015-in.) thick bond line. These two improvements would reduce the frame weight by 10.5 kg (23 pounds). See Table VIII for details.

Potting Compound - Excessive splicing of honeycomb and extensive instrumentation requirements forced the use of an excessive amount of potting material. Improvement in honeycomb procurement and elimination of test instrumentation allows for a weight savings of 46.3 (102 pounds) in a flight frame. See Table IX for details.

Metal Components - The compressor ring can be lightened by proper sculpturing to reduce the weight by 6 kg (13 pounds). A supporting structure for aero instrumentation probes will not be required, saving 7 kg (16 pounds). Total saving in metal component weight is 13 kg (29 pounds). See Table X for details.

Adding up the weight difference between the actual QCSEE test frames and a production flight-weight frame of the same design, the total difference is 114 kg (252 pounds) which results in a flight-weight frame that weighs 204 kg (450 pounds). The weight deltas are summarized below.

Material	Test Frame kg (lb)	Delta kg (lb)	Flight Frame kg (lb)
Graphite/Epoxy	152 (337)	17 (40)	135 (297)
Honeycomb	29 (63)	12 (25)	17 (38)
Glass/Epoxy	15 (33)	15 (33)	0 (0)
Adhesive	34 (75)	10 (23)	24 (52)
Potting Compound	56 (124)	46 (102)	10 (22)
Metal Components	32 (70)	14 (29)	18 (41)
Total	318 (702)	114 (252)	204 (450)

Table VIII. Adhesive Weight.

Area	Film Weight kg (lb)	Paste Weight kg (lb)	Total Weight kg (lb)
Outer Casing	8.06 (17.77)	8.68 (19.15)	16.74 (36.92)
Vanes	0.48 (1.07)	5.09 (11.24)	5.58 (12.31)
Splitter	0.74 (1.64)	2.99 (6.60)	3.74 (8.24)
Core Struts	---	0.84 (1.85)	0.84 (1.85)
Hub	---	1.67 (3.69)	1.67 (3.69)
Wheels	5.44 (12.00)	---	5.44 (12.00)
Total	14.72 (32.48)	19.27 (42.53)	34.01 (75.01)

Table IX. Potting Compound Weight.

	Area	Quantity	Weight kg	Weight (lb)
(a)	* Top Vertical Splitter	1	1.52	(3.36)
(a)	* Top Vertical Inlet Latch	1	3.33	(7.35)
	* Tip Treatment (Interior)	1	9.39	(20.70)
	Sump Drain Funnel	1	0.95	(2.10)
(a)	* Nacelle Probe Fastener	2	3.43	(7.56)
(a)	* Nacelle Probe Link Fastener	3	1.31	(2.88)
(a)	* Square Nacelle Pad (Accel.)	2	0.87	(1.92)
(a)	* Nacelle Probe Pad	1	1.31	(2.88)
	* Top Vertical Attach Posts	17	2.26	(4.98)
(a)	Splitter Probe	1	1.33	(2.94)
(a)	Light Probes	1	2.18	(4.80)
	* Access Cover	1	0.25	(0.56)
	Sump Drain Tunnel	1	1.27	(2.80)
(a)	* Instrumentation Hole	19	1.16	(2.57)
(a)	* Instrumentation Channels	N/A	8.50	(18.75)
(a)	* Honeycomb Splicing	N/A	17.01	(37.50)
		Total	56.07	(123.65)

* Volume potted is substantiated by photographs of region.

(a) Not required for production frame.

Table X. Metal Components Weight.

	Component	Weight kg	Weight (lb)
**	Compressor Ring	9.52	(21.00)
	Latches and Bushings	1.79	(3.94)
	Reinforcing Plates	0.72	(1.58)
	Inserts	6.20	(13.67)
	Bolts	1.41	(3.11)
	Tube Fittings	1.56	(3.45)
	Oil-In Tube	0.67	(1.48)
	GE Variable-Pitch Tube (2)	0.39	(0.86)
*	Probe Support (2)	3.43	(7.56)
*	Probe Base	2.24	(4.94)
*	Probe Bracket (4)	0.78	(1.71)
*	Probe Receptical	0.18	(0.39)
*	Probe Bracket (3)	0.58	(1.28)
	Drain Plate	1.09	(2.41)
	Drain Tube	0.15	(0.34)
	Pressure Tube	0.09	(0.20)
	Pressure Tube	0.09	(0.20)
	Tube	0.11	(0.24)
	Flange	0.02	(0.05)
	Flange	0.05	(0.12)
	Drain Tube	0.03	(0.06)
	Drain Tube (Pylon)	0.66	(1.46)
	Total	31.76	(70.05)

* Not required for flight frame
** Can be modified to 3.62 kg (8 lb) for flight frame.

4.0 FRAME TEST

Testing of the QCSEE OTW composite frame was performed in the General Electric Static Load Lab test facility shown in Figure 52. The entire setup (shown in Figures 53, 54, and 55) was designed and fabricated by Static Load Lab personnel specifically for the QCSEE engine program. As shown in Figures 53 and 56, all loads were applied to the frame through a simulated bearing cone and a simulated inlet, and were reacted through the engine mounts. All applied loads were imposed on the frame with hydraulic cylinders connected in series to load cells which were attached to the simulated forward (No. 1) bearing cone and the simulated inlet. In order to accurately simulate the proper boundary conditions on the frame, the composite frame was bolted to a simulated QCSEE core engine. This frame/core engine asembly was then hung from the Static Load Lab facility through the actual engine mounting locations. The configuration of the mounting locations on the composite frame consisted of a large metal pin positioned in the frame uniball at top vertical, and two links that attached to the small uniball in the thrust brackets located at ±45° down from top vertical. This mount configuration is shown in Figure 18. The aft engine mount (shown in Figure 55) consisted of two vertical links and one horizontal link. This mounting system simulated as close as possible the actual engine mount system that is shown in Figure 57.

At the forward mount all thrust loads are removed through the two links that are attached to the two brackets on the aft wheel. Vertical and side loads are removed through the pin/uniball configuration at top vertical. At the aft mount, all side loads are extracted through the one horizontal link. All vertical and torque loads are removed through the two vertical links.

As shown in Figures 53 and 56, the composite frame contained extensive instrumentation; in all, a total of 19 three-element rosette strain gages, 12 single-element strain gages, and 49 deflection pots were utilized in monitoring the condition of the frame throughout all test conditions. Most of the instrumentation was located in the critically loaded regions of the frame. All applied loads, strain values, and deflections were recorded on a digital monitoring system and put into a computer program. Output from this computer program was loads in the load cells, loads on the frame, frame strains, and frame deflections. A typical printout from this program is shown in Figure 58.

The entire frame test program consisted of seven tests. The first four tests established four critical frame spring constants, and the remaining three tests established frame stresses and deflection for three critical-load conditions. Table XI lists these seven load conditions, the loads applied to the test fixtures, and the resultant loads on the frame. Figures 53 and 56 depict the location of the applied test loads on the simulated inlet and simulated No. 1 bearing cone.

For the first four tests the loads were applied in 20% increments up to 100% and then reduced to 20% of maximum load before returning to zero load. The next two load cases (maximum thrust and crosswind) had loads applied in

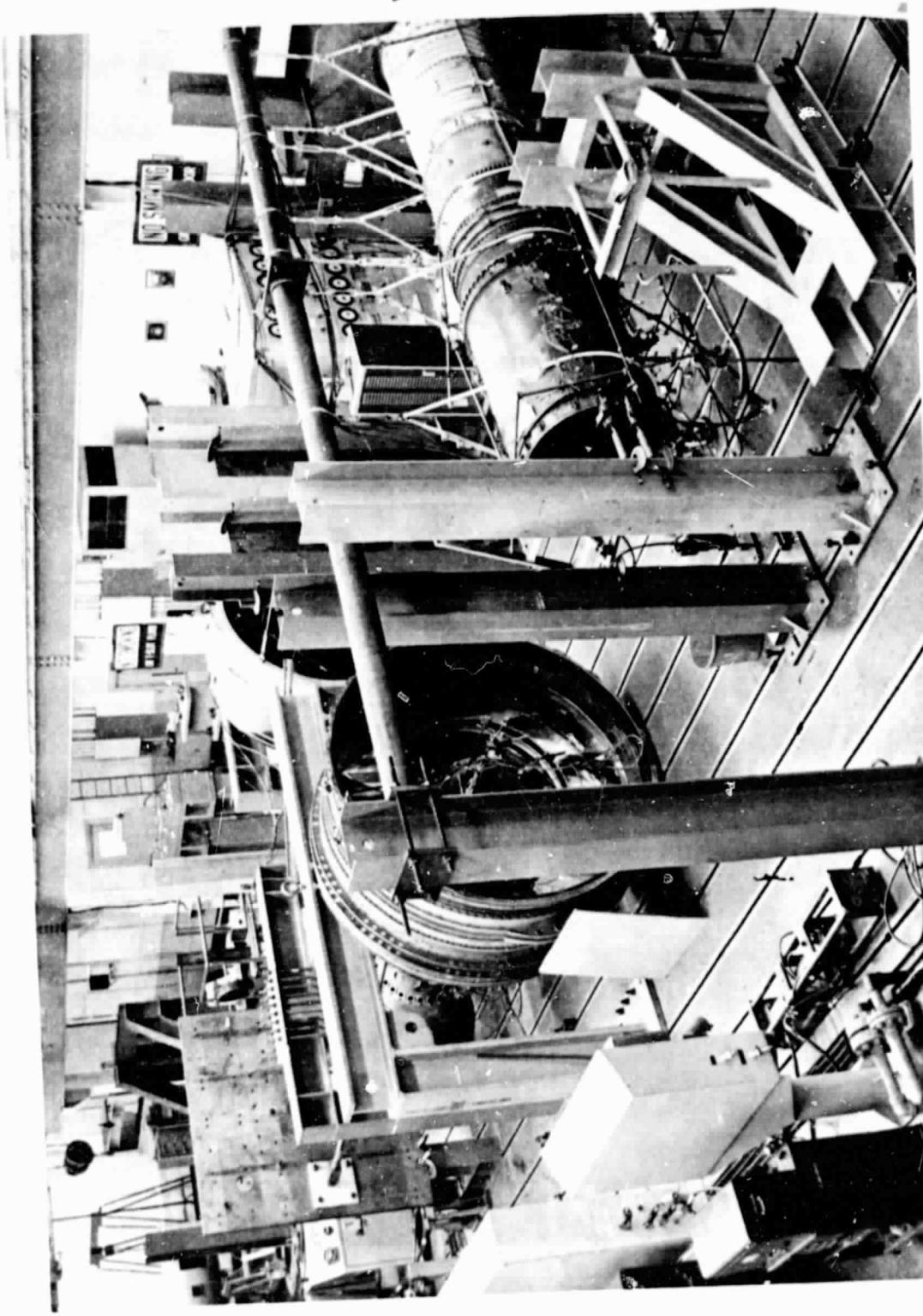

Figure 52. Static Load Lab Facility.

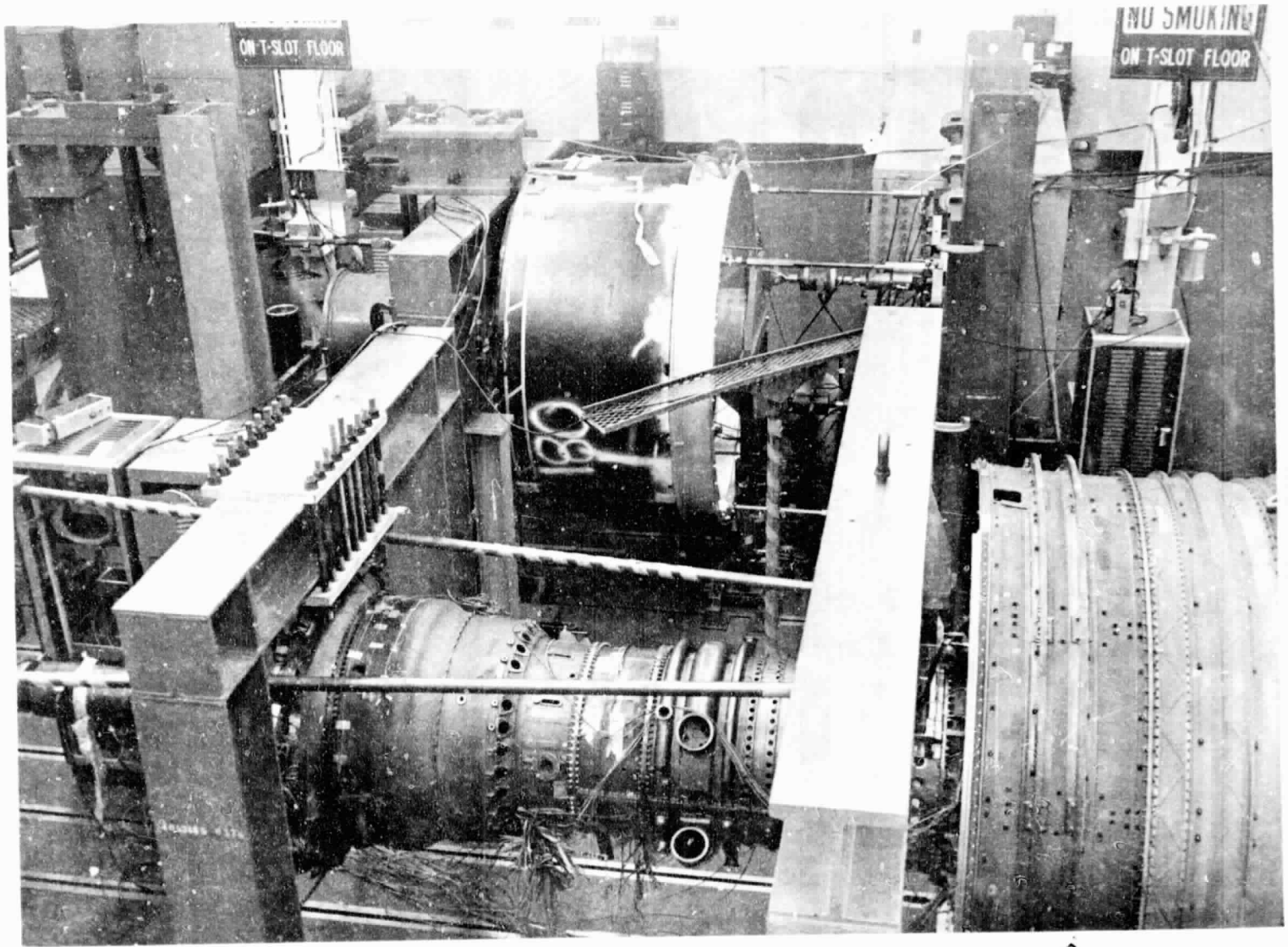

Figure 53. QCSEE Frame Test Setup.

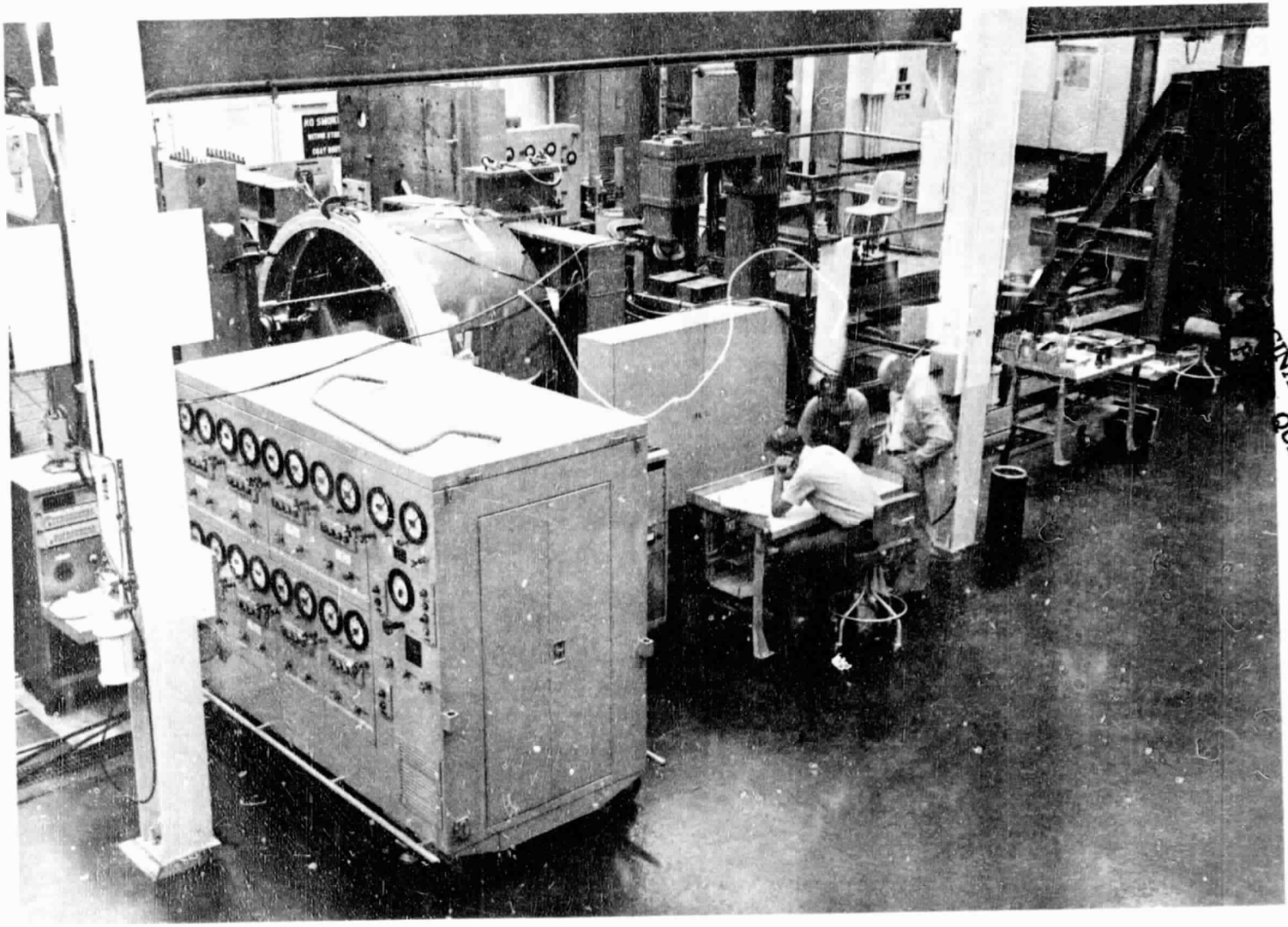

Figure 54. Hydraulic Load Input Cart.

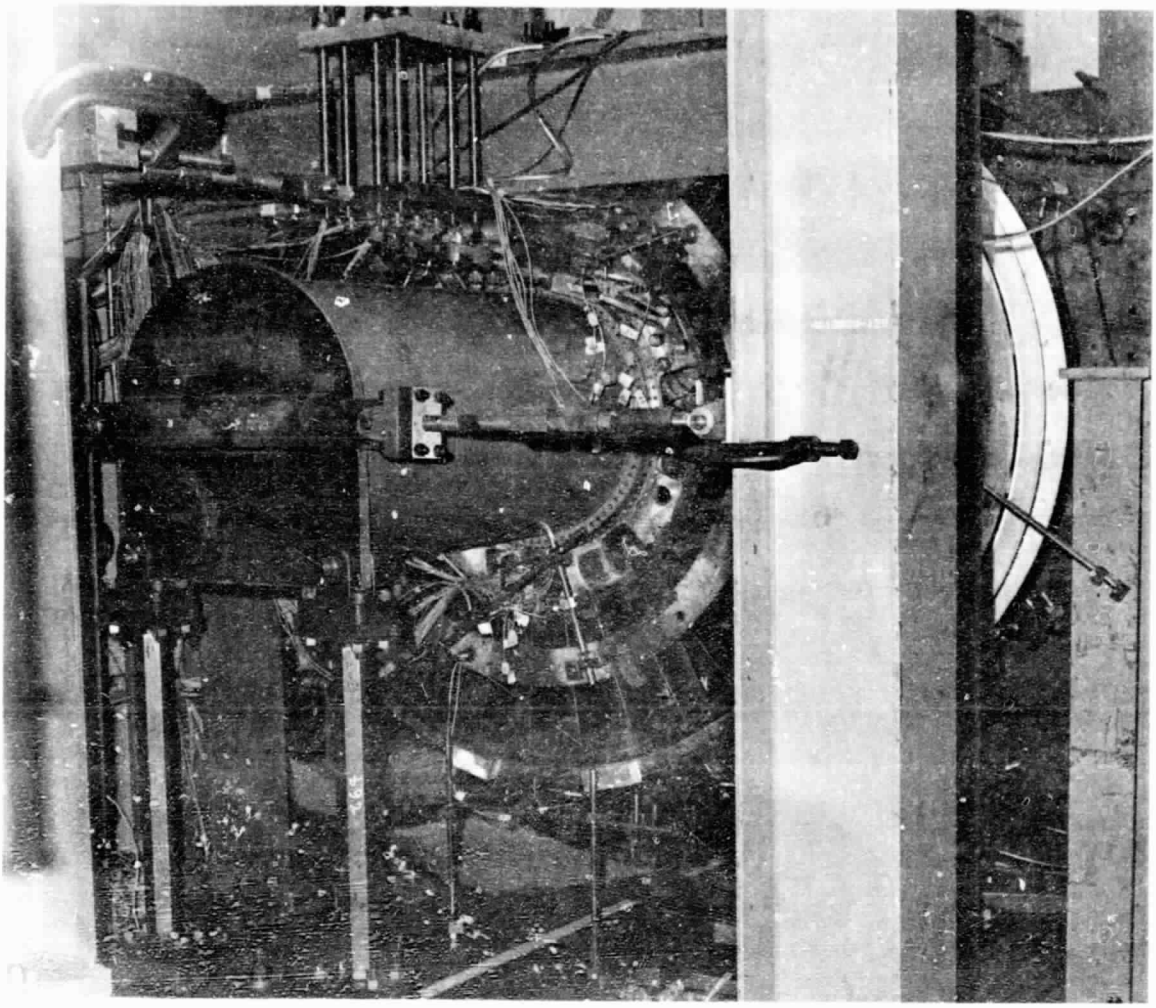

Figure 55. Aft Engine Mount Test Setup.

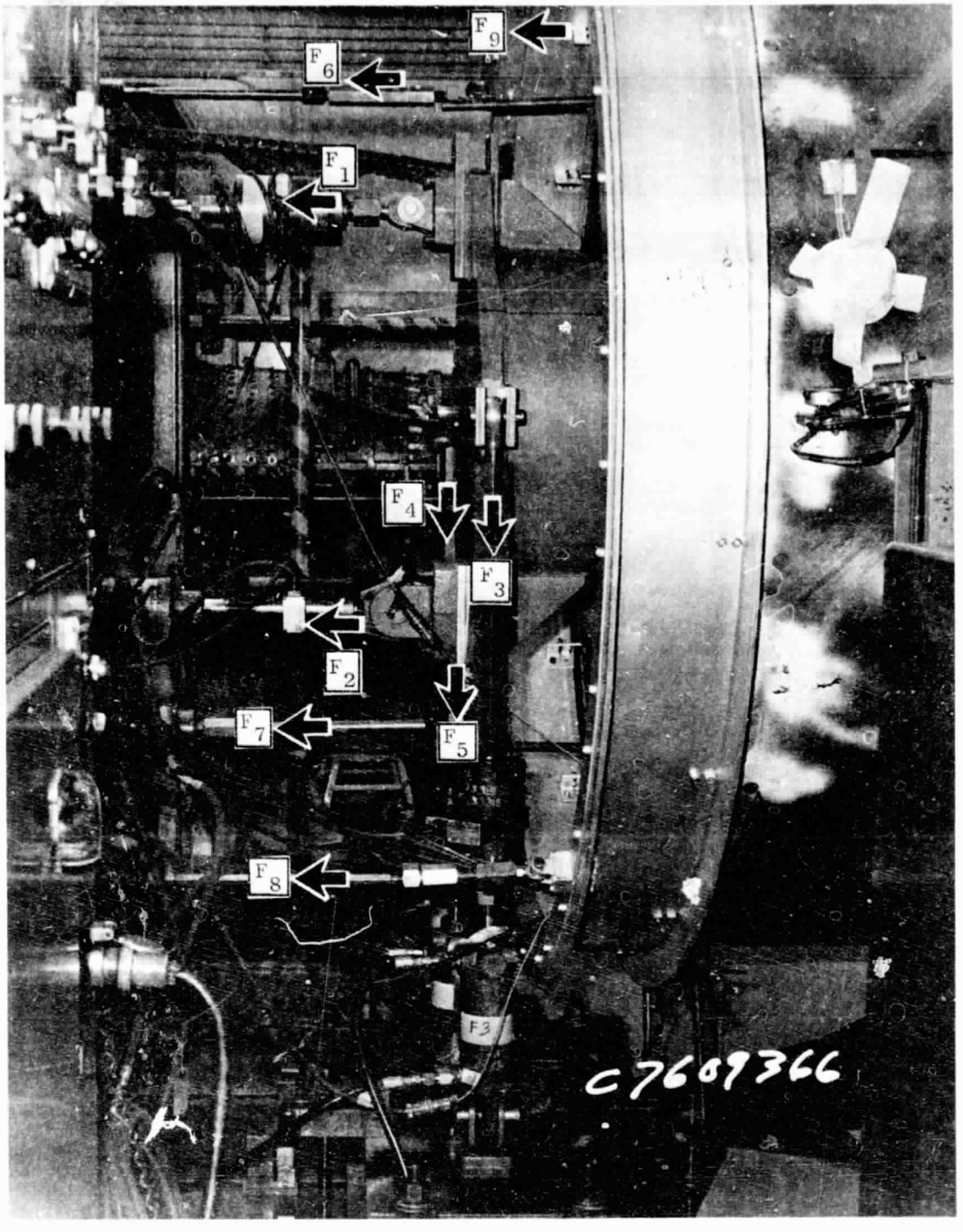

Figure 56. Frame Load Input Setup.

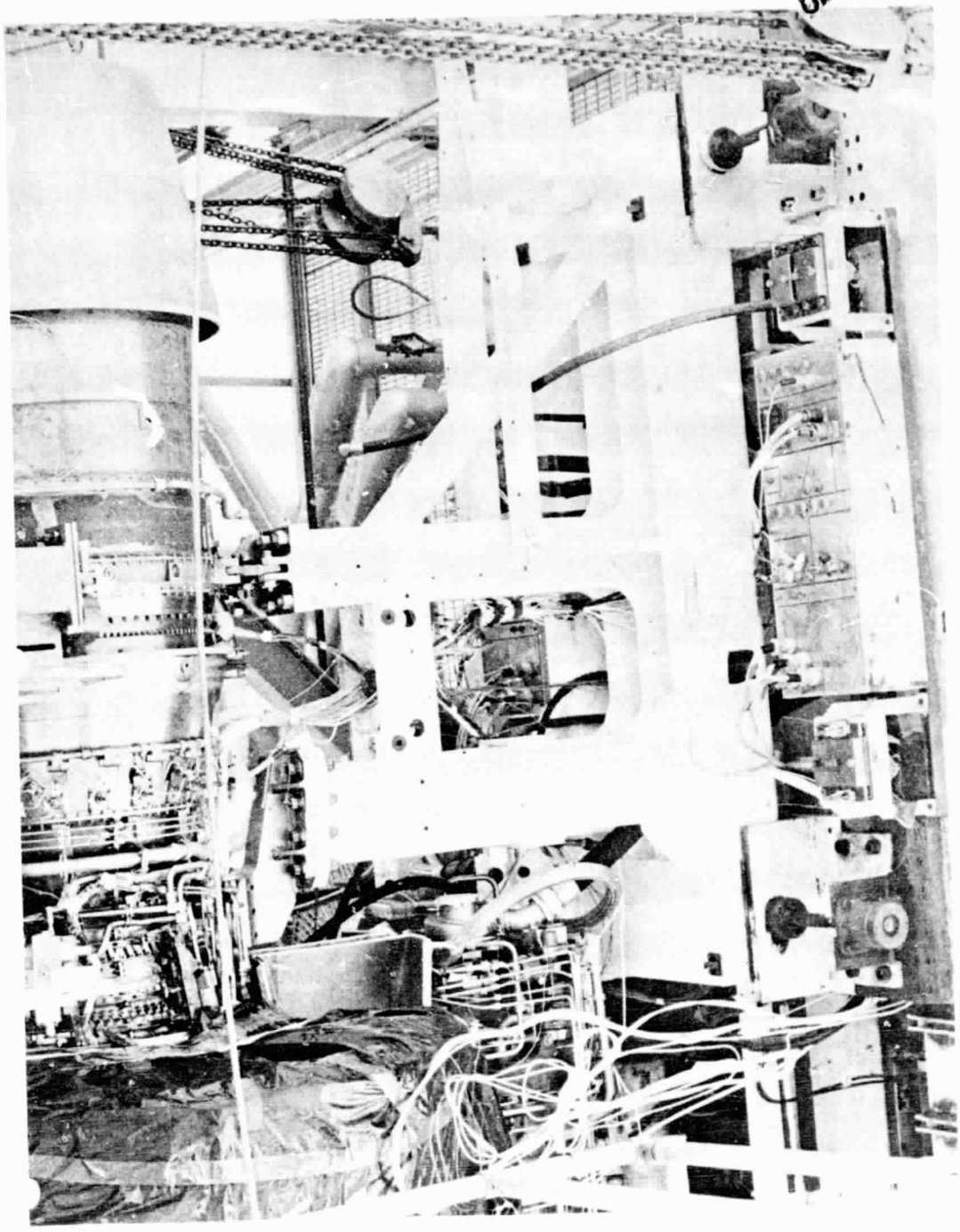

Figure 57. Engine Mounting Configuration.

OCSEE COMPOSITE FRAME

8/27/76 TIME 1935 READING 21

PERCENT LOAD 60

THIS DATA CALCULATED USING ZERO READING NO. 18
S/G DATA IN STRAIN

SPECIAL PARAMETERS

LOD-F1 =	11.9	LOD-F2 =	-4.7	LOD-F3 =	2.4
LOD-F4 =	-11.9	LOD-F5 =	594.8		

ENGINEERING UNITS

NAME	VALUE	NAME	VALUE	NAME	VALUE	NAME	VALUE
RS-1**	1897.0	RSC-1*	6348.0	SG-1A*	13.5	SG-1B*	14.0
SG-1C*	19.2	SG-2A*	19.9	SG-2B*	17.3	SG-2C*	33.8
SG-3**	23.0	SG-4A*	35.7	SG-4B*	24.9	SG-4C*	15.9
SG-5A*	8.7	SG-5B*	27.2	SG-5C*	52.7	SG-6A*	21.5
SG-6B*	13.5	SG-6C*	21.9	SG-7A*	9.4	SG-7B*	8.0
SG-7C*	2.8	SG-8A*	-10.6	SG-8B*	11.9	SG-8C*	8.5
SG-9A*	12.6	SG-9B*	11.5	SG-9C*	-9.1	SG-10A	5.8
SG-10B	13.4	SG-10C	6.3	SG-11A	15.6	SG-11B	7.4
SG-11C	19.4	SG-12A	31.2	SG-12B	33.4	SG-12C	15.1
SG-13A	-25.4	SG-13B	-52.4	SG-13C	10.7	SG-14A	-0.6
SG-14B	17.1	SG-14C	40.5	SG-15A	-5.5	SG-15B	-6.6
SG-15C	0.6	SG-16A	9999.0	SG-16B	27.8	SG-16C	20.1
SG-17A	31.5	SG-17B	23.9	SG-17C	25.1	SG-18A	15.5
SG-18B	15.7	SG-18C	15.7	SG-19*	26.2	SG-20*	11.1
SG-21*	16.4	SG-22*	17.7	SG-23*	22.6	SG-24*	23.8
SG-25*	24.7	SG-26*	16.6	SG-27*	20.3	SG-28*	15.0
SG-29*	16.2	SG-30A	17.7	SG-30B	14.4	SG-30C	18.1
SG-31A	17.1	SG-31B	18.1	SG-31C	24.1	SG-32*	4.9
LOD-F1	11.9	LOD-F2	-4.7	LOD-F3	2.4	LOD-F4	-11.9
LOD-F5	594.8	EX-POT	8360.0	POT-1*	-2.3	EX-POT	8337.0
POT-2*	-0.5	EX-POT	8327.0	POT-3*	-0.3	EX-POT	8357.0
POT-4*	0.0	EX-POT	8368.0	POT-5*	-0.2	EX-POT	8378.0
POT-6*	0.1	EX-POT	8380.0	POT-7*	0.1	EX-POT	8373.0
POT-8*	-0.8	EX-POT	8378.0	POT-9*	0.1	EX-POT	8367.0
POT-10	-0.0	EX-POT	8370.0	POT-11	-0.2	EX-POT	8369.0
POT-12	0.0	EX-POT	8330.0	POT-13	-0.4	EX-POT	8368.0
POT-14	0.2	EX-POT	8376.0	POT-15	-0.1	EX-POT	8374.0
POT-16	-0.0	EX-POT	8375.0	POT-17	-0.2	EX-POT	8375.0
POT-18	-0.3	EX-POT	8378.0	POT-19	-0.9	EX-POT	8332.0
POT-20	1.3	EX-POT	8343.0	POT-21	1.3	EX-POT	8365.0
POT-22	-0.8	EX-POT	8349.0	POT-23	2.1	EX-POT	8364.0
POT-24	-7.5	EX-POT	8362.0	POT-25	0.0	EX-POT	8224.0
POT-26	-0.6	EX-POT	8223.0	POT-27	0.0	EX-POT	8272.0
POT-28	-0.4	EX-POT	8272.0	POT-29	-1.3	EX-POT	8260.0
POT-30	-0.2	EX-POT	8263.0	POT-31	0.2	EX-POT	8268.0
POT-32	0.1	EX-POT	8273.0	POT-33	-2.6	EX-POT	8252.0
POT-34	2.1	EX-POT	8275.0	POT-35	-1.0	EX-POT	8264.0
POT-36	-3.4	EX-POT	8265.0	POT-37	-0.1	EX-POT	8271.0
POT-40	-1.8	EX-POT	8257.0	POT-41	1.0	EX-POT	8267.0
POT-42	0.5	EX-POT	8268.0	POT-43	-1.9	EX-POT	8268.0
POT-44	0.2	EX-POT	8268.0	POT-45	0.0	EX-POT	8269.0
POT-46	-0.0	EX-POT	8269.0	POT-47	-0.2	EX-POT	8269.0
POT-48	0.3	EX-POT	8273.0	POT-49	-1.1		

Figure 58. Typical Test Printout.

Table XI. Test Load Cases.

Test Number	Test Condition	F_1	F_2	F_3	F_4	F_5	F_6	F_7	F_8	F_9	Resultant Loads on Test Part
1	Axial Spring Constant	13,495 (3,034)	8,745 (1,966)	--- ---	--- ---	-4,003 (-900)	--- ---	--- ---	--- ---	--- ---	22,240-N (5,000-lb) Forward Axial Load at Forward Hub
2	Radial Spring Constant	23,650 (5,317)	-23,650 (-5,317)	--- ---	--- ---	-21,795 (-4,900)	--- ---	--- ---	--- ---	--- ---	17,792-N (4,000-lb) Radial Load at Forward Hub
3	Overturning Moment Constant	2,375 (534)	-2,375 (-534)	--- ---	--- ---	-8,451 (-1,900)	--- ---	--- ---	--- ---	--- ---	4,448-N (1,000-lb) Radial Up-Load at Forward Hub Plus a 405,388 cm-N (35,875 in.-lb) Moment About Forward Hub Horizontal Centerline
4	Torsional Spring Constant	2,375 (534)	-2,375 (-534)	-17,792 (-4,000)	17,792 (4,000)	-4,003 (-900)	--- ---	--- ---	--- ---	--- ---	1,356,000 cm-N (120,000 in.-lb) Torque at Forward Hub Applied Clockwise Aft Looking Forward
5	Thrust	49,079 (11,034)	44,329 (9,966)	-74,135 (-16,667)	74,135 (16,667)	-4,003 (-900)	--- ---	--- ---	--- ---	--- ---	93,408-N (21,000-lb) Forward Axial Load and a 5,650,000 cm-N (500,000 in.-lb) Torque at Forward Hub Applied Clockwise Aft Looking Forward
6	Thrust Plus Crosswind	49,079 (11,034)	44,329 (9,966)	-74,135 (-16,667)	74,135 (16,667)	-4,003 (-900)	-7,962 (-1,790)	-7,962 (-1,790)	-7,962 (1,790)	-7,962 (1,790)	93,408-N (21,000-lb) Forward Axial Load and a 5,650,000 cm-N (500,000 in.-lb) Torque at Forward Hub Applied Clockwise Aft Looking Forward Plus a 2,260,000 cm-N (200,000 in.-lb) Overturning Moment at Inlet Applied About Vertical Centerline
7	Thrust Plus 1 Blade-Out	29,441 (6,619)	63,966 (14,381)	-74,135 (-16,667)	74,135 (16,667)	-34,694 (-7,800)	--- ---	--- ---	--- ---	--- ---	Same as Test 5 Plus a 30,691-N (6,900-lb) Radial Up-Load and a 4,294,000 cm-N (380,000 in.-lb) Moment Up About Horizontal Centerline at Forward Hub

*Applied Load Locations Are Shown in Figure 56.

10% increments up to 100% and then reduced to 60% and 20% of maximum load before reduction to zero load. The last load case,the blade-out condition, consisted of first applying the maximum thrust/torque loads in 10% increments up to 100%. At this point the loads were equal to the 100% maximum thrust test case. Radial loads were then imposed in 10% increments up to 100% blade-out condition and were then reduced to a 20% blade-out condition, a 100% and 20% maximum thrust condition, and finally zero load.

The first four tests measured the axial, shear, moment, and torsional spring constants of the frame. All spring constants are for the forward hub ring relative to the aft wheel at the mounting regions. Table XII lists these four spring constants and compares them to predicted values calculated by the analytical computer model.

The next three tests represent the highest loading for different major components of the frame. The first of these tests represented the highest normal operating loads, and consisted of the maximum axial load coupled with the highest torque load. These loads occur from the maximum fan thrust coupled with the torque resulting from the fan reduction gear assembly. The highest measured stresses and deflections during this load case are shown in Tables XIII and XIV.

The next two load cases represent the highest loading on the bypass vanes and core frame. Both of these load cases represent ultimate load cases for the frame and are the worst of the load cases listed in Table I.

The first ultimate load case represents the loads induced by a 100-knot crosswind at a maximum thrust condition. Loads resulting from this condition produce a large moment on the frame outer casing while at the same time imposing the highest axial and torque loads on the core frame. Stresses and deflections resulting from this condition are shown in Tables XIII and XIV.

The last ultimate load condition is the worst condition for the frame. This case induces loads resulting from the loss of one fan blade at the maximum thrust and maximum torque condition. Although the ultimate load case defined in Table I describes a loss of five adjacent fan blades, the test case limited the loading to the loss of one blade. The stresses listed in Tables XIII and XIV show the measured stresses and deflections for the blade-out condition. As seen from the tables, the blade-out condition represents the highest loading on the frame.

Table XII. Frame Spring Constant Comparison.*

Mode	Calculated	Test
Axial	---	7.2×10^6 lb/in.
Radial	1.1×10^7 lb/in.	1.0×10^7 lb/in.
Overturning Moment	3.6×10^9 in.-lb/radian	2.7×10^9 in.-lb/radian
Torsional	1.8×10^9 in.-lb/radian	2.8×10^9 in.-lb/radian

*All Spring Constants Are for the Forward Hub Ring Relative to Aft Splitter Ring.

Table XIII. Maximum Measured Frame Stresses.

Strain Gage Location	Maximum Stresses* N/cm^2 ($lb/in.^2$)		
	Test Case 5	Test Case 6	Test Case 7
	Maximum Operating	100-kn Crosswind	One Blade-Out
Forward Hub Ring	-1420 (-2060)	-1185 (-1718)	-1327 (-1925)
Forward Outer Ring	+1209 (-1753)	+1113 (+1614)	+1755 (+2546)
Middle Hub Ring	+1056 (+1531)	+898 (+1302)	+4717 (+6841)
Inner Splitter Ring	-84 (-122)	-70 (-101)	-2788 (-4044)
Top Vertical Mount	-1549 (-2247)	-2419 (-3508)	-3863 (5602)
Forward Hub Flowpath	-1690 (-2452)	+1778 (+2579)	-2364 (-3428)

*+ = Tensile Stress
- = Compressive Stress

Table XIV. Maximum Measured Frame Deflections.

Deflection Location (Top Vertical)	Direction	Maximum Deflection* cm (in.)		
		Test Case 5	Test Case 6	Test Case 7
		Maximum Operating	100-kn Crosswind	One Blade-Out
Forward Hub Ring	Horizontal	0.0124 (0.0049)	0.0190 (illegible)	0.0294 (0.0116)
	Vertical	0.0030 (0.0012)	0.0028 (0.0011)	-0.0048 (-0.0019)
	Axial	0.0208 (0.0082)	0.0197 (0.0078)	0.0063 (0.0025)
Middle Hub Ring	Horizontal	-0.0015 (-0.0006)	-0.0058 (-0.0023)	-0.0043 (-0.0017)
	Vertical	0.0018 (0.0007)	-0.0013 (-0.0005)	0.0180 (0.0071)
	Axial	0.0089 (0.0035)	0.0015 (0.0006)	0.0195 (0.0077)
Forward Over Casing	Horizontal	0.0023 (0.0009)	-0.0172 (-0.0068)	0.0119 (0.0047)
	Vertical	-0.0020 (-0.0008)	0.0013 (0.0005)	-0.0251 (-0.0099)
	Axial	0.0000 (0.0000)	-0.0033 (-0.0013)	-0.0078 (-0.0031)

*+ Horizontal Is Right; + Vertical Is Up; + Axial Is Forward with Datum F.L.A.(Forward Looking Aft)

5.0 CONCLUSIONS

1. The internal sump cavity of the frame should contain a metal liner. The metal liner would greatly reduce the risk of any oil leakage from the sump into the core frame, whether through components or around tube penetrations.

2. Field repair of both structural and nonstructural components can be accomplished with relative ease.

3. Finite-element analysis should be utilized in the frequency analysis of composite hollow vanes having large amounts of camber.

4. The weight penalties versus the application ease of paste adhesive should be carefully considered for each component application.

5. The channeling of instrumentation should be minimized so as to restrict the volume of honeycomb that would require potting compound.

6. The structure can withstand physical abuse and yet retain its structural soundness.

7. Urethane tape provides excellent erosion protection; its bond strength, however, is degraded by long periods of exposure to jet engine oil.

6.0 REFERENCES

1. Anon., "Structural Design Guide for Advanced Composite Applications," AFML, Wright-Patterson Air Force Base, Ohio, 1971.

2. Anon., "Test Project Report No. 6032, Component Mechanical Lab," General Electric, Evendale, Ohio, 1976.

3. Mitchell, S.C., "Advanced Composite Engine Static Structures Development," AFML-TR-73-158, July 1973.

4. Stotler, C.L., Jr., "QCSEE Composite Fan Frame Subsystem Test Report," NASA CR-135010, August 1977.